1994

Water and electrolyte regulation during space flight and exercise

Susan Elizabeth Doty
Iowa State University

Order Number 9518374

Water and electrolyte regulation during space flight and exercise

Doty, Susan Elizabeth, Ph.D.

Iowa State University, 1994

U·M·I

300 N. Zeeb Rd.
Ann Arbor, MI 48106

Water and electrolyte regulation during space flight and exercise

by

Susan Elizabeth Doty

A Dissertation Submitted to the

Graduate Faculty in Partial Fulfillment of the

Requirements for the Degree of

DOCTOR OF PHILOSOPHY

Department: Chemical Engineering
Interdepartmental Program: Biomedical Engineering

Co-majors: Chemical Engineering
Biomedical Engineering

Approved:

Signature was redacted for privacy.

In Charge of Major Work

Signature was redacted for privacy.

For the Interdepartmental Program

Signature was redacted for privacy.

For the Major Department

Signature was redacted for privacy.

For the Graduate College

Iowa State University
Ames, Iowa

1994

TABLE OF CONTENTS

NOMENCLATURE iii

INTRODUCTION 1

GENERAL BACKGROUND INFORMATION 6

Body Water Compartments 6
Interactions between Body Water Compartments 9
Osmosis 14
Regulation of Body Water 17

MODELING KIDNEY FUNCTION 21

Description of the Urinary System 21
Cardiovascular System 33
Renal Function 37
Hormonal Systems 42
Sodium and Potassium Balance 48
Testing the Kidney Model 51

MODELING THERMOREGULATION 56

Insensible Perspiration 56
Sensible Perspiration 61
Energy Balances 68

SPACE FLIGHT 75

Water and Sodium Balance 75
Thermoregulation 83
Calcium Balance 91

EXERCISE 124

CONCLUSIONS 136

BIBLIOGRAPHY 139

ACKNOWLEDGMENTS 148

NOMENCLATURE

Symbol	Description	Typical value
A	concentration of angiotensin II in plasma (ng/l)	27.0
A	surface area of the body (m^2)	1.8
ADH	concentration of ADH in plasma (munits/l)	4.0
ALD	concentration of aldosterone in the plasma (ng/l)	85.0
c	time constant (min^{-1})	0.04
C	concentration of cortisol in the plasma (mg/l)	0.15
Ca^{++}	concentration of ionized calcium in plasma (mg/l)	55
C_{cl}	clothing thermal conductance (N/sec·^oC·m)	*
CO	cardiac output (l/min)	5.0
C_p	heat capacity (kcal/g·^oC)	
C_s	humid heat of air (J/kg·K)	1090
C_0	concentration of water in the papillary dermis (g/cm^3)	0.879
C_1	concentration of water at the interface between the viable epidermis and stratum corneum (g/cm^3)	0.87
C_2	concentration of water at the surface of the stratum corneum (g/cm^3)	0.2
D	steady state GFR during exercise (ml/min)	*
D_{AB}	molecular diffusivity of water vapor and air (cm^2/s)	0.25
D_{ADH}	clearance rate of ADH (l/min)	0.206
D_C	clearence rate of cortisol (l/day)	144
D_{PTH}	clearance rate of PTH (l/day)	3334
D(T)	diffusivity as a function of temperature (g/cm^2)	*
DV_E	excess fluid in extracellular compartment (l)	0.0
D_0	reference diffusivity, determined by extrapolating experimental data to 0 K (cm^2/s)	
D_1	diffusivity of water through the hydrated skin layer (cm^2/s)	$6.9x10^{-6}$
$D_{1,25(OH)2D3}$	clearence rate of 1,25-$(OH)_2D_3$ (l/day)	2.4
D_2	diffusivity of water through the stratum corneum (cm^2/s)	$2.5x10^{-10}$
E_a	activation energy of diffusion (kcal/mole)	
E_{max}	maximum evaporative capacity of the environment (kcal/hr)	*
$FAb_{Ca++,int}$	fraction of ingested and secreted calcium which is absorbed by the intestine (dimensionless)	0.5
$F_{Na,DT}$	rate of flow of sodium into the distal tubule (mEq/min)	0.89

$F_{Na,LH}$	rate of flow of sodium into the loop of Henle (mEq/min)	4.44
$F_{Na,PT}$	filtered load of sodium (mEq/min)	17.75
$F_{Na,U}$	rate of excretion of sodium (mEq/min)	0.128
$FRe_{Ca++,DT}$	fraction of calcium delivered to the distal tubule which is reabsorbed by the distal tubule and collecting duct	0.61
$FRe_{W,LH}$	fraction of water reabsorbed in the loop of Henle	0.33
FT	flight time (day)	*
$F_{W,DT}$	rate of flow of water into the distal tubule (ml/min)	
$F_{W,LH}$	rate of flow of water into the loop of Henle (ml/min)	31.25
$F_{W,U}$	urine flow rate (ml/min)	1.0
GFR	glomerular filtration rate (ml/min)	125.0
GFR_{ave}	average GFR during exercise (ml/min)	*
GFRrest	GFR at rest (ml/min)	*
Gr	Grashof number (dimensionless)	*
GTB	fraction of filtered load of sodium reabsorbed in the proximal tubule	0.75
h_c	convective heat transfer coefficient (kcal/m^2·^oC·hr)	*
$h_{c,f}$	convective heat transfer coefficient for forced convection (kcal/m^2·^oC·hr)	*
$h_{c,n}$	convective heat transfer coefficient for natural convection (kcal/m^2·^oC·hr)	*
h_d	convective mass transfer coefficient (kg/m^2·hr)	*
$h_{d,f}$	convective mass transfer coefficient for forced convection (kg/m^2·hr)	*
$h_{d,n}$	convective mass transfer coefficient for natural convection (kg/m^2·hr)	*
h_r	radiative heat transfer coefficient (kcal/m^2·^oC·hr)	*
h_y	heat transfer coefficient (J/s·K·m^2)	*
H	partition coefficient (g H_2O per cm^3 air/g H_2O per cm^3 stratum corneum)	8.04×10^{-5}
Hct	hematocrit (unitless)	0.45
H_{vap}	heat of vaporization (kcal/g)	0.58
im	ability of water vapor to pass through clothing (dimensionless)	*
In_{Na}	rate of ingestion of sodium (mEq/min)	*
IN_W	rate of ingestion of water (ml/min)	*
j	flux of water through the skin (g/cm^2·s)	3.22×10^{-7}
j_M	mass transfer j factor (dimensionless)	*
j_l	flux of water through the hydrated layer (g/cm^2·s)	3.22×10^{-7}

j_2	flux of water through the stratum corneum ($g/cm^2 \cdot s$)	3.22×10^{-7}
k	thermal conductivity of the body ($kcal/m \cdot hr \cdot {}^oC$)	0.4
k_C	mass transfer coefficient	*
k_y	mass transfer coefficient (mole/s·mole fraction)	*
Kf	capillary filtration coefficient (ml/min·kg·torr)	0.061
K_1	bone formation rate constant (l/day)	9.27
K_2	bone destruction rate constant (mg/day)	510
L	characteristic length (m)	
m_{sw}	rate of sweat mass production (g/hr)	180
mtot	total rate of water loss through the skin (g/hr)	200
M	total metabolic rate (kcal/hr)	*
M_o	basal metabolism ($kcal/m^2 \cdot hr$)	37
M_B	molecular weight of air (kg/mole)	0.0288
M_E	metabolic rate due to exercise ($kcal/m^2 \cdot hr$)	*
Na_I	intracellular concentration of sodium (mEq/l)	10.0
Na_{pl}	extracellular concentration of sodium (mEq/l)	142.0
$Na_{,sw}$	sweat sodium concentration (mEq/l)	12.5
$Na_{TOT,E}$	total extracellular sodium (mEq)	2130.0
$Na_{TOT,I}$	total intracellular sodium (mEq)	250.0
Nu	Nusselt number (dimensionless)	*
$1,25\text{-}(OH)_2D_3$	concentration of 1,25-dihydroxycholecalciferol in plasma (mg/l)	0.00003
OS_{pl}	plasma osmolality (mEq/l)	299.6
OT_E	total extracellular osmotic components other than sodium (mEq)	2418.0
OT_I	total intracellular osmotic components other than sodium	7555.0
P	ambient pressure (torr)	760
P_a	partial pressure of water in the ambient air (torr)	*
P_{ar}	arterial pressure (torr)	100.0
Pc	capillary hydrostatic pressure (torr)	27.0
Pi	interstitial hydrostatic pressure (torr)	1.0
PK	extracellular concentration of potassium (mEq/l)	5.0
$P_{m,s}$	mean systemic pressure (torr)	7.0
Pr	Prandlt number (dimensionless)	*
P_S	partial pressure of water in the air at the skin's surface (torr)	44
PTH	concentration of parathyroid hormone in the plasma (mg/l)	0.00045
Q_{conv}	heat transfered through convection ($kcal/m^2 \cdot hr$)	*

Q_{evap}	heat transfered through evaporation (kcal/m^2·hr)	*
Q_{rad}	heat transfered through radiation (kcal/m^2·hr)	*
R	gas constant (kcal/mole·K)	0.00199
R	concentration of renin in plasma (GU/l)	0.06
Re	Reynolds number (dimensionless)	*
$Re_{Na,DT}$	rate of reabsorption of sodium from the distal nephron segments (mEq/min)	0.757
$Re_{Na,LH}$	rate of reabsorption of sodium from the loop of Henle (mEq/min)	3.55
$Re_{Na,PT}$	rate of reabsorption of sodium from the proximal tubule (mEq/min)	13.3
$Re_{W,DT}$	rate of reabsorption of water in the distal nephron segments (ml/min)	19.7
$Re_{W,LH}$	rate of reabsorption of water in the loop of Henle (ml/min)	10.55
$Re_{W,PT}$	rate of water reabsorption in the proximal tubule (ml/min)	93.75
R_f	rate of calcium input to the bones (mg/day)	510
$R_{f,actual}$	rate of calcium input to the bones when the plasma cortisol level is elevated (mg/day)	*
$R_{f,normal}$	rate of calcium input to the bones when the plasma cortisol level is normal (mg/day)	510
R_r	rate of calcium output from the bones (mg/day)	510
$R_{r,actual}$	rate of calcium output from the bones when the plasma cortisol level is elevated (mg/day)	*
$R_{r,normal}$	rate of calcium output from the bones when the plasma cortisol level is normal (mg/day)	510
$R_{t,p}$	total peripheral resistance (torr/l·min)	20.0
RVR	resistance to venous return (torr/l·min)	1.4
S_A	rate of formation of angiotensin II (ng/min)	105.0
S_{ADH}	release rate of ADH (munits/min)	0.825
$S_{ADH,P}$	release rate of ADH due to plasma osmolality (munits/min)	0.84
$S_{ADH,V}$	release rate of ADH due to diminished fluid volume (munits/min)	0.81
S_{ALD}	rate of secretion of aldosterone (ng/min)	52.7
Sc	Schmidt number (dimensionless)	*
S_C	secretion rate of cortisol (mg/day)	21.6
$S_{Ca,B}$	net rate of ionized calcium release by the bones (mg/day)	0
$S_{Ca,I}$	net rate of ionized calcium absorbtion by the intestine (mg/day)	178

Sh	Sherwood number (dimensionless)	*
SL	stress level (dimensionless)	0.83
S_{PTH}	rate of secretion of parathyroid hormone (mg/day)	1.51
S_R	rate of release of renin (GU/min)	0.008
$S_{1,25(OH)2D3}$	rate if secretion of 1,25-$(OH)_2D_3$ (mg/day)	0.00072
t	time (min or day)	
T	temperature (K)	*
T_a	ambient temperature (^oC)	*
T_c	average core temperature (^oC)	37
T_m	average muscle temperature (^oC)	34.7
T_s	average skin temperature (^oC)	33.6
T_{su}	temperature at the surface of the skin (^oC)	33.1
T_r	radiant temperature (^oC)	*
$U_{Ca,K}$	urinary loss of ionized calcium (mg/day)	178
v	air velocity (cm/s)	15
V_{bl}	blood volume (l)	5.0
V_E	extracellular fluid volume (l)	15.0
v_{eff}	effective velocity (m/s)	*
$V_{E,N}$	normal extracellular fluid volume (l)	15.0
V_I	intracellular fluid volume (l)	25.0
VO2,max	maximum oxygen consumption (ml/kg•min)	49
V_{pl}	plasma volume (l)	3.0
VR	venous return (l/min)	5.0
V_W	total body water (l)	40.0
$V_{W,L}$	body water contained in the lower extremities (l)	12
$V_{W,U}$	body water contained in the upper body (l)	28
w	fraction of skin wetted by perspiration (dimensionless)	0.06
X_c	thickness of the core layer (cm)	3.2
X_m	thickness of the muscle layer (cm)	1.6
X_{mc}	average distance between the muscle and core layers (cm)	2.4
X_s	thickness of the skin layer (cm)	0.8
X_{sm}	average distance between the skin and muscle layers (cm)	1.2

Greek

α_+	gain for body temperature above normal ($^oC^{-1}$)	0.25
α_-	gain for body temperature below normal ($^oC^{-1}$)	0.5

β	volumetric coefficient of expansion (K^{-1})	
γ	control constant (hr/^oC)	0.042
δ_{PD}	thickness of the papillary dermis (cm)	0.015
δ_{SC}	thickness of the stratum corneum	0.00093
δ_{VE}	thickness of the viable epidermis	0.00407
μ	air viscosity (g/cm·s)	18
πc	capillary oncotic pressure (torr)	25.0
πi	interstitial oncotic pressure (torr)	0.0
ρ	density (g/cm^3)	
ρa	fluid density (g/cm^3)	*

(* determined from experimental conditions)

INTRODUCTION

The success of long-term space flight critically depends upon the design of a life support system, since this system is responsible for providing an environment which can comfortably sustain human life. A life support system must therefore supply food, clean water, oxygenated air, and an appropriate atmospheric temperature and humidity. Through eating and breathing, humans take in material. This material is used to produce energy and consequently material, in a somewhat different form, and energy are returned to the environment. The life support system recovers the output material and energy to convert it for future use when possible or to eliminate it from the environment. The exact output of material and energy from a crew member depends on diet, activity level, gender, age, the ambient conditions, and many other factors. The design of a life support system for long-term space flight must therefore include aspects of the crew's physiology and of the mechanical equipment which sustains the environment. A diagram of the interactions between a crew and the life support system is shown in Figure 1. The contents within the dashed lines, which are mainly concerned with the human water balance, represent the physiological processes which will be described in this dissertation.

This dissertation is describes the development of a quantitative and reliable mathematical description of how humans produce, internally redistribute, and exchange water with their environment, as a function of activity level and environmental conditions. Since the movement of water

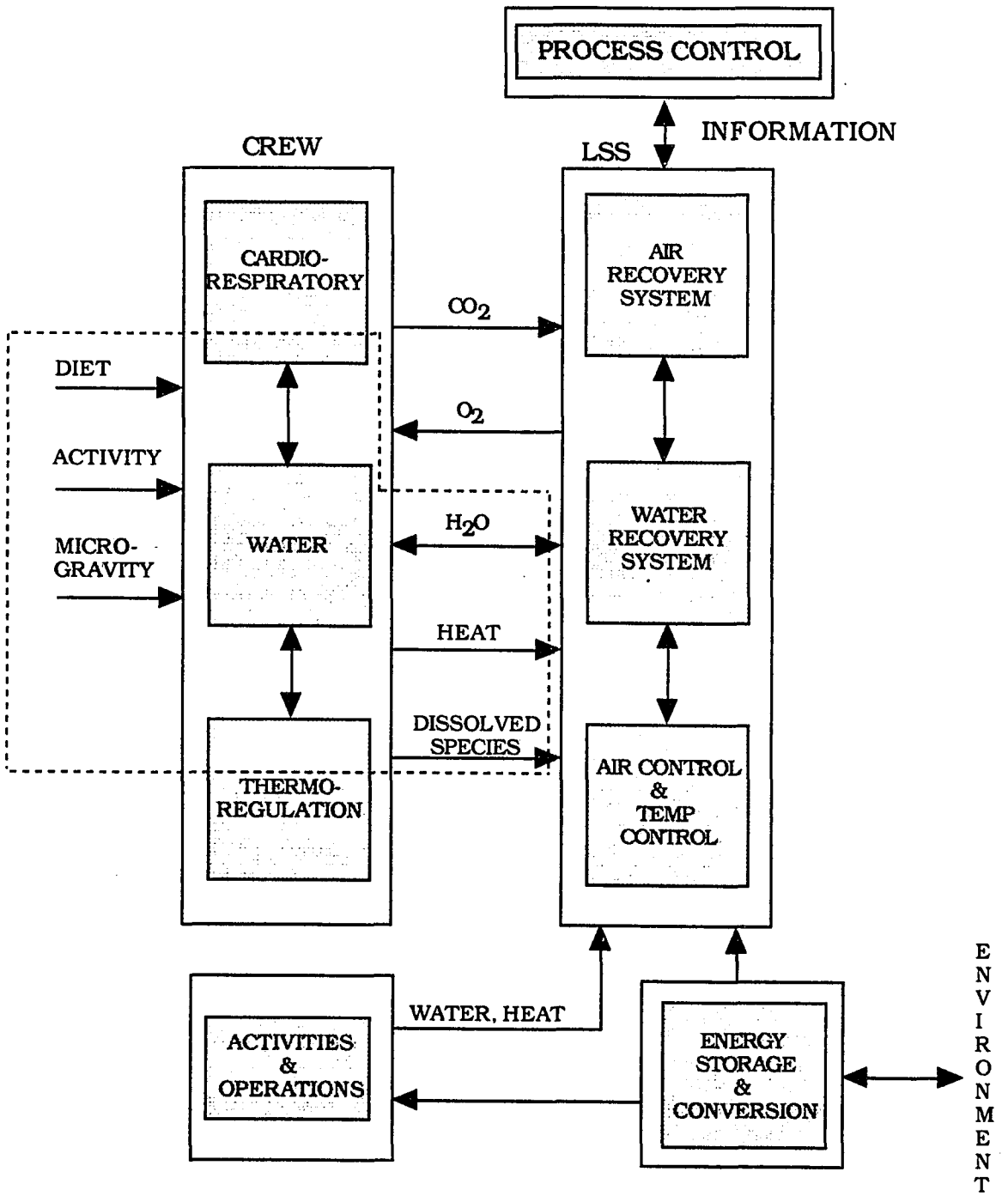

Figure 1: Interactions between a crew and a life support system.

into, within, and out of the body is coupled to the movement of dissolved electrolytes, this mathematical description will also include the movement of sodium ions and calcium ions. Some of the conditions experienced during space flight and their effect on humans, such as microgravity and reduced barometric pressure, will be addressed. Moreover, since exercise may play an important role in preventing detrimental effects caused by space flight conditions, the model is extended to include a full range of activity levels.

The model is initially developed for an average-sized human at rest in a neutral environment. This initial model mainly describes kidney function since, under these conditions, the kidneys are the primary regulators of body water content and electrolyte composition. As shown in Figure 2, the basic kidney model divides body water into an intracellular compartment and an extracellular compartment. Hormones involved in water and/or electrolyte regulation, which are mainly confined to the extracellular fluid compartment, are included in this model. Since water can also leave the body in the form of perspiration, this water loss must also be considered. The perspiration rate depends primarily on body temperature, therefore, the basic kidney model is coupled with a thermoregulation model. The thermoregulation model predicts the core, muscle, and skin temperatures as a function of the metabolic rate, ambient conditions, and clothing type. To include the effects of space flight and exercise, variations to the basic kidney-thermoregulation model must be made. During space flight, water which is normally pooled in the lower extremities shifts headward. To

account for this fluid shift, the extracellular and intracellular fluid compartments are further divided to represent upper and lower fluid compartments. Since space flight can drastically alter calcium regulation by demineralizing bone tissue, calcium regulation is considered at this time. Exercise affects the rate at which the kidneys filter fluid from the extracellular compartment. This rate is called the glomerular filtration rate (GFR) and variations to it during physical activity are considered in the exercise section. Figure 2 illustrates how space flight conditions and exercise are included with the basic kidney-thermoregulation model.

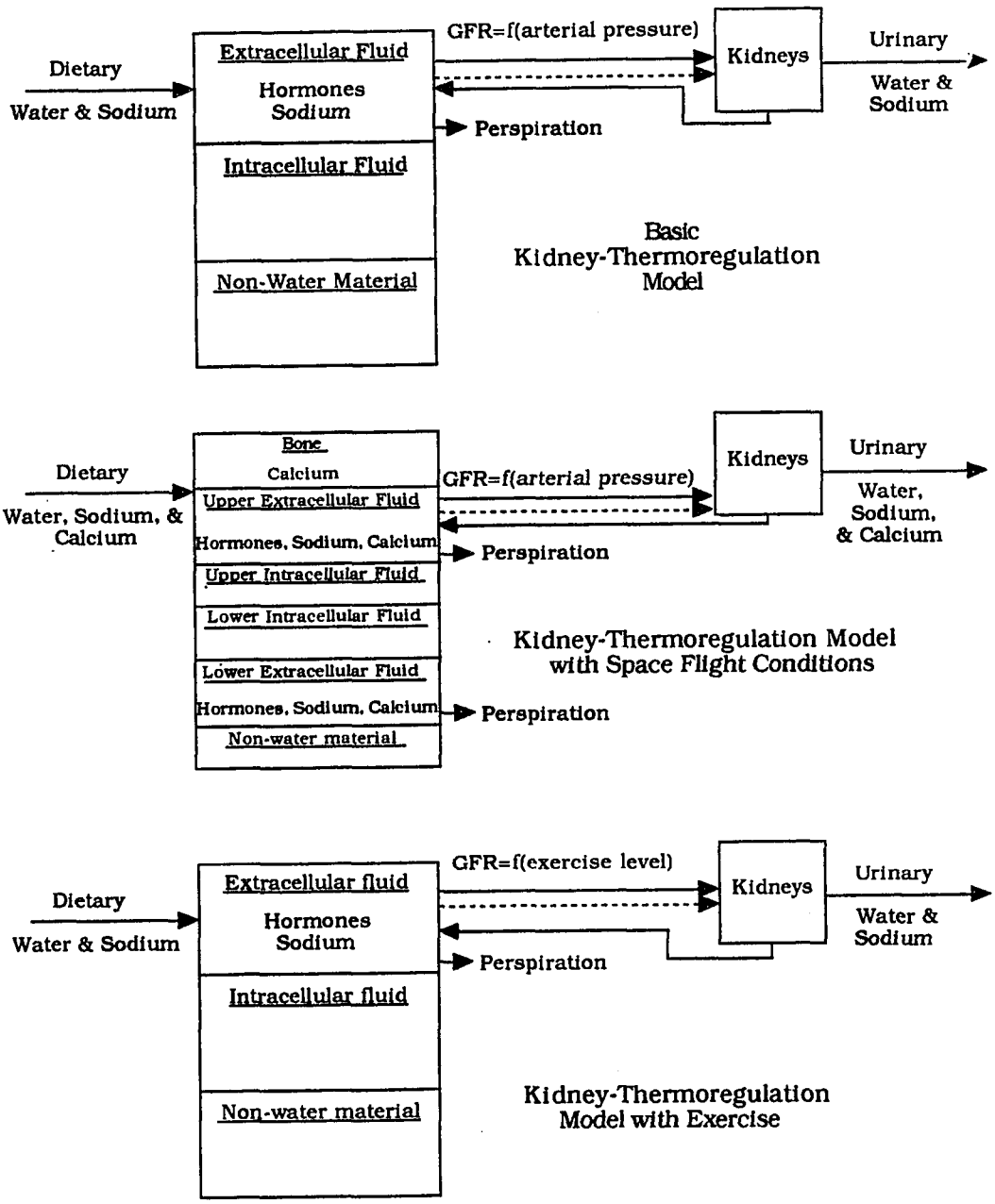

Figure 2: Illustration of relation between the basic kidney-thermoregulation model, space flight, and exercise where the solid line = flow of water and dissolved species and the dashed line = flow of other information.

GENERAL BACKGROUND INFORMATION

Body Water Compartments

The most abundant compound in the human body is water, accounting for 40% to 80% of the body weight depending upon the amount of adipose tissue present. The body contains the highest proportion of water at infancy, up to 80%, and then the water content decreases as old age is approached. The average water content of an adult male is 60% of the body weight whereas the average water content of an adult female is 50% of the body weight. This difference is due to the varying content of subcutaneous fat.

The total body water can be categorized as existing in two main compartments: intracellular water and extracellular water. The intracellular water consists of all the water within the cells and constitutes over half of the total body water. Since red blood cells are surrounded by plasma, and all other cells are surrounded by interstitial fluid, the intracellular compartment has been sub-divided to represent these two cell types in Figure 3. The extracellular water, which includes all of the fluid outside of the cells, can be further sub-divided into compartments that represent interstitial fluid, circulating blood plasma, lymph, and transcellular water. The interstitial fluid surrounds cells outside of the vascular system whereas plasma is contained within the blood vessels. Avascular tissues such as dense connective tissue and cartilage contain interstitial water which slowly equilibrates with tracers used to determine extracellular fluid volume. For

this reason, additional compartments are sometimes used to represent the interstitial fluid of these avascular tissues. Lymph is interstitial fluid which has flowed into the lymphatic vessels and is eventually returned to the vascular system. A small fraction of the extracellular fluid is separated from other extracellular compartments by a layer of epithelium. This compartment, which includes cerebrospinal fluid, aqueous and vitreous humor, synovial fluid, and fluid secretions of glands, makes up the transcellular compartment. These body water compartments, and the interactions between them, are shown in Figure 3. The average size of each compartment, in terms of percent body weight, has been determined for adult males and females (West, 1985) and is included in this figure. The lymph compartment, which is often included in the interstitial compartment, has been determined to be approximately 2% of the body weight (Pitts, 1974). The size of the lymph compartment for females was determined by multiplying 2% by 5/6, since that the average female body is about 50% water and the average male body is about 60% water.

Cerebrospinal fluid and aqueous humor, which make up a part of the transcellular compartment, are formed by epithelial cells secreting sodium ions into the associated chamber (Guyton, Taylor, & Granger, 1975). The secretion of positively charged sodium ions creates a potential difference with respect to the blood, causing negatively charged ions to flow from the plasma, into the epithelial cells, and eventually into the chambers. The excess ions then cause water to flow across the epithelial membranes by osmosis. Water flows from the intracellular fluid of the epithelial cells into

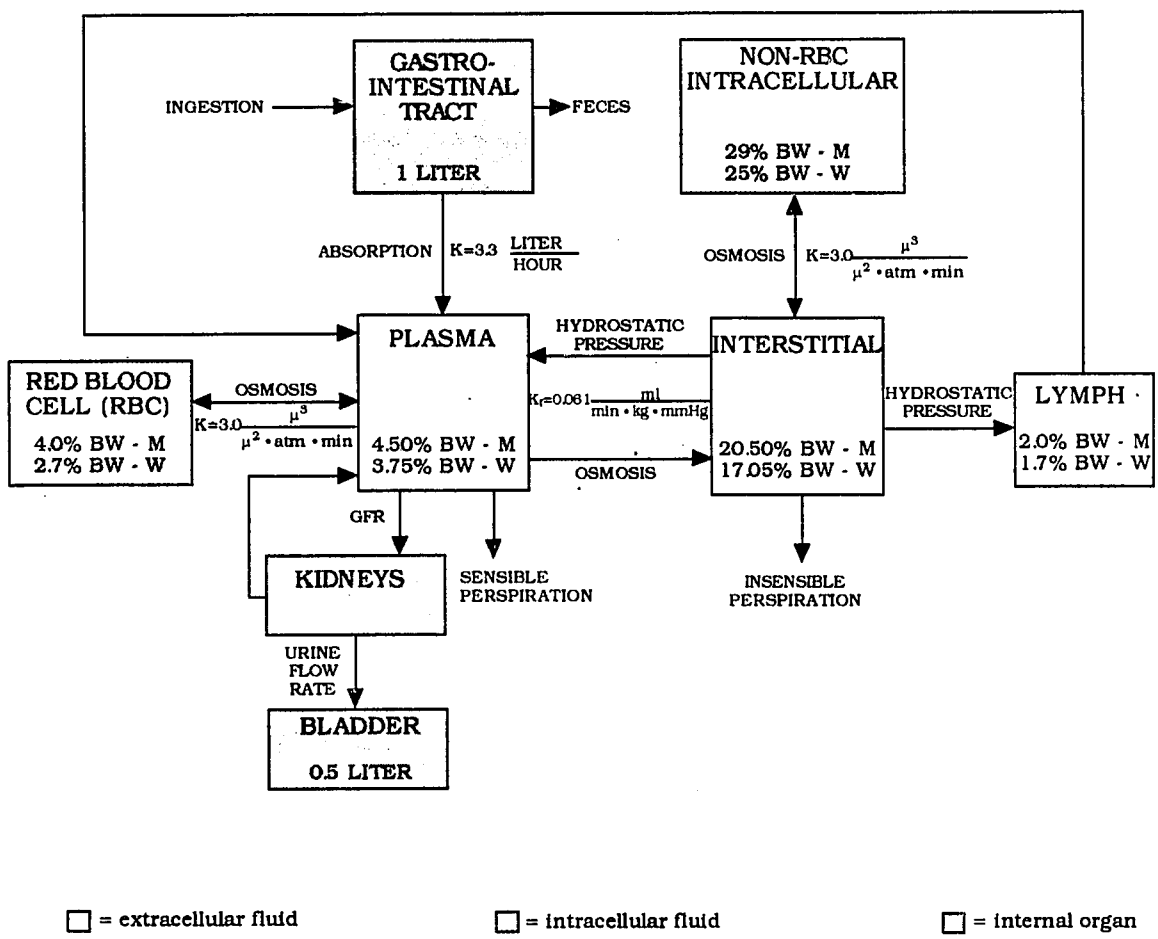

Figure 3: Body water compartments and the forces which cause flow between them. Membrane permeability is represented by K. The size of each compartment is shown for both males (M) and females (F) where BW = body weight.

the chambers by osmosis. Since osmosis is also the primary force for the flow of water between the cellular compartment and the interstitial compartment, and since the transcellular compartment accounts for less than 2% of the body weight, this compartment has been lumped together with the interstitial compartment in Figure 3.

Interactions between Body Water Compartments

Water enters the body through the digestive tract and moves across the mucosa of the small and large intestines in response to osmotic gradients (Ganong, 1991). Previous studies have estimated that water is absorbed from the gastrointestinal tract (GI tract) at a constant rate with a zeroth-order rate constant of 3.3 liters/hour (Reeve & Guyton, 1967). The volume of the stomach, which is given in Figure 3, is about one liter (Hole, 1987). Water is also produced by the intracellular metabolism of nutrients. The movement of water between the fluid compartments is controlled by hydrostatic pressure, osmotic pressure, or both.

Fluid movement between the extracellular and intracellular compartments is built on three main points: (1) that water can easily move between the two compartments; (2) that most of the solutes on each side of the cell membrane will not penetrate the membrane easily; and (3) that hydrostatic pressure differences do not play a major role in the final fluid distribution (Coleman, Norman, & Manning *in* Guyton, Taylor, & Granger, 1975). In other words, water will cross the cell membrane until osmotic

equilibrium has been attained between the two compartments. Hydrostatic pressures are not a major factor in this osmotic equilibrium since the cell wall is extremely flexible and marked volume changes do not produce significant intracellular hydrostatic pressure differences (Coleman, Norman, & Manning *in* Guyton, Taylor, & Granger, 1975).

To determine the rate at which water penetrates the cells, the cell membrane permeability and surface area must be known. The hydraulic permeability of the human cell membrane to water is approximately 3.0 μ^3 water/μ^2·min·atm (West, 1985). The surface area of the red blood cell compartment, which is near osmotic equilibrium with the plasma compartment, can be calculated from the blood volume, hematocrit (Hct), red blood cell volume, and red blood cell surface area. The blood volume can be calculated with the following equation.

$$\text{Blood volume} = \frac{\text{Plasma volume}}{1 - \text{Hct}} \qquad (1)$$

The average normal hematocrit is 0.47 for men and 0.42 for women (Ganong, 1991). The volume and surface area of a normal red blood cell are 9.7×10^{-8} µl and 135 μm^2, respectively (West, 1985). The surface area of the non-red blood cell compartment, which is near osmotic equilibrium with respect to the interstitial fluid, can be calculated from the average cell size and the volume of the non-red blood cell compartment. The average cell is roughly cubic with dimensions of 10µm x 10µm x 10µm (Martini, 1989).

The exchange of fluid between the plasma and interstitial

compartments can be described by what are called Starling forces. This exchange occurs across the capillary walls and is responsible for supplying cells with oxygen and nutrients while removing cellular wastes. Capillary hydrostatic pressure and interstitial osmotic pressure forces fluid out of the capillaries and into the interstitial spaces. Conversely, the interstitial hydrostatic pressure and the plasma osmotic pressure force fluid back into the capillaries. The composition of the plasma is almost identical to that of the interstitial fluid with the exception of the protein content. Most of the relatively large protein molecules cannot penetrate the capillary wall. Therefore, the protein content is substantially higher in the plasma and causes the osmotic effects. The protein osmotic pressure is sometimes referred to as the oncotic pressure. Typically the plasma hydrostatic pressure declines from about 37 mm Hg to 17 mm Hg along the length of a capillary whereas the oncotic pressure and interstitial hydrostatic pressure remain relatively constant at 25 mm Hg and 1 mm Hg, respectively. Consequently, fluid is forced out of the arteriole end of the capillary and fluid is forced into the venous end of the capillary. This situation is shown in Figure 4.

Fluid movement is related to the Starling forces through the following expression.

$$\text{Fluid movement} = K_f[(P_c+\pi_i) - (P_i+\pi_c)] \qquad (2)$$

where K_f = capillary filtration coefficient (ml/min·kg·mm Hg)

P_C = capillary hydrostatic pressure (mm Hg)

P_i = interstitial hydrostatic pressure (mm Hg)

π_C = capillary oncotic pressure (mm Hg)

π_i = interstitial oncotic pressure (mm Hg)

For the entire body, K_f has been found to be approximately 0.061 ml fluid/min·kg body weight·mm Hg (Landis & Pappenheiner, 1963).

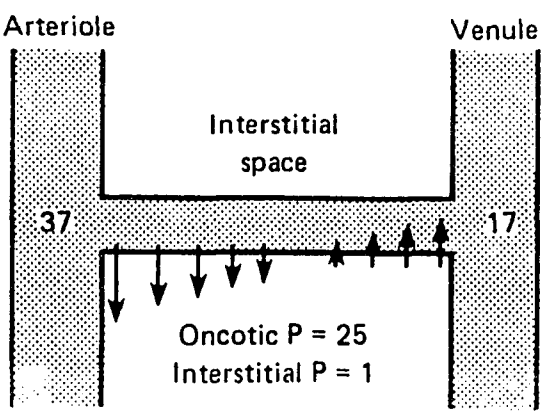

Figure 4: Representation of pressure gradients across the wall of a muscle capillary. The arrows indicate the approximate magnitude and direction of fluid movement. (taken from Ganong, 1991)

During a 24 hour period, about 2 liters more fluid is filtered across the capillary walls than is reabsorbed (Little, 1989). This fluid then flows into the lymphatic system due to a hydrostatic pressure difference. However, since the flow rate of this interstitial fluid and the distance to a lymphatic capillary is extremely small, the pressure gradient between the

interstitial spaces and lymphatic capillary is too slight to be measurable (Guyton, Taylor, & Granger, 1975). A primary characteristic of the lymphatic system is that under normal conditions any excess fluid that collects in the tissues is returned back to the circulation (Guyton, 1984). Previous studies have found that the rate of lymph flow can increase up to 20 times the resting level (Guyton, Taylor, & Granger, 1975). This phenomena is mainly due to the structure of the lymphatic capillaries. Endothelial cells of the lymphatic vessels overlap to form pores (see Figure 5).

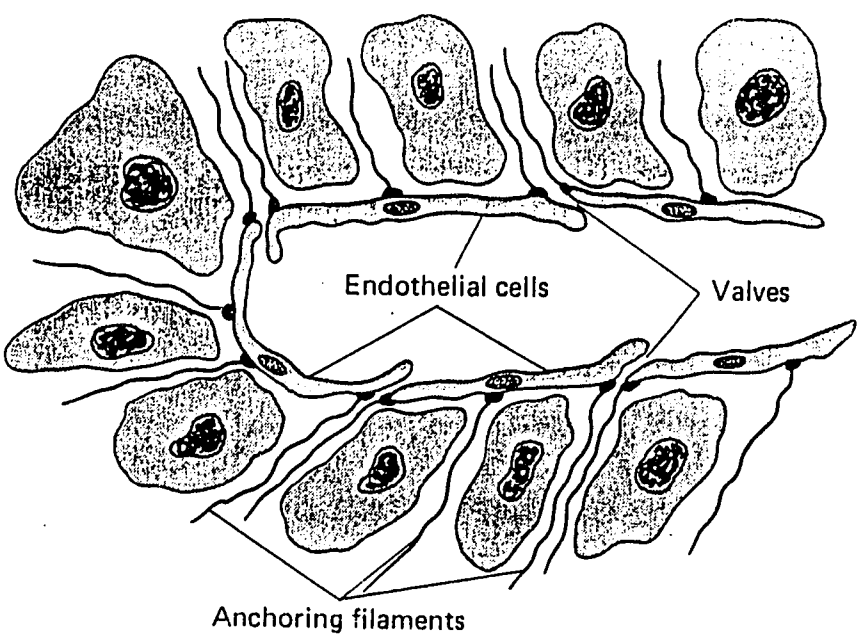

Figure 5: Structure of the lymphatic capillaries which allows for the variable, one directional flow of lymph. (taken from Guyton, 1984)

As the interstitial space fills with liquid, the tissue swells and the endothelial cells are pulled apart causing the pores to open wider. Therefore, the greater the tissue pressure, the greater the lymph formation rate. The overlapping edges of the endothelial cells also prevent fluid from flowing out of the lymphatic capillary so any compressive force will cause lymph to flow forward through the vessel (Guyton, 1984).

For the above stated reasons, it is assumed that the lymph flow rate is equal to the net formation of interstitial fluid in Figure 3. Figure 6 illustrates the effect of capillary pressure on interstitial fluid pressure, interstitial fluid volume, and lymph flow. From Figure 6, it can be seen that the interstitial fluid volume remains relatively constant as the capillary pressure and interstitial pressure are increased until edema, which is an accumulation of fluid in the tissue spaces, occurs. Over this range of capillary pressures, the lymph flow increases 15 to 20 times normal. Therefore, the lymphatic regulatory system which prevents the buildup of interstitial fluid performs close to its maximum level before edema occurs. Once edema results, the lymphatic system continues to operate at the maximum level thereby alleviating the swelling as quickly as possible.

Osmosis

In this work, osmosis refers to the movement of water across a semipermeable membrane which is permeable to water but not to solutes. A cell membrane, which is freely permeable to water but not to most solutes,

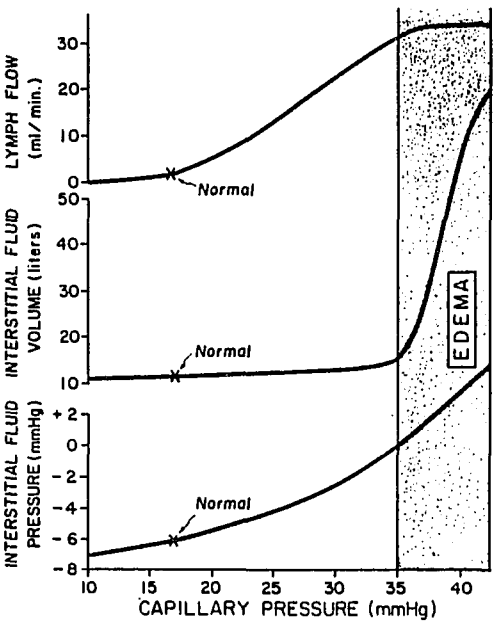

Figure 6: Computed effects of progressive increase in capillary pressure on interstitial fluid pressure, interstitial fluid volume, and lymph flow. (taken from Guyton, Taylor, and Granger, 1975)

is an example of such a semipermeable membrane. Osmosis is similar to diffusion in that a concentration gradient is the driving force behind the movement of molecules. However, diffusion refers to the movement of solute molecules whereas osmosis refers to the movement of water molecules. Additionally, osmosis and diffusion occur in opposite directions, since a higher concentration of solute molecules corresponds to a lower water concentration. The process of osmosis is illustrated in Figure 7, where the small spheres represent water molecules and the large spheres represent solute molecules. The two solutions on each side of the semipermeable

membrane initially have different solute concentrations (step 1). The solvent molecules, in this case water, begin crossing the membrane from the side with the lower solute concentration to the side with the higher solute concentration. This process continues until the concentration of solute is the same on both sides (step 2a). The larger the solute concentration difference on each side, the stronger the driving force, or osmotic force, for water movement. This osmotic force is sometimes called the osmotic pressure. If a downward pressure is applied to side b (step 2b), the movement of water across the membrane can be eliminated and this downward pressure is equal to the osmotic pressure.

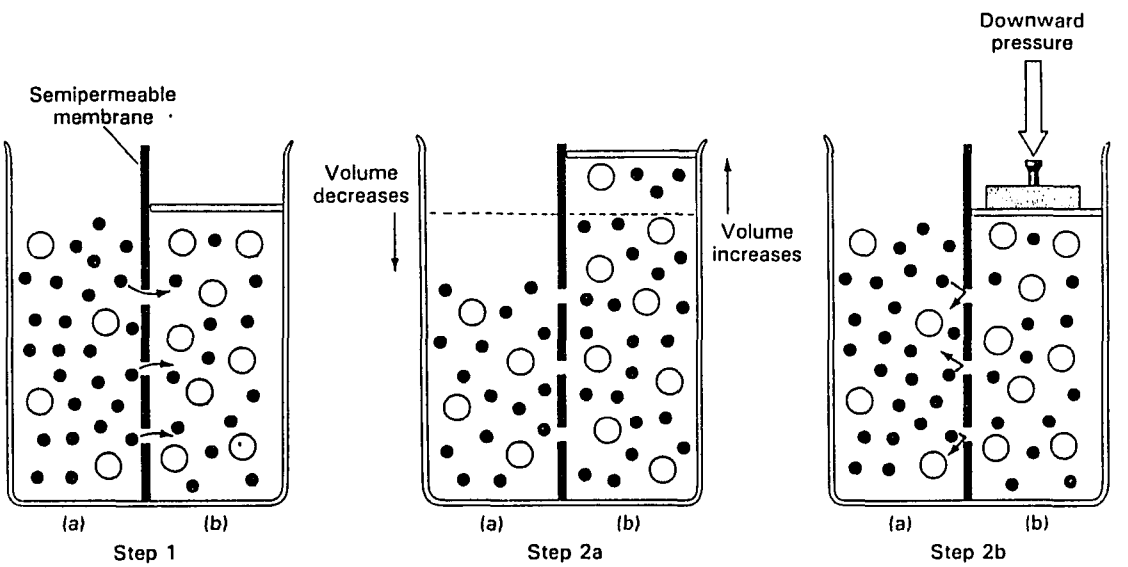

Figure 7: An example of osmosis where the small spheres represent water molecules and the large spheres represent solute molecules. (taken from Martini, 1989)

Regulation of Body Water

Water can enter the body as a liquid, with moist food, and as the result of intracellular oxidative metabolism of various nutrients. The primary regulator of water intake is thirst, and although the thirst mechanism is poorly understood, it seems to involve the osmotic pressure of extracellular fluid and a thirst center in the hypothalamus (Hole, 1987).

Water is lost from the body through four primary routes: sensible perspiration, insensible perspiration, urine, and feces. Water lost by sensible perspiration, or sweating, is a necessary part of the body's temperature control mechanism; water loss in feces accompanies the elimination of undigested food materials and other waste products; and water losses through diffusion and evaporation (insensible perspiration) are largely unavoidable (Hole, 1987). The primary mechanism by which water loss is regulated is the formation of urine. The urine flow rate, which can vary from less than 0.7 ml/min to more than 14 ml/min, is determined primarily by arterial blood pressure and the plasma level of antidiuretic hormone (ADH) (West, 1985). ADH is secreted from the posterior pituitary gland and the secretion rate is controlled by a center located in the hypothalamus.

The osmolality of the body fluids is regulated by the thirst mechanism and by the renal excretion rate of electolytes. Ingesting excess hypotonic liquids will dilute the extracellular water compartment and therefore reduce

plasma osmolality. ADH and another hormone, aldosterone, regulate the urinary loss of sodium and potassium.

The thirst center and the ADH secretion rate are primarily stimulated by two physiological conditions, increases in plasma osmolality and decreases in plasma volume (West, 1985). Changes in plasma osmolality are sensed by nerve cells called osmoreceptors that are located in the hypothalamus. It is believed that the osmoreceptors become reduced in volume by osmotic dehydration when plasma osmolality is elevated. This triggers thirst and increases ADH release (Cowley *in* Guyton, Taylor, & Grange, 1975). Changes in plasma volume are sensed by stretch receptors located in the heart and blood vessels and by the juxtaglomerular apparatus of the kidney. The stretch receptors are stimulated by distention and their afferent nerve fibers pass via the glossopharyngeal and vagus nerves to the medulla (Ganong, 1991). The juxtaglomerular apparatus secretes an enzyme, renin, in response to a decreased blood volume or decreased blood pressure. Renin converts a circulating blood protein which is produced by the liver, angiotensinogen, to angiotensin I. Angiotensin I is then converted in lung tissue to angiotensin II. The actions of angiotensin II include vasoconstriction, which elevates the blood pressure, increased secretion rates of aldosterone and ADH, and stimulation of the thirst center. A change in plasma osmolality of 1% doubles the plasma level of ADH, and the thirst center is stimulated when the plasma osmolality changes by 1 to 2%, whereas the change in blood volume necessary to cause these responses is on the order of 10 to 15% (Cowley *in* Guyton, Taylor, and Granger, 1975).

However, if the osmoreceptors and volume receptors provide conflicting information, for example a low blood volume with a low osmolality, the volume regulating mechanism will be the predominant mechanism. Since the stretch receptors adapt to abnormal blood volumes over a period of several days, and the osmoreceptors do not adapt to abnormal plasma osmolalities (Cowley *in* Guyton, Taylor, and Granger, 1975), the volume regulating mechanism is active only when considering short-term regulation. The osmolality mechanism will be active for both short-term and long-term body water regulation. The effects of plasma osmolality and volume on the circulating level of ADH are shown in Figure 8. The relationship between the intensity of thirst and the plasma osmolality is shown in Figure 9.

An increase in arterial pressure increases the amount of fluid the kidneys withdraw from the vascular compartment and hence increases the urine flow rate. The relationship between renal arterial pressure and urine production is shown later in Figure 17 and will be discussed in more detail.

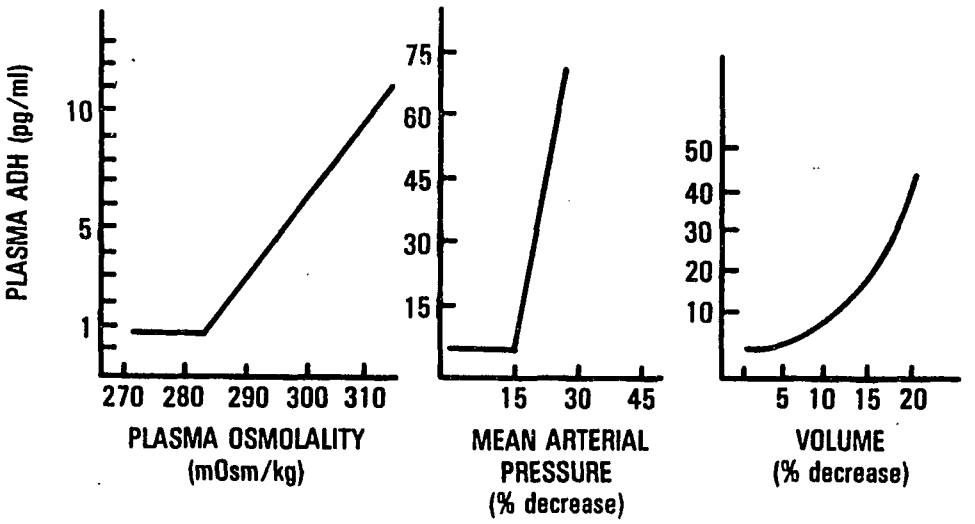

Figure 8: Control of plasma ADH concentration by osmolality, mean arterial pressure, and circulatory volume. (taken from West, 1985)

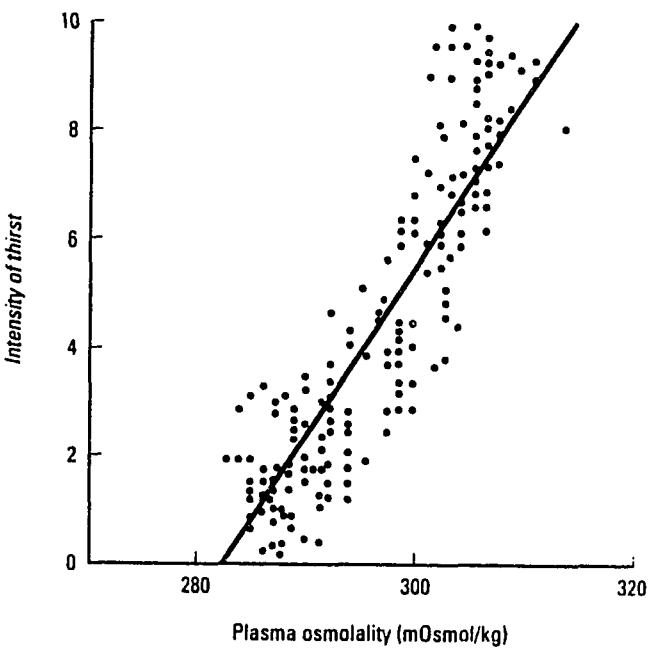

Figure 9: Relation of plasma osmolality to thirst in healthy adult humans during infusion of hypertonic saline. The intensity of thirst is measured on a qualitative analog scale. (taken from Ganong, 1991)

MODELING KIDNEY FUNCTION

Description of the Urinary System

The urinary system includes the kidneys, ureters, bladder, and urethra. The primary function of this system is to maintain homeostasis of the body fluids by adjusting the composition of circulating blood. The kidneys receive about 25% of the cardiac output and filters out a fluid similar to plasma. The composition of this filtered fluid changes as it flows through the kidney tubules since compounds are continually being secreted and reabsorbed. Ultimately, the plasma-like fluid becomes urine. Through this mechanism, the kidneys eliminate wastes while conserving body water, electrolytes, and metabolites.

The kidneys are shaped similar to lima beans and weigh about 300 grams apiece. The internal structure of the kidney can be divided into two parts, an outer portion called the cortex and an inner portion called the medulla (see Figure 10). The medulla of each kidney contains 6-18 conical renal pyramids, with tips, or papillae, each surrounded by a minor calyx (Martini, 1989). Several minor calyces combine to form a major calyx and the major calyces join within the renal pelvis which is connected to a ureter. The nephron is the functional unit of the kidney and consists of a renal tubule and an expanded end or Bowman's capsule (see Figure 11). Each human kidney contains about 1.3 million nephrons. The Bowman's capsule surrounds a capillary bed, the glomerulus, which receives blood through

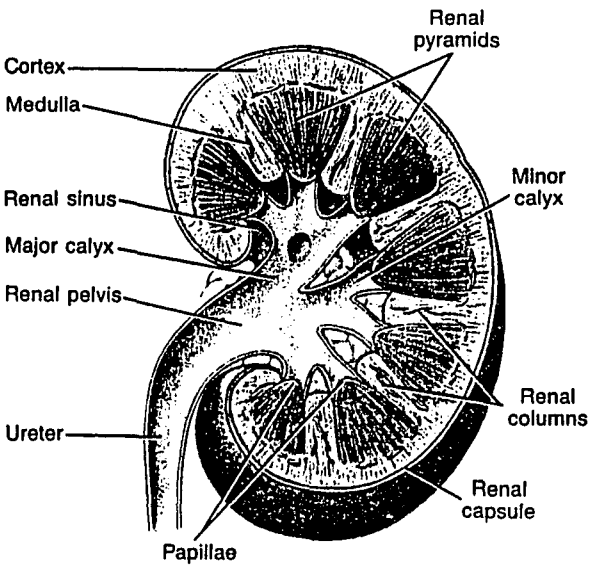

Figure 10: Gross anatomy of the right kidney, in sectional view. (taken from Martini, 1989)

an afferent arteriole and discharges blood, less some filtrate, through an efferent arteriole. Fluid must penetrate three layers, the fenestrated capillary endothelium, the basement membrane which surrounds the capillary wall, and the glomeular epithelium, before it can enter the capsular space (see Figure 12). The structure of these membranes allow water and other small molecules to cross easily but restricts the passage of larger molecules such as plasma proteins. The forces which control the filtration of plasma fluid into Bowman's capsule include the capillary hydrostatic pressure and capsular oncotic pressure, which force fluid into the capsular space, and the plasma oncotic pressure and capsular hydrostatic pressure, which force fluid into the capillaries. The renal capillary pressure is normally 60 mm Hg, whereas the colloid pressure in the glomerulus is

normally 32 mm Hg (Guyton, 1984). The pressure in Bowman's capsule is about 18 mm Hg, and the colliod osmotic pressure in the capsule is essentially zero (Guyton, 1984). The capillary hydrostatic pressure may be varied considerably by the constriction of the afferent or efferent arterioles. The rate at which filtrate enters the capsule is called the glomerular filtration rate (GFR). Typically, 180 liters of fluid enter the renal tubules each day although only about one liter of urine is produced due to the secretion and reabsorption processes which occur along the length of the nephron.

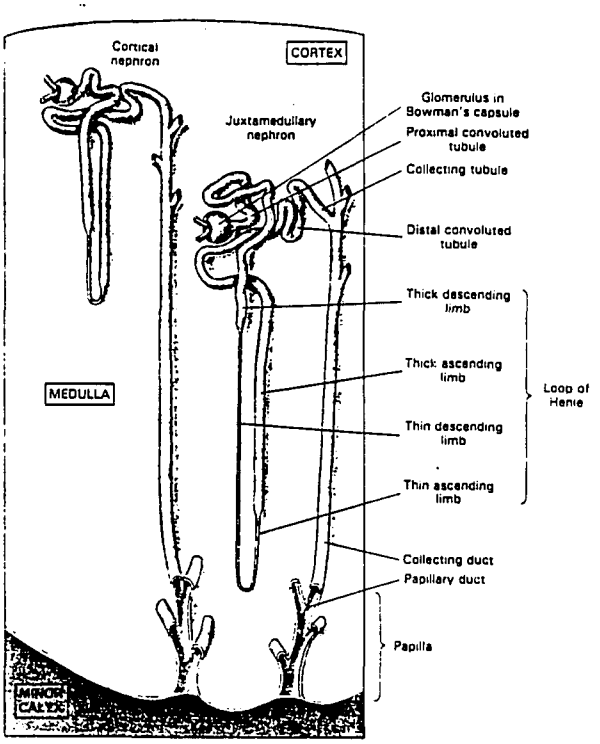

Figure 11: The functional nephron. (taken from Martini, 1989)

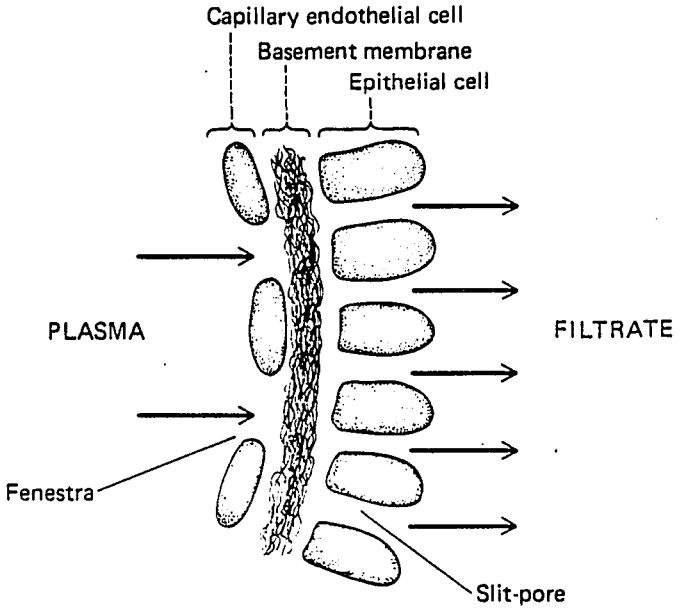

Figure 12: Structure of the glomerular membrane. (taken from Guyton, 1984)

The glomerular filtrate passes from the capsular space into the proximal convoluted tubule due to a hydrostatic pressure gradient. Simple cuboidal epithelial cells with microvilli line this portion of the nephron. The function of the proximal tubule is to actively reabsorb electrolytes and nutrients from the filtered fluid. As these solutes are absorbed, water flows into the epithelial cells and eventually into the interstitial fluid by osmosis. Consequently, the tubular fluid remains isotonic with respect to plasma as it travels through the proximal tubule. By the time the tubular fluid reaches the next segment of the nephron, the loop of Henle, 60 - 70% of the filtered solutes and water have been removed (Ganong, 1991).

From Figure 11, it can be seen that the loop of Henle consists of a descending limb and an ascending limb, each of which has thin and thick

segments. The length of the loop of Henle depends upon the location of the nephron within the kidney. Nephrons in the outer portions of the kidney, or cortical nephrons, have short loops, whereas nephrons closer to the medulla, or juxtamedullary nephrons, have longer loops. For the juxtamedullary nephrons, a concentration gradient exists within the interstitial fluid along the length of the loop of Henle. The variation of osmolality within the medulla is shown in Figure 13.

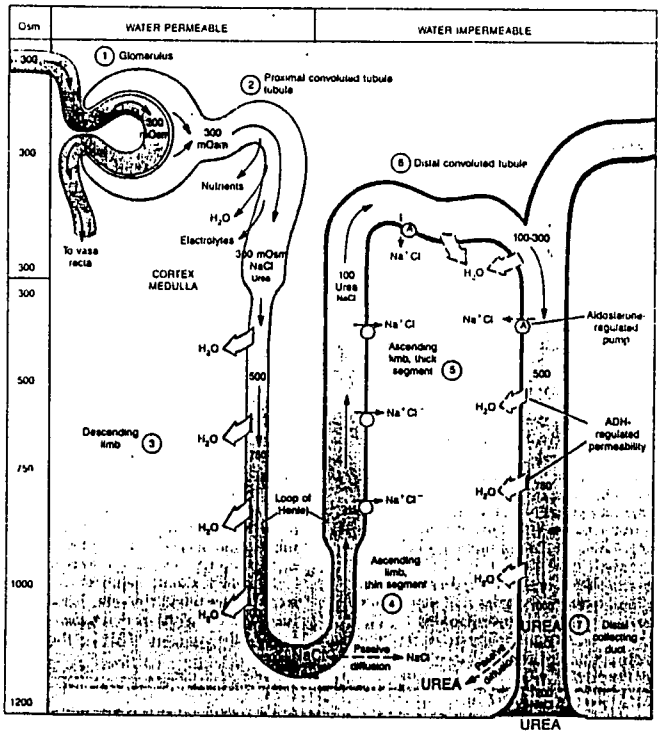

Figure 13: An overview of kidney function. (taken from Martini, 1989)

The descending limb of Henle is freely permeable to water and relatively impermeable to ions (Martini, 1989). Since the osmolality of the interstitial fluid increases with depth into the medulla, water is reabsorbed from this segment by osmosis. The ascending thin limb of Henle is impermeable to water and permeable to electrolytes. The ascending thick limb is also impermeable to water and actively reabsorbs sodium. Since the rate of active transport is proportional to the concentration, more sodium is reabsorbed in the deeper portion of the ascending limb than in the superficial portion of the ascending limb. This active transport aids in creating the osmotic gradient within the medullary interstitial fluid. By the time the tubular fluid reaches the next portion of the nephron, the distal convoluted tubule, the osmolality has fallen to 100 mosm.

Near the portion of the nephron where the afferent and efferent arterioles permeate the Bowman's capsule, the ascending limb of Henle ends and forms a tight bend that places a portion of the distal tubule in direct contact with the arterioles (see Figure 14). The cells of the distal tubule which contact the arterioles are known as the macula densa, and the associated smooth muscle cells in the wall of the afferent arteriole are called the juxtaglomerular cells. Together, the macula densa and the juxtaglomerular cells make up the juxtaglomerular apparatus, a secretory complex which releases renin and erythropoietin in response to a lowered blood pressure and/or lowered sodium concentration in the tubular fluid. Renin converts circulating angiotensinogen to angiotensin I which is converted to angiotensin II, a powerful vasoconstrictor, in the lung

capillaries. Angiotension II also increases the secretion rates of ADH and aldosterone. The renin-angiotensin system is shown in Figure 15. Erythropoietin stimulates the formation of red blood cells in the bone marrow and therefore maintains or in some cases increases the oxygen carrying capacity of the blood.

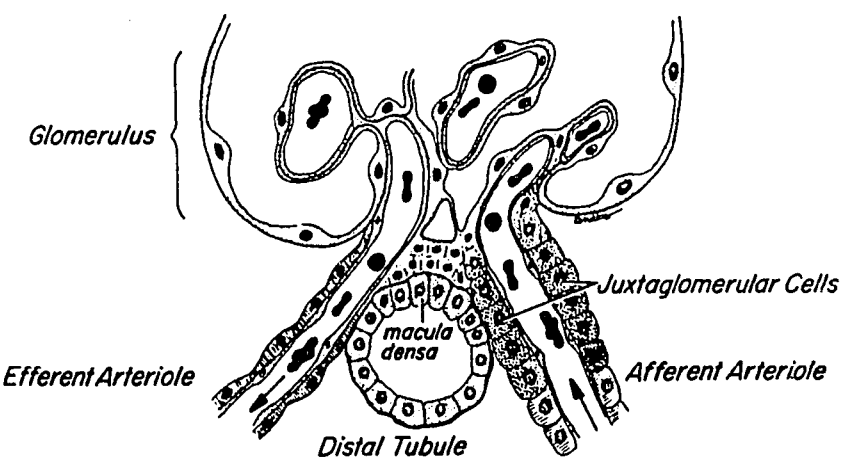

Figure 14: The juxtaglomerular apparatus. (taken from Brown & Stubbs, 1983)

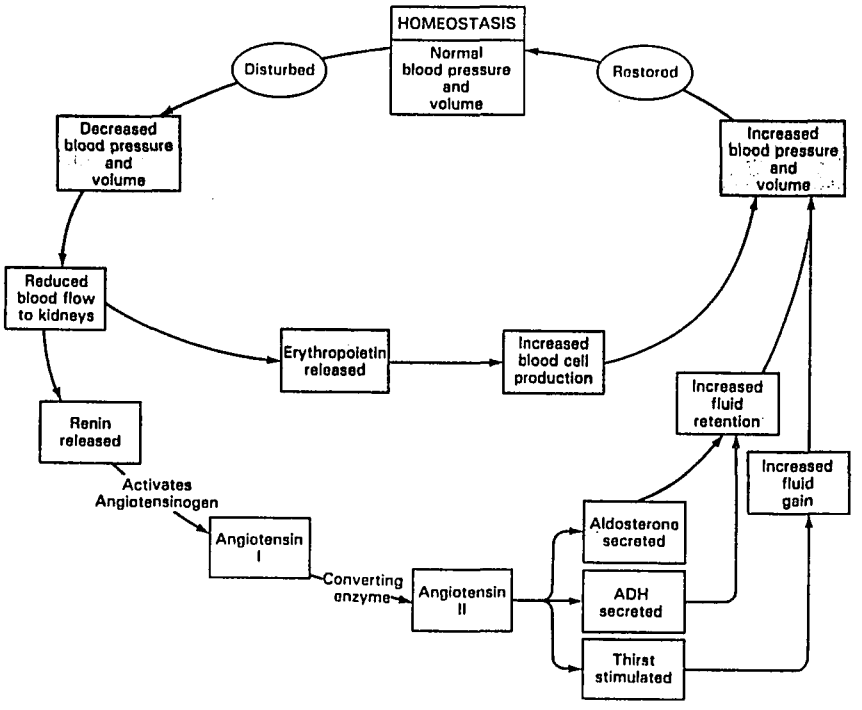

Figure 15: The renin-angiotensin system. (taken from Martini, 1989)

The distal convoluted tubule, collecting tubule, and collecting duct are essentially impermeable to water unless ADH is present in the body fluids. ADH in the interstitial kidney fluid binds to receptors located in the basal membranes of cells in these portions of the nephron (see Figure 16). This coupling of receptor and ADH activates adenyl cyclase, an enzyme associated with the cell membrane, which catalyzes the production of cyclic adenosine monophosphate (cAMP) (Sullivan, 1982). Although the mechanism in not completely established, the rise in intracellular cAMP results in the insertion of vesicles containing water channels into the apical membrane of the cell (Koeppen & Stanton, 1992). In high concentrations, ADH increases the amount of water absorbed in these nephron segments,

thereby causing the formation of a concentrated urine. Conversely, in the absence of ADH, large amounts of a dilute urine will be formed.

The reabsorption of sodium from the tubular fluid within the distal convoluted tubule, collecting tubule, and collecting duct is controlled by the hormone aldosterone, which is secreted from the adrenal gland when plasma levels of angiotensin II or potassium are elevated. Aldosterone stimulates ion pumps in these portions of the nephron, which then exchange sodium ions for potassium ions. Therefore, aldosterone increases the urinary loss of potassium while reducing this loss of sodium.

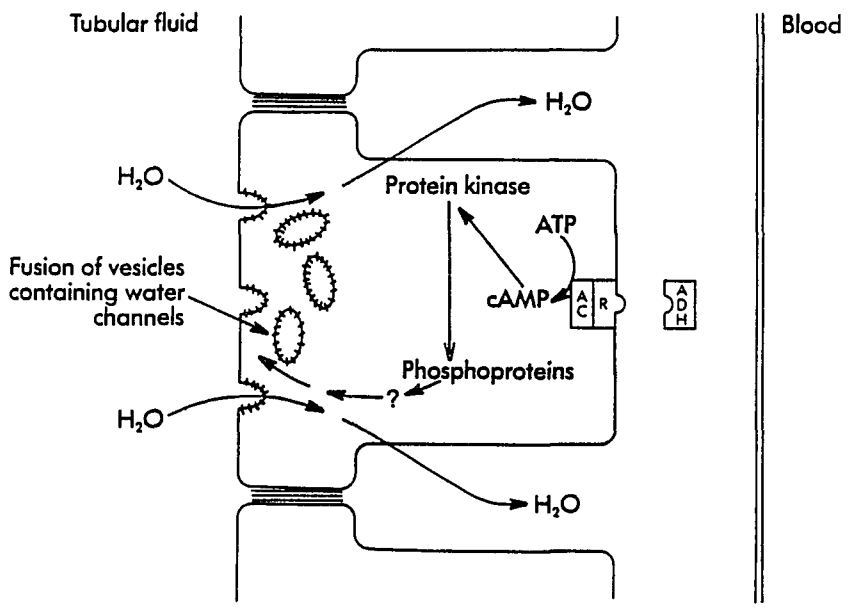

Figure 16: The binding of ADH to cells of the distal tubule and collecting duct. R, ADH receptor; AC, adenyl cyclase. (taken from Koeppen & Stanton, 1992)

Sodium accounts for over 90% of the cations in the extracellular fluid (Guyton, 1984). Due to electroneutrality of the extracellular fluid, the amount of cations automatically controls the number of anions present, so by regulating the concentration of sodium, over 90% of the ions are also controlled. Since the ions account for most of the dissolved species in the bodily fluids, the concentration of sodium is directly related to the fluid osmolality. Therefore, in terms of regulating the body fluid compartments, the renal handling of water and sodium will be the most important factors to consider when modeling kidney function.

In regulating the body fluid compartments, volume is controlled primarily by the arterial pressure, sodium concentration primarily by anti-diuretic hormone, and potassium levels primarily by aldosterone (Guyton & Young *in* Guyton, Taylor, and Granger, 1975). Increasing the arterial pressure slightly increases renal blood flow and the glomerular filtration rate, however, the urine flow rate can be greatly increased. Furthermore, urine production may cease altogether if the arterial pressure falls below 60 mm Hg. The variations of renal blood flow, GFR, and urine flow are shown as a function of arterial pressure in Figure 17. A depleted blood volume, which causes a drop in blood pressure, will decrease urine flow and tend to alleviate the problem. Alternatively, an expanded blood volume, which causes an elevated blood pressure, will increase the urine flow rate thereby decreasing the blood volume.

The secretion rate of ADH and the thirst center response are strongly related to the plasma osmolality. A change in plasma osmolality of 1%

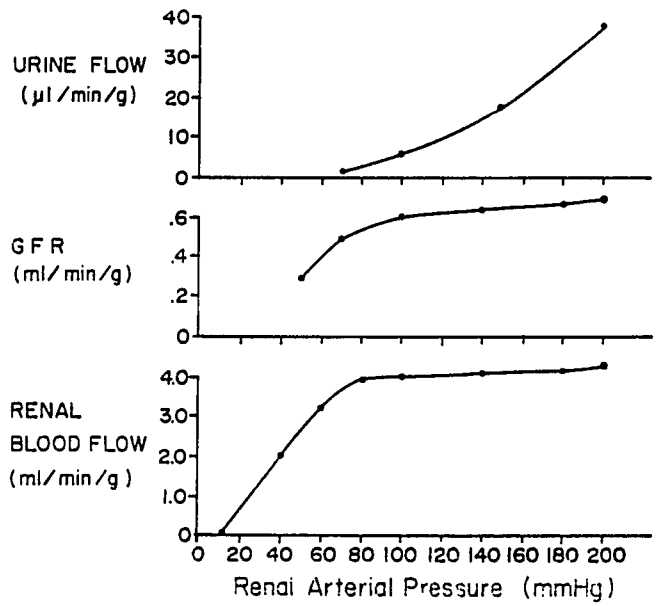

Figure 17: Effect of acute changes in arterial pressure on the important hemodynamic variables of renal function that relate to renal volume excretion. (taken from Navar & Guyton, 1975)

doubles the plasma level of ADH, and the thirst center is stimulated when the plasma osmolality changes 1 to 2% (Cowley *in* Guyton, Taylor, and Granger, 1975). An elevated plasma level of ADH is usually believed to increase the blood volume by reducing the urinary water loss and increasing the amount of water ingested. Increasing the plasma ADH level initially will increase the blood volume, but only by a small extent because of the associated increase in arterial pressure and urine flow rate (see Figure 17). The urine which is formed will have a high solute to water ratio. Consequently, persistently high levels of ADH will cause a slight increase in the blood volume but will also decrease the plasma osmolality due to a high

flow rate of concentrated urine. Since sodium is responsible for about 90% of the plasma osmolality, ADH primarily affects the sodium concentration of the extracellular fluid.

Aldosterone causes cells in the later portion of the nephron to absorb sodium from the tubular fluid with the simultaneous secretion of potassium. It would therefore be expected that aldosterone would control the sodium and potassium levels in the extracellular fluid. However, previous studies have found that aldosterone plays about ten times as much role in the control of potassium concentration as in the control of sodium ion concentration (Guyton & Young *in* Guyton, Taylor, and Granger, 1975). The reason for this is that the ADH-thirst mechanism is a very potent mechanism for control of sodium ion concentration, so potent that the aldosterone mechanism, in competing with this more potent mechanism, is indeed a very poor competitor (Guyton & Young *in* Guyton, Taylor, and Granger, 1975).

Since sodium accounts for over 90% of the cations in the extracellular fluid, and the number of cations is balanced by the number of anions, considering only the renal handling sodium and water should sufficiently describe the relationship between the plasma compartment and kidneys. The following mathematical description has been adapted from a previous model of normal renal function in man (Uttamsingh, Leaning, Bushman, Carson, & Finkelstein, 1985).

Cardiovascular System

The cardiovascular system consists of a pump, the heart, an assortment of conducting channels, the vessels, and a flowing fluid, the blood. These components are illustrated in Figure 18. Arteries carry blood away from the heart and veins return blood to the heart. The blood vessels, which make up the circulatory system, can be sub-divided into two parts. Pulmonary vessels bring blood to and from the lungs whereas systemic vessels service the rest of the body.

Blood pressure, which affects the glomerular filtration rate, is directly related to the blood volume. An increased blood volume increases the cardiac output and, consequently, the blood pressure. Additionally, an increased blood volume stretches elastic fibers located in the vessel walls causing the fibers to contract more powerfully and elevate the blood pressure. A decreased blood volume causes the opposite effects. The experimental relationship between the blood volume, V_{bl}, and the mean systemic pressure, $P_{m,s}$, can be described by

$$P_{m,s} = 3.5(V_{bl} - 3) \qquad (3)$$

where the mean systemic pressure is the average pressure within the blood vessels from the root of the aorta to the end of the great veins and has a typical value of 7 mm Hg (Uttamsingh, Leaning, Bushman, Carson, & Finkelstein, 1985).

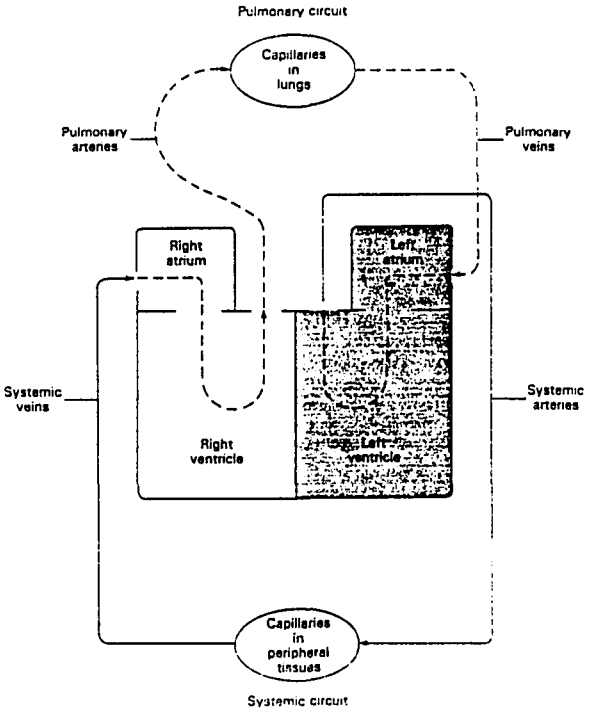

Figure 18: The cardiovasular system. (taken from Martini, 1989)

The mean systemic pressure is also called the mean filling pressure since it is the average effective pressure of the blood in the peripheral circulation that tends to promote return of blood toward the heart (Guyton, 1976). Experiments have demonstrated that the rate of blood flow from the systemic vessels through the veins to the heart is directly proportional to the systemic filling pressure minus the right atrial pressure (Guyton, 1976). The right atrial pressure usually remains at about 0 mm Hg except under very extreme conditions such as heart failure or massive blood transfusion. Therefore, the rate of blood return to the heart, which is equal to the cardiac output, should be approximately proportional to the mean systemic pressure. Since blood flow is zero when the mean systemic pressure is zero

and the cardiac output is about 5 liters per minute when the mean systemic pressure is 7 mm Hg, a linear relationship can be used as an approximation.

$$CO = 0.7\ (P_{m,s}) \tag{4}$$

where CO is the cardiac output and is about 5 liters/minute at rest.

Since angiotensin II is a powerful vasoconstrictor, it will influence the peripheral resistance, which is the resistance to blood flow caused by friction with the vessel walls. Short term, neural control of vascular tone is neglected in this model. The relationship between the resistance of the entire circulatory system, or total peripheral resistance ($R_{t,p}$), and the plasma level of angiotensin II [A] can be approximated for humans by the following equations (Uttamsingh, Leaning, Bushman, Carson, & Finkelstein, 1985). It should be noted that small arteries and arterioles are the principal site of the peripheral resistance.

$$R_{t,p} = 19 + 0.037[A] \qquad \text{for } [A] \leq 27 \text{ ng/l} \tag{5}$$

$$R_{t,p} = 12.2 + 5.44 \log[A] \qquad \text{for } [A] > 27 \text{ ng/l} \tag{6}$$

The simplest relationship between flow and resistance is analogous to Ohm's law for electrical circuits where I = V/R in which I is the current flow,

V is the voltage, and R is the resistance of the circuit. The analogy for flow through a hydraulic circuit is given by

$$\text{Flow} = \frac{\Delta P}{\text{Resistance}} \tag{7}$$

Poiseuille's law, which is given by equation 8, is an example of this type of equation. $\mathcal{Q}$ represents the flow rate (volume/time) and the resistance is given by $\frac{8\mu L}{\pi R^4}$. Poiseuille's law is valid for steady, uniform, and laminar flow where the fluid is Newtonian and incompressible and the no-slip condition is valid.

$$\mathcal{Q} = \frac{\pi R^4}{8\mu L}\Delta P \tag{8}$$

In considering the entire systemic circuit, the flow rate would be the cardiac output, ΔP is the difference between the arterial and venous pressure, and the peripheral resistance would be given by equations 5 and 6. Since the venous pressure is close to zero, the following relationship for the arterial pressure (P_{ar}) can be derived from equation 7. From the conditions given for the validity of Poiseuille's law, it can be seen that this equation will only be an approximation when considering flow in blood vessels.

$$P_{ar} = CO(R_{t,p}) \tag{9}$$

Renal Function

The nephron segments considered by the model, and the corresponding flows of sodium and water, are illustrated in Figure 19.

Glomerular function The forces which control the filtration of plasma fluid into Bowman's capsule include the capillary hydrostatic pressure and capsular oncotic pressure, which force fluid into the capsular space, and the plasma oncotic pressure and capsular hydrostatic pressure, which force fluid into the arterioles. These latter three pressures remain relatively constant under normal physiological conditions, therefore, the glomerular filtration rate will depend mainly upon the pressure within the arterioles. The following relationship between the arterial pressure and glomerular filtration rate has been previously determined (Goldstein & Rypins, 1992).

$$GFR = 4.50 - 1.62P_{ar} + 0.100(P_{ar})^2 - 1.2\times10^{-3}(P_{ar})^3 + 5.73\times10^{-6}(P_{ar})^4 - 9.89\times10^{-9}(P_{ar})^5 \quad (10)$$

Chemical analysis of glomerular filtrate has found that it has approximately the same sodium concentration as plasma (Uttamsingh, Leaning, Bushman, Carson, & Finkelstein, 1985) so the rate of filtration of sodium into the proximal tubule ($F_{Na,PT}$) is given by

$$F_{Na,PT} = GFR[Na_{pl}] \quad (11)$$

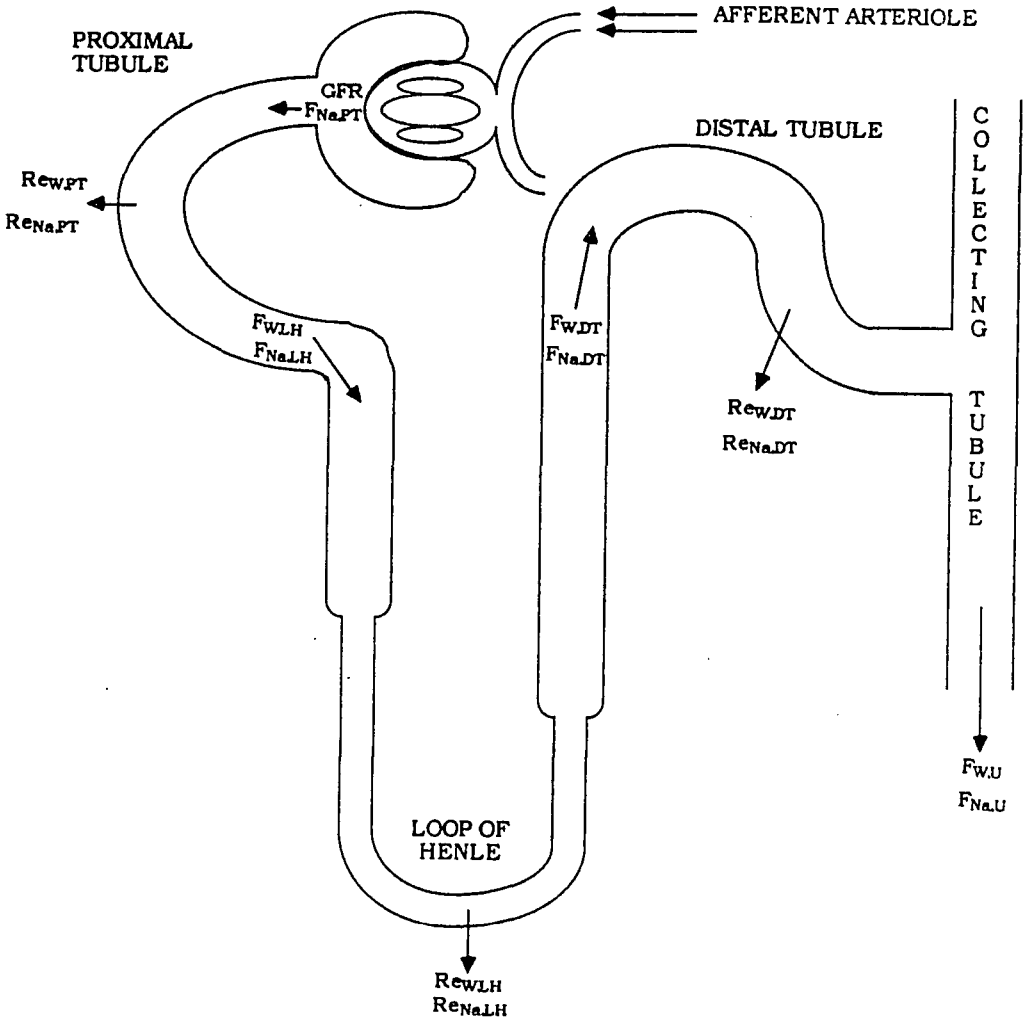

Figure 19: Nephron segments and associated flow rates of sodium and water.

Proximal tubule Electrolytes are actively reabsorbed in this portion of the nephron. The rate of sodium reabsorption ($Re_{Na,PT}$) can be described by an active transfer coefficient multiplied by the sodium concentration of the tubular fluid.

$$Re_{Na,PT} = GTB(F_{Na,PT}) \quad (12)$$

where GTB is the glomerular tubular balance or active transfer coefficient. Through micropuncture techniques, where micropipets are inserted into a nephron and the tubular fluid analyzed, this coefficient is known to be a function of the sodium concentration of the tubular fluid. Since the concentration of sodium in the proximal tubule is nearly equal to the concentration of sodium in the plasma $[Na_{pl}]$, the following linear relationship has been previously derived as a first-order approximation (Uttamsingh, Leaning, Bushman, Carson, & Finkelstein, 1985).

$$GTB = 5.815 - 0.0357[Na_{pl}] \quad (13)$$

As electrolytes are pumped out of this portion of the tubule, water follows by osmosis. Sodium makes up the majority of the cations in the filtered fluid, and as sodium is removed from the tubule, negatively charged ions follow due to an electrical gradient. The fraction of water reabsorbed in the proximal tubule will be nearly equal to the fraction of sodium reabsorbed.

$$Re_{W,PT} = GTB(GFR) \quad (14)$$

where $Re_{W,PT}$ is the rate of water reabsorption in the proximal tubule. From equations 12 and 14, the flow rates of sodium ($F_{Na,LH}$) and water ($F_{W,LH}$) into the loop of Henle can be determined.

$$F_{Na,LH} = F_{Na,PT} - Re_{Na,PT} \quad (15)$$

$$F_{W,LH} = GFR - Re_{W,PT} \quad (16)$$

Loop of Henle Examinations of the reabsorptive characteristics of sodium and water for the entire loop have demonstrated that the fraction of water reabsorbed ($FRe_{W,LH}$) is a function of transit time, or an inverse function of flow rate, whereas the fraction of sodium reabsorbed remains fairly constant with flow rate. The following relationships for the rate of reabsorption of sodium ($Re_{Na,LH}$) and water ($Re_{W,LH}$) have been derived for this portion of the nephron (Uttamsingh, Leaning, Bushman, Carson, & Finkelstein, 1985).

$$FRe_{W,LH} = -0.01F_{W,LH} + 0.65 \quad (17)$$

$$Re_{W,LH} = FRe_{W,LH}(F_{W,LH}) \quad (18)$$

$$Re_{Na,LH} = 0.8F_{Na,LH} \quad (19)$$

The flow rate of water ($F_{W,DT}$) and sodium ($F_{Na,DT}$) into the distal tubules is given by

$$F_{W,DT} = F_{W,LH} - Re_{W,LH} \quad (20)$$

$$F_{Na,DT} = F_{Na,LH} - Re_{Na,LH} \quad (21)$$

Distal and collecting tubules In these portions of the nephron, the amount of water reabsorbed is controlled by antidiuretic hormone (ADH) and the amount of sodium reabsorbed by aldosterone (ALD). Using data from previous experiments, relationships for the rate of water reabsorbed ($Re_{W,DT}$) and the rate of sodium reabsorbed ($Re_{Na,DT}$) have been derived (Uttamsingh, Leaning, Bushman, Carson, & Finkelstein, 1985 and Goldstein & Rypins, 1992).

$$Re_{W,DT} = 0.0 \quad \text{for } [ADH] \leq 0.765 \quad (22)$$

$$Re_{W,DT} = F_{W,DT}\,(0.383ADH - 0.293) \quad \text{for } 0.765 < [ADH] \leq 3.0 \quad (23)$$

$$Re_{W,DT} = F_{W,DT}\,(-0.0383[ADH]^2 + 0.364[ADH] + 0.109) \quad \text{for } 3.0 < [ADH] \leq 5.0 \quad (24)$$

$$Re_{W,DT} = F_{W,DT}\,(0.0012[ADH] + 0.9653) \quad \text{for } 5.0 < [ADH] \quad (25)$$

Where the maximum effective concentration of anti-diuretic hormone is 7.2 mu/l (Sullivan, 1982).

$$Re_{Na,DT} = F_{Na,DT}(0.003[ALD] + 0.596) \quad \text{for } 0 \leq [ALD] \leq 85 \quad (26)$$

$$Re_{Na,DT} = F_{Na,DT}(0.00021[ALD] + 0.833) \quad \text{for } 85 < [ALD] \leq 800 \quad (27)$$

$$Re_{Na,DT} = F_{Na,DT} \quad \text{for } [ALD] > 800 \quad (28)$$

Urine flow ($F_{W,U}$) is then given by

$$F_{W,U} = F_{W,DT} - Re_{W,DT} \quad (29)$$

and the urinary excretion rate of sodium ($F_{Na,U}$) is given by

$$F_{Na,U} = F_{Na,DT} - Re_{Na,DT} \quad (30)$$

Note that these equations predict that ADH can produce large percentage changes in fluid reabsorption whereas aldosterone has only a small modulating effect on sodium reabsorption. This agrees with the discussion at the end of the previous section (Description of the urinary system) which stated that ADH is the primary controller of sodium in the extracellular fluid and the urinary sodium excretion rate. However, a full analysis requires the inclusion of aldosterone.

Hormonal Systems

Having derived equations for the reabsorption of sodium and water in the latter portions of the nephron, which depend upon ADH and

aldosterone, the levels of these hormones must now be estimated.

Control of ADH concentration Plasma ADH concentration is determined by three factors: the rate of ADH release from the posterior pituitary gland which depends upon signals from osmoreceptors and stretch receptors, the rate of clearance of ADH from the body by the liver and kidneys, and the volume in which the ADH is dispersed. As seen in Figure 8, plasma ADH levels, and consequently the ADH release rate, increase as plasma osmolality increases and blood volume decreases. Equations for ADH secretion as a function of plasma sodium ($S_{ADH,P}$) (Sullivan, 1982) and extracellular compartment volume ($S_{ADH,V}$) (Uttamsingh, Leaning, Bushman, Carson, & Finkelstein, 1985) have been derived from experimental data.

$$S_{ADH,P} = 0.2374[Na_{pl}] - 32.89 \quad \text{for } [Na_{pl}] \geq 138.5 \text{ mosm/l} \tag{31}$$

$$S_{ADH,P} = 0.0 \quad \text{for } [Na_{pl}] < 138.5 \text{ mosm/l} \tag{32}$$

$$S_{ADH,V} = 0.0 \quad \text{for } DV_E \geq 1.8 \tag{33}$$

$$S_{ADH,V} = 0.15 - 0.083DV_E \quad \text{for } 1.8 > DV_E \geq 1.0 \tag{34}$$

$$S_{ADH,V} = 0.813 - 0.75DV_E \quad \text{for } 1.0 > DV_E \geq -1.2 \tag{35}$$

$$S_{ADH,V} = 1.71 \quad \text{for } -1.2 > DV_E \tag{36}$$

where DV_E is the deviation of the extracellular compartment volume (V_E) from the normal value ($V_{E,N}$).

$$DV_E = V_E - V_{E,N} \tag{37}$$

The signals for ADH release in response to variations in plasma osmolality and blood volume are additive if both signals tend to increase the ADH release rate (ie. increased plasma osmolality with decreased blood volume). However, if both the plasma osmolality and blood volume are above normal, the signal for blood volume will be the primary signal. Recall that volume overrides tonicity. For this case the net rate of ADH (S_{ADH}) release is given by the following equations (Uttamsingh, Leaning, Bushman, Carson, & Finkelstein, 1985).

$$S_{ADH} = \frac{17.0(DV_E)(S_{ADH,V}) + S_{ADH,P}}{17.0(DV_E) + 1.0} \tag{38}$$

for $OS_{pl} > 299.6$ mosm/l and $DV_E > 2.0$

$$S_{ADH} = \frac{\{33.0(DV_E) - 32.0\}(S_{ADH,V}) + S_{ADH,P}}{33.0(DV_E) - 31.0} \tag{39}$$

for $OS_{pl} > 299.6$ mosm/l and $1.0 \leq DV_E \leq 2.0$

For all other cases

$$S_{ADH} = \frac{S_{ADH,V} + S_{ADH,P}}{2.0} \tag{40}$$

The maximum secretion rate of ADH is 16.5 munits/min (Guyton, 1976).

The rate of clearance of ADH from the plasma (D_{ADH}) has been found to be related to the plasma concentration of ADH (Uttamsingh, Leaning, Bushman, Carson, & Finkelstein, 1985).

$$D_{ADH} = 0.206 \qquad \text{for [ADH]} > 4.0 \text{ munits/l} \qquad (41)$$

$$D_{ADH} = 0.374 - 0.042\,[ADH] \qquad \text{for [ADH]} \leq 4.0 \text{ munits/l} \qquad (42)$$

where the clearance rate of a substance is a fictitious amount of blood completely cleared of the substance per unit time. In reality, a particular substance cannot be completely removed from the blood as it passes through the kidneys, however, the clearance value can be useful in many calculations. The clearance rate of 0.206 l/min, which is given for ADH in equation 41, means that the amount of ADH which is being removed from the entire blood supply is equivalent to removing ADH completely from 0.206 liter of blood each minute.

Previous studies have found that ADH is distributed within a volume equivalent to two thirds of the extracellular volume (Cowley, 1975). A material balance on ADH yields

$$0.67(V_E)\frac{d[ADH]}{dt} = S_{ADH} - D_{ADH}[ADH] \qquad (43)$$

Control of aldosterone concentration Aldosterone release is one of the final consequences of the renin/angiotensin system, the function of which is to provide feedback control on the rates of sodium and potassium excretion, and thereby to influence the volume of the extracellular and intracellular compartments (see Figure 15). In absence of more explicit data, a linear relationship has been postulated for the rate of renin release (S_R) as a function of the amount of sodium entering the distal tubule (Uttamsingh, Leaning, Bushman, Carson, & Finkelstein, 1985).

$$S_R = 0.0163 - 0.0093F_{Na,DT} \tag{44}$$

This equation is consistent with the fact that the macula densa, which secretes renin into the plasma compartment, monitors fluid within the distal tubule. Renin is distributed in a volume approximately equal to the plasma volume and is removed from the circulation on passage through the liver (Uttamsingh, Leaning, Bushman, Carson, & Finkelstein, 1985). From steady state considerations, where $\frac{d[R]}{dt} = 0$, the clearance of renin can be found to be 0.143 l/min. A material balance on renin yields

$$(V_{pl})\frac{d[R]}{dt} = S_R - 0.143[R] \tag{45}$$

where [R] is the plasma concentration of renin.

Renin catalyses the reaction which converts circulating angiotensinogen to angiotensin I. Angiotensin I is rapidly converted to

angiotensin II by enzymes in the lungs. The following equation has been derived for the rate of formation of angiotensin II (S_A) (Uttamsingh, Leaning, Bushman, Carson, & Finkelstein, 1985).

$$S_A = 583.3[R](V_{pl}) \tag{46}$$

Angiotensin II is confined mainly to the plasma compartment (Uttamsingh, Leaning, Bushman, Carson, & Finkelstein, 1985) and the steady state rate of clearance for this hormone can be found to be 3.78 l/min. A material balance on angiotensin II yields

$$(V_{pl})\frac{d[A]}{dt} = S_A - 3.78[A] \tag{47}$$

The major factor which regulates the release of aldosterone from the adrenal gland is the plasma concentration of angiotensin II. From previous animal studies, the following relationships for the rate of aldosterone release (S_{ALD}) as a function of plasma angiotensin II concentration have been derived (Uttamsingh, Leaning, Bushman, Carson, & Finkelstein, 1985).

$$S_{ALD} = 0.75[A] + 7.76 \quad \text{for } [A] < 18 \text{ ng/l} \tag{48}$$

$$S_{ALD} = 3.32[A] - 38.5 \quad \text{for } 18 \leq [A] < 34.0 \tag{49}$$

$$S_{ALD} = 0.585[A] + 54.6 \quad \text{for } [A] \geq 34.0 \tag{50}$$

From the steady state situation, the clearance rate of aldosterone from the plasma can be found to be 0.602 l/min which leads to the following material balance.

$$(V_{pl})\frac{d[ALD]}{dt} = S_{ALD} - 0.602[ALD] \tag{51}$$

Sodium and Potassium Balance

The overall model of the body water compartments is concerned mainly with water and sodium, since sodium ions account for almost 95% of the cations in the extracellular fluid. The present model will assume that the extracellular potassium concentration remains constant at a typical value of 4 meq/l. The time-average daily ingestion rate of sodium (IN_{Na}) and the urinary excretion rate of sodium ($F_{Na,U}$) will determine the amount of sodium in the extracellular fluid ($Na_{TOT,E}$).

$$\frac{d[Na_{TOT,E}]}{dt} = In_{Na} - F_{Na,U} \tag{52}$$

Since cellular membranes are relatively impermeable to electrolytes when compared to water, the amount of sodium in the intracelluar fluid will remain constant.

$$\frac{d[Na_{TOT,I}]}{dt} = 0 \tag{53}$$

The concentration of sodium in the extracellular compartment [Na_{pl}] and the intracellular compartment [Na_I)]will then be given by

$$[Na_{pl}] = \frac{Na_{TOT,E}}{V_E} \tag{54}$$

$$[Na_I] = \frac{Na_{TOT,I}}{V_I} \tag{55}$$

where V_E is the extracellular fluid volume and V_I is the intracellular fluid volume.

Total body water balance A mass balance on total body water (V_W) gives

$$\frac{dV_w}{dt} = In_W - F_{W,U} - F_{W,P} \tag{56}$$

where IN_W is the flow rate of water into the body, which includes water entering from the intestine and metabollically produced water, and $F_{W,P}$ is water lost through perspiration. Water absorbed by the intestine enters the plasma or extracellular compartment whereas metabolically produced water is formed in the intracellular compartment. For an average diet, about 0.133 grams of water is formed for every kcal of energy produced (McArdle, Katch, & Katch, 1985). Water lost as a result of urine production $F_{W,U}$, accounts for almost all of the water lost from the body in a thermally neutral environment. In the following section, $F_{W,P}$ is estimated but considered insignificant for the calculations made in this section.

Assuming instantaneous osmotic equilibration between the intracellular and extracellular compartments

$$\frac{Na_{TOT,E} + OT_E}{V_E} = \frac{Na_{TOT,I} + OT_I}{V_I} \tag{57}$$

where OT_E and OT_I are constants which represent the other dissolved species within the extracellular and intracellular compartments, respectively. The assumption of instantaneous osmotic equilibrium between the extracellular and intracellular compartments can be tested from the mass transfer coefficient given in Figure 3 ($K = 3.0\mu^3/m^2 \cdot atm$). A maximum water loss from the extracellular compartment would be about 9.3 ml/min which includes 1 ml/min lost from the kidneys and 8.3 ml/min lost via perspiration. The osmotic pressure of each compartment is given by

$$\pi = nRT/V_m \tag{58}$$

where n is the moles of dissolved species, R is the gas constant, T is the temperature, and V_m is the volume of pure solvent. The driving force for water movement from the intracellular compartment to the extracellular compartment is the osmotic pressure difference between these compartments, $\Delta\pi$. Using the mass transfer coefficient and assuming a water loss of 9.3 ml/min, the volume of the extracellular and intracellular compartments can be calculated along with the osmotic pressure of each compartment. This computation is shown in Figure 20.

Figure 20 shows that the osmotic pressure of the intracellular compartment is nearly the same as that of the extracellular compartment with the difference being less than a tenth of a percent. Therefore the assumption of osmotic equilibrium is valid.

Since $V_W = V_E + V_I$, the size of the intracellular and extracellular compartments can be derived from equation (57).

$$V_E = \frac{V_W}{1 + \frac{Na_{TOT,I} + OT_I}{Na_{TOT,E} + OT_E}} \tag{59}$$

$$V_I = \frac{V_W}{1 + \frac{Na_{TOT,E} + OT_E}{Na_{TOT,I} + OT_I}} \tag{60}$$

Testing the Kidney Model

To test the validity of the proposed kidney model, results predicted by the model will be compared to actual data involving injected or ingested fluids and subsequent urine flow rates. Under these conditions, water enters the body through the plasma compartment and leaves the body through the formation of urine. Intravenously injected fluids enter the plasma compartment immediately whereas ingested fluid must first be absorbed by the intestines. The rate constant for water absorption from the gastrointestinal tract has been estimated to be 3.33 liters/hour (see Figure

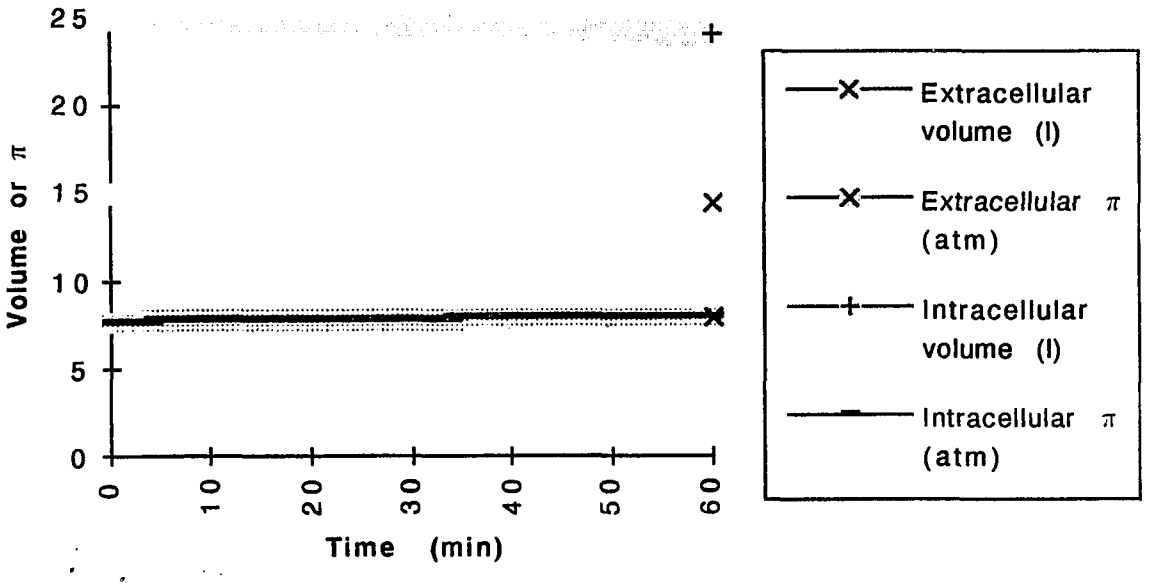

Figure 20: Extracelluar and intracellular compartment volumes (liter) and the osmotic pressure of each compartment (atm) when 9.3 ml/min of water is withdrawn from the extracellular compartment.

through sensible and insensible perspiration should be relatively small and will be neglected in these cases. Water loss through perspiration is considered in more detail in following sections.

Steady state urinary losses and hormone levels are shown in Figures 21 and 22. Comparison of the model simulation to actual data following the ingestion of 1 liter of water is shown in Figure 23. Assuming a zero order rate constant of 3.33 liters/hour for the absorption of water from the intestines most likely contributed some error in this figure. In Figure 24, the model simulation is shown with actual data for the intravenous infusion

of hypertonic saline. Using a 10% aqueous solution, 0.91 g/kg body weight of NaCl was infused during the first 65 minutes of this experiment.

The model results shown in Figures 21, 22, 23, and 24, were calculated by writing a computer program using the previously given model equations. The program was written using Macintosh Extend software. Integrations of the mass balances were carried out with this software by using one time step per minute.

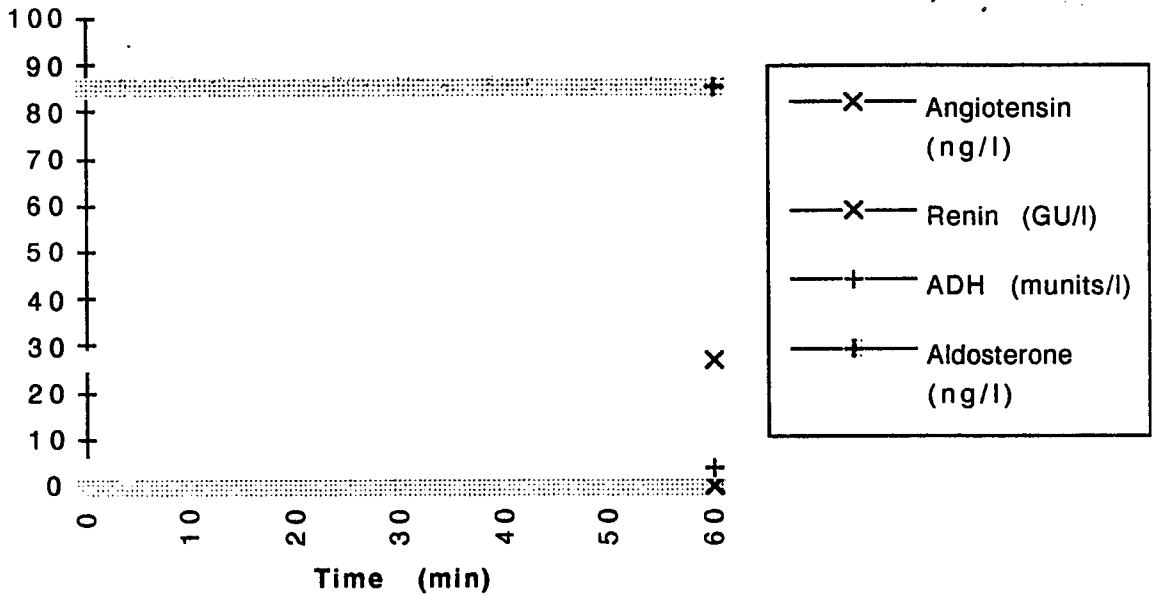

Figure 21: Steady state hormone levels.

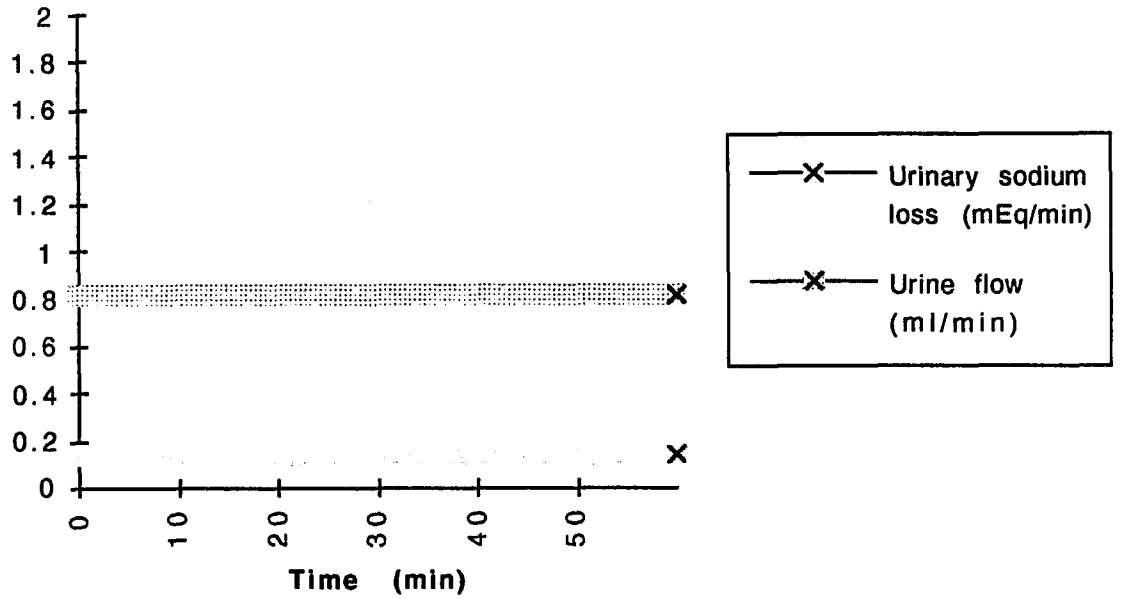

Figure 22: Steady state urinary loss of water and sodium.

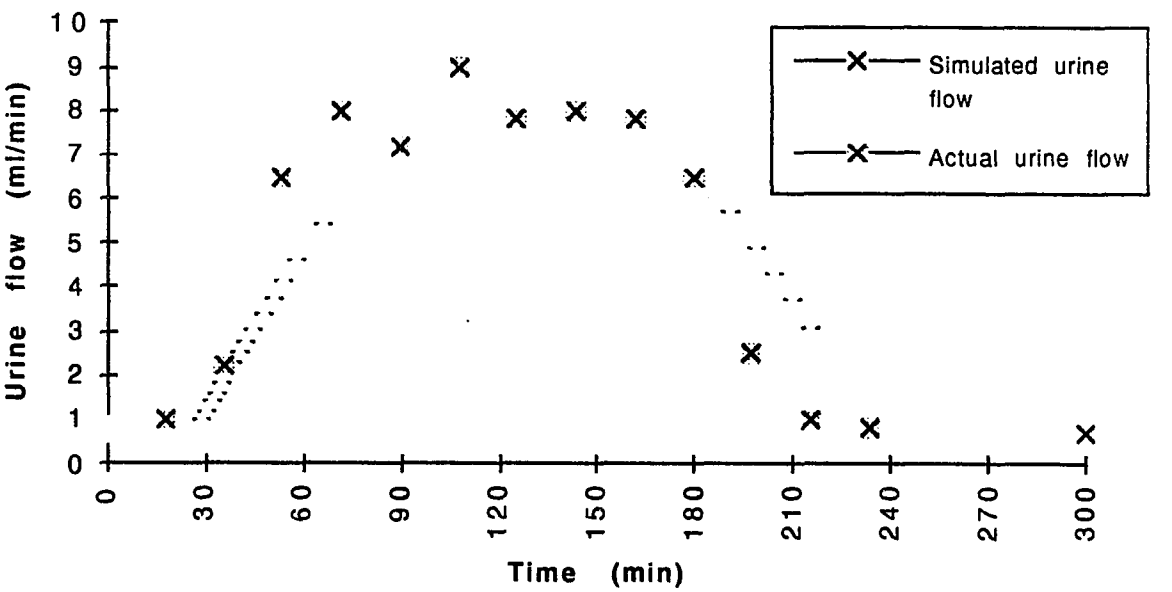

Figure 23: Results from the model simulation and experimental data following ingestion of 1 liter of water. (actual data taken from Baldes & Smirk, 1934)

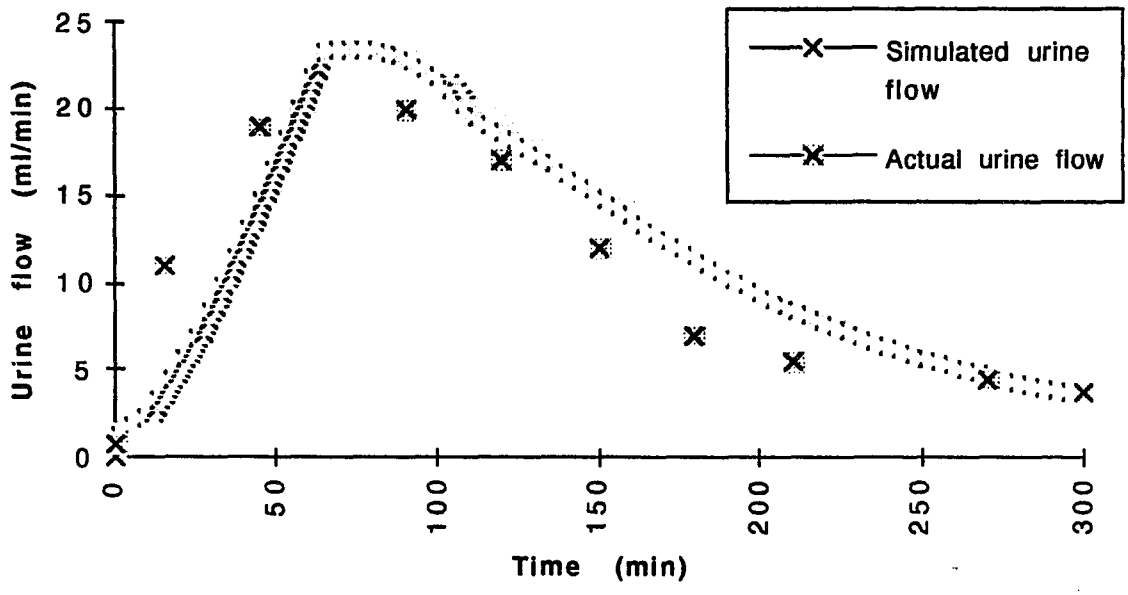

Figure 24: Results from the model simulation and experimental data with the infusion of 9.8 g/min of a 10% NaCl solution during the first 65 minutes of the experiment. (actual data taken from Dean & McCance, 1949)

MODELING THERMOREGULATION

The evaporation of perspiration from the skin's surface has a cooling effect on the skin. When constructing mass and energy balances around the body, it can be seen that through this mechanism, the water mass balance will be coupled to the energy balance. Therefore, a thorough consideration of the human water balance must include the overall energy balance. The following sections describe perspiration and how the perspiration rates fit into the overall human energy and mass balances.

Insensible Perspiration

Insensible perspiration includes water which is lost from the skin and lungs by diffusion and evaporation. Although skin is water resistant, it is not water proof, and interstitial body water slowly diffuses to the skin's surface where it evaporates into the air. Water also evaporates from the respiratory system as inhaled air is humidified to protect the lungs. The amount of water lost from the system can be determined if the water content of the incoming air is known since the outgoing air is approximately saturated at body temperature. A model for describing the insensible water loss from the skin is given below.

The skin behaves as if it consists of two layers, each of which have different diffusion properties. Previously, the percutaneous absorption of liquids and gases has been mathematically described by modeling the skin

as a composite membrane (Scheuplein, 1978 and Cussler, 1984).

The upper portion of skin which resists the diffusion of materials can be divided into three layers: the papillary dermis, the viable epidermis, and the stratum corneum. These three layers act in series to constitute a composite membrane. For an adult, the portion of the upper papillary dermis which resists the diffusion of water is approximately 150 μm thick (Scheuplein , 1978). The thickness of the viable epidermis and the stratum corneum is 40.7 μm and 9.3 μm, respectively (Holbrook, 1982). Since the diffusivity of water in the stratum corneum is 3 to 4 orders of magnitude less than that for the viable epidermis and papillary dermis, these latter hydrated layers can be treated as one phase and described with a single diffusivity (Scheuplein, 1978). This model is illustrated in Figure 25.

It has been shown that the transfer of isotopic water is linear with the gradient over a fivefold range in concentration difference (Parmley and Seeds, 1970). Assuming a steady state situation, Fick's first law of diffusion may be applied to each layer yielding:

$$j_1 = D_1\left[\frac{(C_0-C_1)}{(\delta_{PD} + \delta_{VE})}\right] \tag{61}$$

$$j_2 = D_2\left[\frac{(C_1-C_2)}{\delta_{SC}}\right] \tag{62}$$

eliminating C_1 by recognizing that $j_1=j_2$:

$$j = \frac{(C_0 - C_2)}{\left[\frac{(\delta_{PD}+\delta_{VE})}{D_1} + \frac{\delta_{SC}}{D_2}\right]} \qquad (63)$$

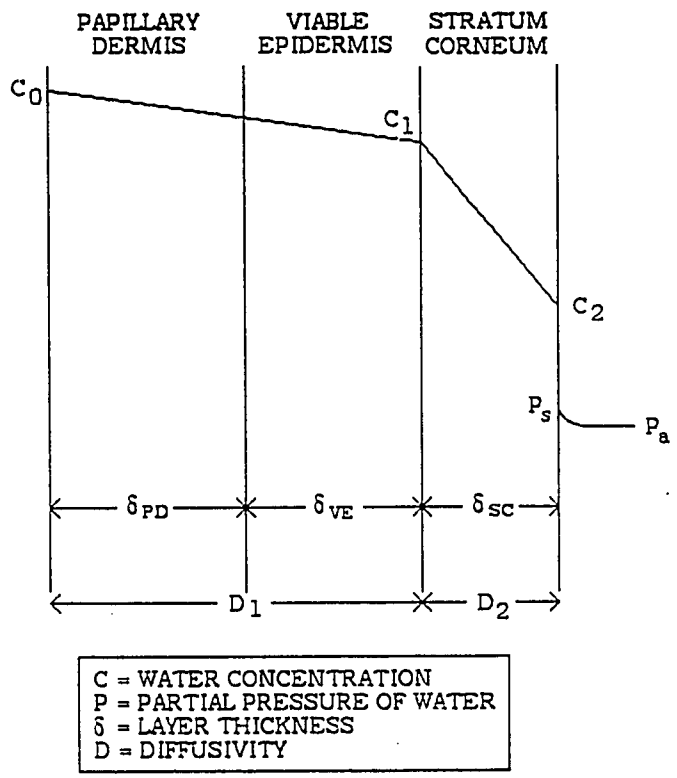

Figure 25: Skin as a composite membrane. (Adapted from Scheuplein, 1978)

The diffusivity of water in the hydrated skin layer and the cornified layer has been determined from absorption experiments as a function of temperature (Scheuplein, 1978). It has been shown that the diffusivity of water through the skin is independent of the direction of flow (Parmley & Seeds, 1970 and Rothman, 1954). In other words, the diffusivity is the same regardless of whether the water is flowing from the skin's surface into

the dermis or from the dermis to the skin's surface. The diffusivity can be expressed as a function of temperature using an Arrhenius equation (Scheuplein, 1978) of the form:

$$D(T) = D_O \exp(-\frac{E_a}{RT}) \tag{64}$$

For the diffusion of water through hydrated stratum corneum, the activation energy is 15.7 kcal/mole and the reference diffusivity is 69.5 cm^2/s. The activation energy is about 4.70 kcal/mole and the reference diffusivity is 0.063 cm^2/s for the hydrated skin layer (Scheuplein, 1978).

To solve equation 63, the concentration of water in the papillary dermis (C_O) and at the surface of the skin (C_2) must be known. For an adult, C_O is about 0.879 g/cm^3 (Scheuplein & Blank, 1971). C_2, which varies with the ambient humidity, can be estimated from water vapor isotherms for excised stratum corneum (Scheuplein & Blank, 1971). In other words, the partial pressure of water at the air-skin interface is approximately equal to the partial pressure of water in the ambient air. These partial pressures can be related to C_2 with a partition coefficient where:

$$P_a \approx P_s = HC_2 \tag{65}$$

The partition coefficient or Henry's Law constant can be determined by calculating the slope of the water vapor isotherm. From a water vapor

isotherm constructed in a temperate environment (Blank, 1952), it can be found that H is 8.04×10^{-5} g H_2O per cm^3 air/g H_2O per cm^3 stratum corneum for a relative humidity between 40% and 70%.

The resistance to the diffusion of water can be calculated for the hydrated skin layer and the stratum corneum if the diffusivities and layer thicknesses are known. These resistances are shown in the denominator of equation 63. An additional resistance to the diffusion of water exists in the boundary layer of air at the skin's surface and can be expressed as a reciprocal of the mass transfer coefficient. Reasonable heat and mass transfer results can be obtained by assuming a cylindrical body shape while keeping the volume and surface area constant (Coffey & Seagrave, 1972). The mass transfer coefficient can then be determined from a correlation for flow past a single cylinder (McCabe, Smith, & Harriott, 1985). Expressing the flux of water in terms of the mass transfer coefficient:

$$j = k_c(P_s - P_a) \tag{66}$$

By combining equations 63, 65, and 66, C_2 and P_s can be eliminated and the following relationship is obtained:

$$j = \frac{(H C_0 - P_a)}{\left[\frac{H(\delta_{PD} + \delta_{VE})}{D_1} + \frac{H\delta_{SC}}{D_2} + \frac{1}{k_c}\right]} \tag{67}$$

When comparing the magnitude of the resistances in the denominator of equation 67, it can be found that the stratum corneum accounts for over 98% of the total resistance (Doty, 1992). Therefore, equation 67 can be simplified to give:

$$j = \frac{(HC_o - P_a)}{\frac{H\delta_{sc}}{D_2}} \tag{68}$$

Sensible Perspiration

There are two types of sweat glands present in the human body: apocrine and eccrine (see Figure 26). These glands consist of a coiled tube lined with sweat secreting epithelia and a duct which opens on the surface of the skin as a pore. Apocrine glands are associated with hair follicles and are found mainly in the underarms. These glands, which are stimulated by increased blood adrenalin levels, secrete a milky fluid in response to emotional or mental stress (Keele, Neil, & Joels, 1982).

Eccrine glands are generally found over the entire body but are mainly concentrated on the palms of the hand, soles of the feet, forehead, back, and neck. These glands respond to an elevated body temperature, via the sympathetic nervous system, by secreting a dilute aqueous solution of sodium chloride, urea, and lactic acid (Keele, Neil, & Joels, 1982). Eccrine glands are also responsible for perspiration which forms on the palms and soles due to emotional stress. The maximum rate of thermal sweat secretion

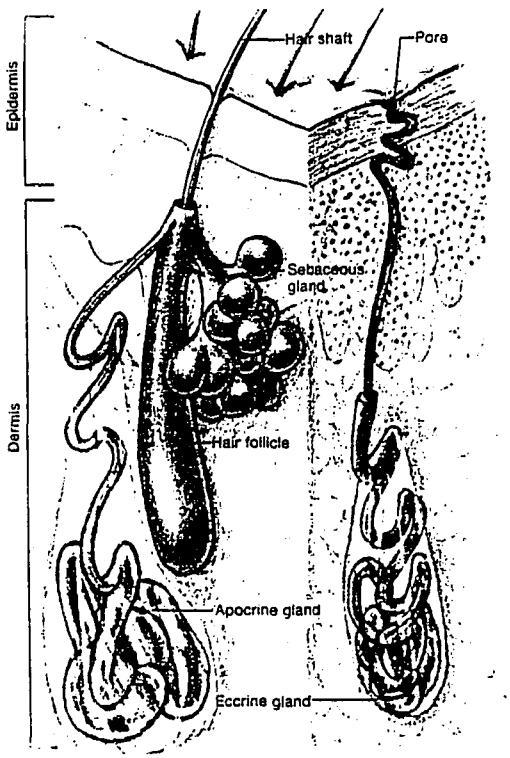

Figure 26: Apocrine and eccrine sweat glands. (taken from Hole, 1987)

can be as high as 12 liters per day (Keele, Neil, & Joels, 1982). Since sensible perspiration is mosty made up of eccrine gland secretions, only these sweat glands will be considered when describing sensible perspiration.

Water and electrolytes secreted by eccrine sweat glands initially come from the blood stream and therefore rapid sweating demands a large cutaneous blood flow (Keele, Neil, & Joels, 1982). The flow rate and composition of sweat depend upon epithelial cells which line both the coiled and duct portions of the gland. Cells which line the coil secrete a fluid similar to plasma into the lumen of the gland and the cells which line the

duct modifiy the primary secretion by reabsorbing sodium chloride (Quinton, 1988). Although sweat is almost always hypotonic to plasma, the final composition varies with the rate of flow. The concentrations of sodium and chloride normally range from 10-15 mEq/l at low rates to 40-50 mEq/l at high rates (Quinton, 1988). For comparison, the sodium and chloride concentrations in plasma are 145 mEq/l and 102 mEq/l, respectively. Assuming a simple linear relationship between sweat flow rate and sodium concentration, the following equation can be derived.

$$[Na_{,sw}] = 0.06771(m_{sw}) + 12.5 \quad (69)$$

The amount of heat removed from the body through the evaporation of perspiration cannot always be calculated from the sweat rate since some perspiration may drip off without yielding any evaporative cooling. The sweat secretion rate has been found to depend upon body temperatures, skin wettedness, metabolic rate, and the amount of heat which has accumulated in the body (a function of body temperatures) (Shapiro, Pandolf, & Goldman, 1982). Since core temperature and skin temperature are the main inputs to the thermoregulatory center, and the sweat glands are the major thermoregulatory effectors in hot environments, the sweat glands will receive more impulses from the sympathetic nervous system when heat production or storage increases and inhibitory feedback will result as the skin becomes wetted and skin temperatures decrease (Shapiro, Pandolf, & Goldman, 1982). The rate at which sweat can evaporate from the

body is a function of environmental conditions and type of clothing. From a mass balance, the amount of sweat which runs off of the body without evaporating will be given by the difference between the sweat secretion rate and sweat evaporation rate.

The sweat secretion rate has previously been described as a function of core and skin temperatures (Nadel, Bullard, and Stolwijk, 1971).

$$m_{sw} = [4.87\Delta T_c + 0.569\Delta T_s]\exp(0.1\Delta T_s) \qquad (70)$$

where the delta's represent a change from the steady state temperature. The exponential term accounts for the observation that the sweat glands become more responsive as their temperature increases (a Q_{10} effect) (Nadel, Bullard, and Stolwijk, 1971).

Using a copper manikin, heat transfer coefficients for radiation and convection have been determined as a function of clothing type and air velocity (Givoni & Goldman, 1972). The combined coefficients are given in equation 71.

$$Q_{conv} + Q_{rad} = 0.8604C_{cl}(T_a - T_s) \qquad (71)$$

C_{cl} is the effective clothing thermal conductance and therefore measures the effect that clothing has on the rate of thermal transfer from the skin to the environment. This term must be included in equation 71 since clothing has insulating properties.

Through the Lewis relation, the convective mass transfer coefficient for evaporation can be determined from the convective heat transfer coefficient, which was determined from the manikin. For the air-water system the following equation, the Lewis relation, is very nearly correct (McCabe, Smith, and Harriott, 1985).

$$\frac{h_y}{M_B k_y} = c_s \tag{72}$$

where h_y is the heat transfer coefficient, k_y is a form of the mass transfer coefficent, M_B is the molecular weight of air, and c_s is the humid heat. After several unit conversions, the following relationship can be derived.

$$E_{max} = 1.893(im)(A)(C_{cl})(P_s - P_a) \tag{73}$$

The maximum sweat evaporation rate occurs when the skin is completely wetted.

Since clothing affects both the rate of heat transfer and mass transfer from the skin, an addition factor, im, is included in equation 73. As previously stated, C_{cl} includes the clothing effect on heat transfer and therefore is included in the heat transfer coefficient (see equation 71). Since clothing offers an additional resistance to the flow of water vapor from the skin, it will affect the mass transfer coefficient. im is a measure of the ability of water vapor to penetrate the clothing and has been determined experimentally (Givoni & Goldman, 1972). If clothing could be neglected,

the Lewis relation would give the mass transfer coefficient directly from the heat transfer coefficient, and im would equal unity. Values for C_{cl} and im are given in Table 1 for various air velocities and clothing types. The effective velocity, v_{eff}, includes the velocity of the flowing air and the air motion which is caused by body movement. Since body motion causes additional air movement around the clothing, it will have the effect of increasing C_{cl} and im. In other words, body motion causes additional convective heat and mass transfer. The effective velocity has been related to the metabolic rate through the following expression:

$$v_{eff} = v + 0.004(M - 105) \tag{74}$$

Table 1: Effective properties of clothing including surrounding air layer (taken from Johnson, 1991)

Clothing Type	Effective Clothing Thermal Conductance (C_{cl}) ($N/sec \cdot {}^oC \cdot m$)	Ability of Water to Pass through Clothing (im) (dimensionless)
Shorts	$11.3(v_{eff})^{0.30}$	$1.20(v_{eff})^{0.30}$
Shorts and short-sleeved shirt	$8.7(v_{eff})^{0.28}$	$0.94(v_{eff})^{0.28}$
Standard fatigues	$6.5(v_{eff})^{0.25}$	$0.75(v_{eff})^{0.25}$
Standard fatigues and overgarment	$4.3(v_{eff})^{0.20}$	$0.51(v_{eff})^{0.20}$

The total amount of water lost from the skin, m_{tot}, will be equal to the sensible water loss plus the amount of water lost by diffusion through the skin (insensible water loss).

$$m_{tot} = m_{sw} + (1x10^4)jA \tag{75}$$

where the factor of 10^4 is used to convert square meters to square centimeters.

Previous thermoregulatory models (Gagge, 1973 and Gagge, Stolwijk, & Nishi, 1971) and this model will assume that the evaportion rate from the skin, E_{sk}, will be given directly from m_{tot} unless the evaporation rate exceeds the maximum evaporation rate. In this case, the skin evaporation rate will equal the maximum evaporation rate.

$$E_{sk} = m_{tot}(Hvap) \quad \text{for } E_{sk} \leq E_{max} \tag{76}$$

$$E_{sk} = E_{max} \quad \text{for } E_{sk} > E_{max} \tag{77}$$

The fraction of the body which is completely wetted with perspiration, w, will then be given by

$$w = \frac{E_{sk}}{E_{max}} \tag{78}$$

Equation 76 assumes that the sweating effectiveness is 100%, in other

words, all of the secreted perspiration evaporates when $E_{sk} \leq E_{max}$. In dry environments, where E_{max} is large and the percentage of wetted skin is small, this equation should be valid. However, as the amount of water in the ambient air increases, the driving force for mass transfer (P_s - P_a) decreases, and the percentage of wetted skin must increase in order to maintain the same evaporation rate. Some perspiration may run off before the skin is completely wetted since the sweat glands are not evenly distributed over the body. Candas et al. (1979) reported a decrease in skin efficiency when the wetted skin area exceeds 74%. In this model, it will be assumed that this error is small and equations 76 and 77 will be used to describe the relationship between the sweat rate and rate of evaporative cooling.

Energy Balances

Since D_2, Q_{conv}, Q_{rad}, P_s, and m_{sw} are functions of skin and/or core temperature, an energy balance must be constructed around the body so that the body temperatures can be estimated over time. To simplify a human's complex geometry, a layered cylinder model may be used with reasonable accuracy (Coffey & Seagrave, 1972). The cylinder is divided into three layers which represent the body core, muscle, and skin. The skin layer can be further divided to include the layers that resist the diffusion of water, namely the hydrated layer which includes the upper portion of the

papillary dermis plus the viable epidermis and the stratum corneum. This model is shown in Figure 27.

An energy balance can be written for each layer yielding:

$$\rho C_p \Delta X_c \left(\frac{dT_c}{dt}\right) = M_o - \frac{k(T_c - T_m)}{\Delta X_{mc}} \tag{79}$$

$$\rho C_p \Delta X_m \left(\frac{dT_m}{dt}\right) = M_E + \frac{k(T_c - T_m)}{\Delta X_{mc}} - \frac{k(T_m - T_s)}{\Delta X_{sm}} \tag{80}$$

$$\rho C_p \Delta X_s \left(\frac{dT_s}{dt}\right) = \frac{k(T_m - T_s)}{\Delta X_{sm}} - Q_{conv} - Q_{rad} - Q_{evap} \tag{81}$$

where:

$$Q_{evap} = 3600(j\Delta H_{vap}) + \frac{E_{sk}}{A} \tag{82}$$

and $Q_{conv} + Q_{rad}$ is given by equation 71.

The thickness of the core, muscle, and skin layers have been determined for adults and infants (Coffey & Seagrave, 1972). Since the themal conductivity, k, is approximately the same for each layer (Coffey & Seagrave, 1972), the temperature profile will be linear for the model shown in Figure 27. Although k does not vary between the different layers, it will vary depending upon a subject's physiological state. k represents an

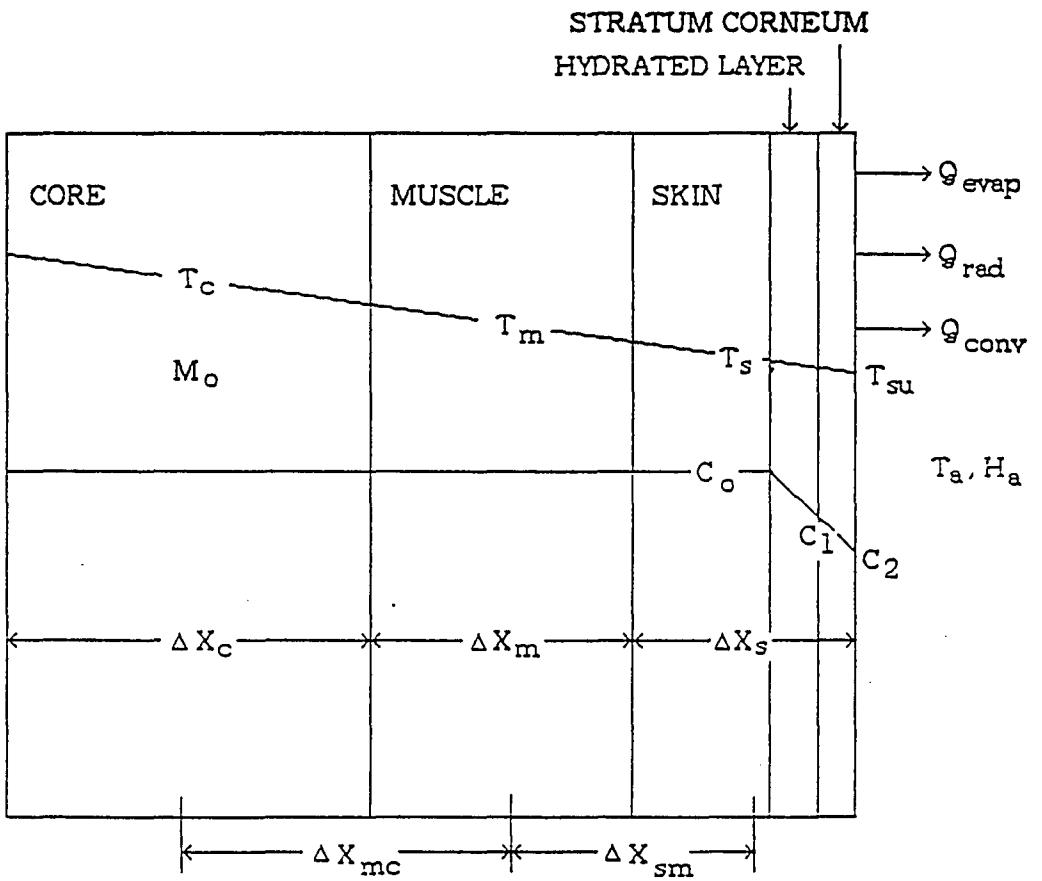

Figure 27: Layered cylinder model. (Adapted from Coffey & Seagrave, 1972)

effective, internal thermal conductivity which describes heat transfer by conduction and also heat which is transfered by the flowing blood (convection). Cool environments lower body temperature and cause vasoconstriction. In this state, blood is shunted to the inner body layers thereby decreasing k. Warm environments or exercise tend to increase body temperature and cause vasodilation. Blood flow to the skin increases with a consequent increase in k. Equations which describe this variation of k with

body temperature are given below (Coffey & Seagrave, 1972).

$$k = k_o[1 + \alpha_+ \Delta T_b + \gamma_k \frac{dT_b}{dt}] \qquad \text{for } \Delta T_b > 0 \tag{83}$$

$$k = k_o[1 + \alpha_- \Delta T_b + \gamma_k \frac{dT_b}{dt}] \qquad \text{for } \Delta T_b < 0 \tag{84}$$

Core and skin temperatures predicted by the model are compared with actual data in Figures 28, 29, 30, and 31.

The model results were determined by programming the model equations with Macintosh Extend software. Intergration of mass and energy balances were carried out with this software using one time step per minute.

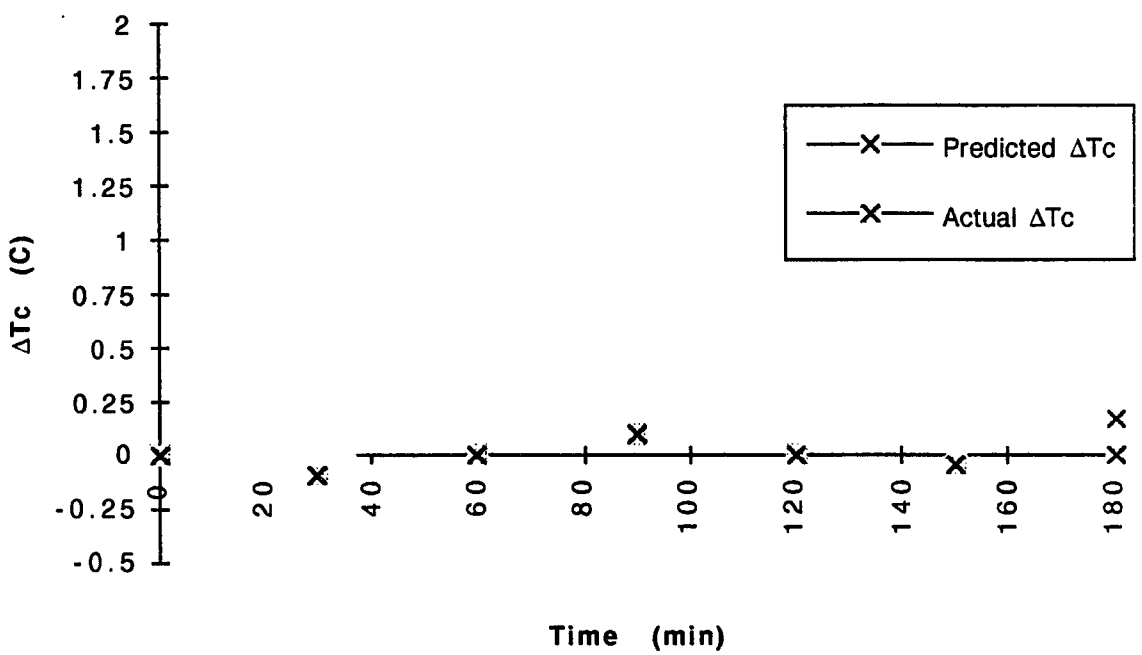

Figure 28: Predicted and actual core temperature for a subject at rest wearing standard fatigues. $T_a = 35^oC$, $P_a = 20$ mmHg, and v = 5 m/s. (Actual data taken from Givoni & Goldman, 1972)

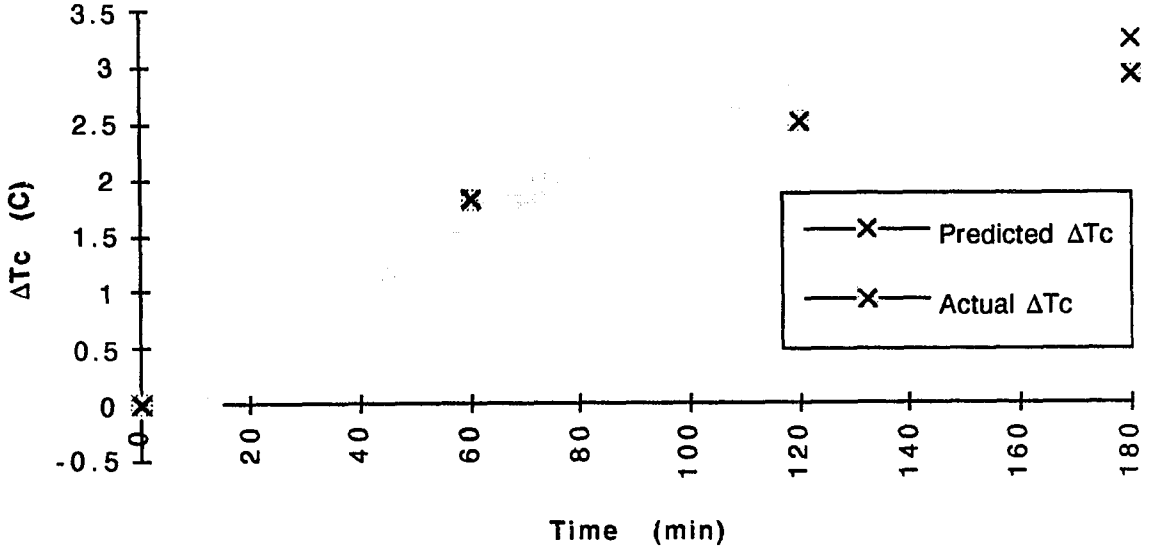

Figure 29: Predicted and actual core temperatures for subjects wearing shorts. M_E = 1.69 kcal/m²·min, T_a = 35.6°C, H = 100%, v=0.75m/s. (Actual data taken from Givoni & Goldman, 1972)

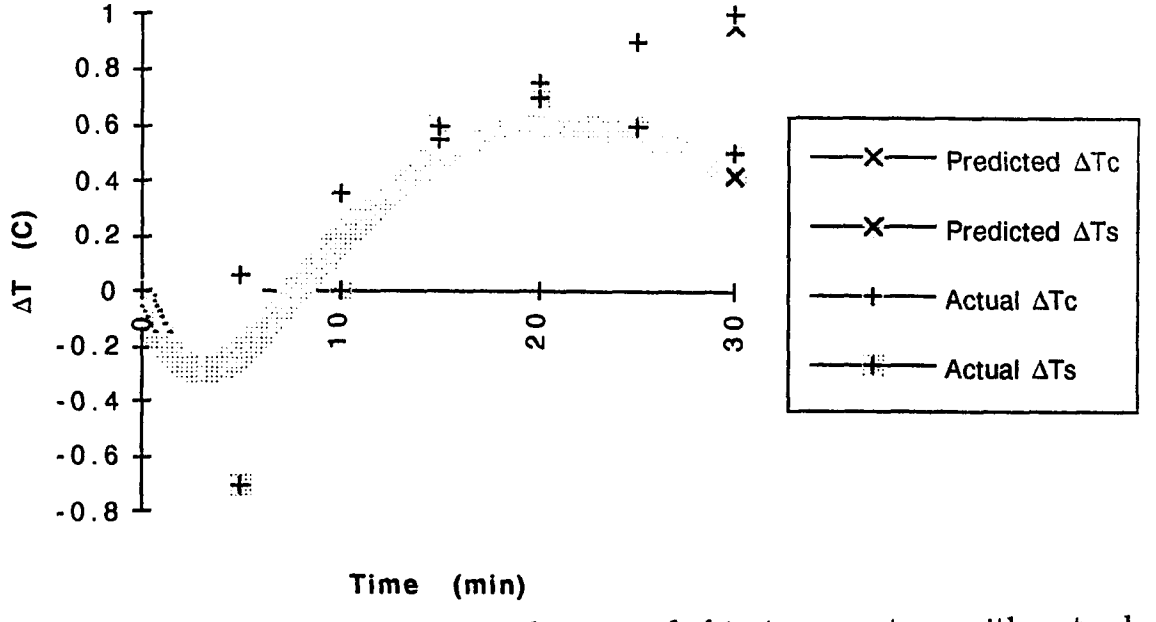

Figure 30: Comparison of predicted core and skin temperature with actual data. M_E = 6.22 kcal/m²·min, T_a = 26.5°C, H = 35%, still air, shorts. (Actual data taken from Mathews, Fox, and Tanzi, 1969)

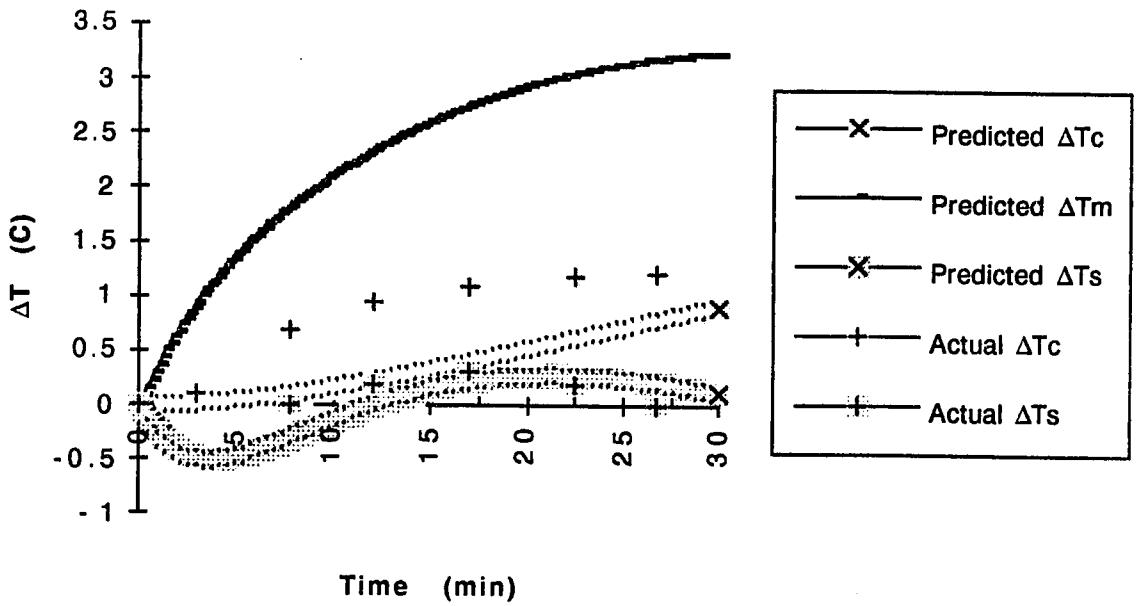

Figure 31: Comparison of predicted core and skin temperature with actual data. M_E = 6.2 kcal/m^2·min, T_a = 36°C, Pa = 16 mmHg, still air, shorts. (Actual data taken from Nadel, Cafarelli, Roberts, & Wenger, 1979)

The above four figures show that the layered cylinder model, which includes environmental conditions, type of clothing, and metabolic activity, adequately predicts the skin and core temperature during rest and exercise. In Figures 30 and 31, where the metabolic rate is high, some discrepancies exist between the model and actual data since the model tends to underestimate the core temperature. The most likely cause of the underestimation is the assumption that metabolic heat due to exercise (M_E) is created in the muscle layer only (see equation 80). In actuality, a fraction of M_E is produced within the core layer because the heart and lungs, which are included in the body core, are functioning at an increased pace. More sophisticated thermoregulatory models do exist (Johnson, 1991) but the

layered cylinder model will be used due to its simplicity and reasonable results.

To connect the layered cylinder model to the kidney model, metabolically produced water and water lost through respiration and perspiration (determined from the layered cylinder model) is included in the body water compartments used in the kidney model. The combined model is accurate for subjects at rest but additional factors due to exercise, such as increased cardiac output and blood pressure, have not yet been included. The effect of exercise on the water and electrolyte balance is incorporated into the model in the exercise section. Various levels of exercise in this section were considered only to test the validity of the layered cylinder thermoregulation model.

SPACE FLIGHT

To include conditions characteristic of space flight, the proposed model must be modifed. The primary space flight condition which needs to be described by the model is microgravity. Reduced barometric pressure, which is sometimes used to reduce leaking from the space craft, is also considered.

Water and Sodium Balance

The blood pressure in any vessel below the heart is increased and that in any vessel above the heart is normally reduced due to the effect of gravity (see Figure 32). When one is exposed to microgravity, the hydrostatic pressure gradient in the blood column is diminished causing fluid which is otherwise pooled in the lower extremities to be redistributed headward by the elastic forces and tone of the tissues (Leach, 1979). The transferred fluid consists mainly of intravascular fluid, or blood, although a small amount of interstitial fluid also shifts headward (Hargens, 1982). The small amount of interstitial fluid enters the blood supply because of the reduced capillary pressure and resulting changes in the Starling forces (see Figure 4). It is believed that the upward shift of this fluid increases both central blood volume and blood pressure. Stretch receptors located in the atrial walls, aortic arch, and carotid sinuses respond to the increased upper-body blood volume and pressure by blocking the release of antidiuretic hormone

(ADH) from the pituitary gland. The secretion rate of renin, and the subsequent release of aldosterone, are also decreased because of the rise in renal blood pressure (recall that renin is released by the juxtaglomerular apparatus in response to a decreased blood pressure, see Figure 15). These actions should cause an increased urinary loss of sodium and water.

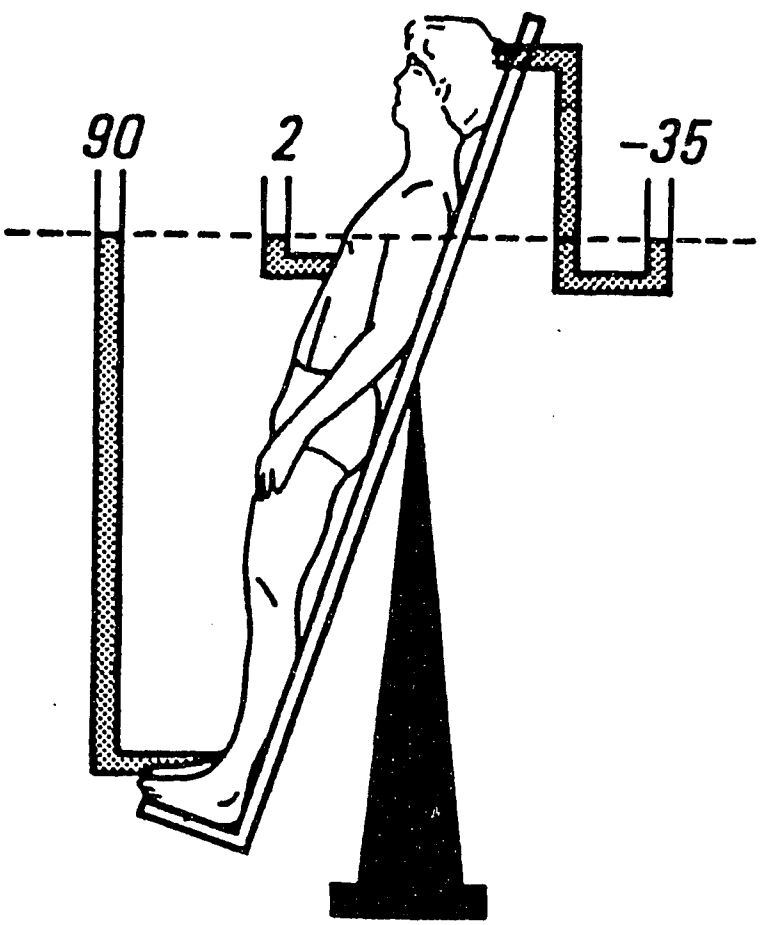

Figure 32: Venous pressures illustrating the hydrostatic pressure gradient in the body's blood column (taken from West, 1985)

To include the effects of weightlessness in the model, total body water (V_W) is divided into two compartments, which represent the water in the lower extremities by ($V_{W,L}$) and the water in the upper portion of the body by ($V_{W,U}$).

$$V_W = V_{W,L} + V_{W,U} \tag{85}$$

For a 70 kg person, V_W is about 40 liters and total leg volume is approximately 18 liters (Johnson, Nicogossian, Bergman, & Hoffler, 1976). Since the body is about 60% water, $V_{W,L}$ should be about 12 liters and consequently $V_{W,U}$ will be about 28 liters. Since the fluid which shifts between these compartments is mainly blood or intravascular fluid (Hargens, 1982), it will consist of extracellular fluid (plasma) and intracellular fluid (from the red blood cells). The amount of each fluid type is determined by the hematocrit.

Previous studies have found that as the body adjusts to a weightless state, the hematocrit remains fairly constant since while the kidneys are removing fluid from the plasma compartment and subsequently increasing the urine flow rate, red blood cell destruction by the spleen increases (Nicogossian, Huntoon, & Pool, 1989). It is believed that this increase in splenic red blood cell destruction is the result of a feedback mechanism which is triggered by the decrease in plasma volume (Nicogossian, Huntoon, & Pool, 1989). The details of the feedback mechanism have yet to be resolved. Red blood cell destruction by the spleen involves rupturing the

cells as they pass through the splenic blood vessels. Consequently, the intracellular contents are released into the circulation which makes up part of the extracellular compartment.

To simulate weightlessness with the proposed model, fluid, which is mostly blood, is transferred from the lower body water compartment to the upper body water compartment (see Figure 33). The kidneys respond to the increased upper body volume by increasing the rate at which fluid is filtered from the plasma compartment, and the subsequent urine flow rate. Since red blood cell destruction by the spleen keeps the hematocrit relatively constant, fluid and electrolytes from the ruptured red blood cells are transferred from the intracellular fluid compartment ($Na_{TOT,I}$ and OT_I) to the extracellular compartment ($Na_{TOT,E}$ and OT_E). The rate at which fluid is transferred from the lower to upper body is estimated from experimental data (Blomquist, Nixon, Johnson, & Mitchell, 1979).

Actual data obtained from space flights provide information on general adaptive changes which occur during weightlessness, however, due to operational constraints, it is very difficult to collect detailed physiological data during the initial stages of flight (Blomquist, Nixon, Johnson, & Mitchell, 1979). Therefore, detailed information must be obtained from ground-based weightlessness simulation studies. One procedure which diminishes the hydrostatic pressure gradient in the body's blood column is 5^o head-down tilt (see Figure 34). Head-down tilt causes many of the same responses as weightlessness, such as engorgement of the neck veins and facial tissues, headache, congestion, reduced leg volume, and diuresis. 5^o

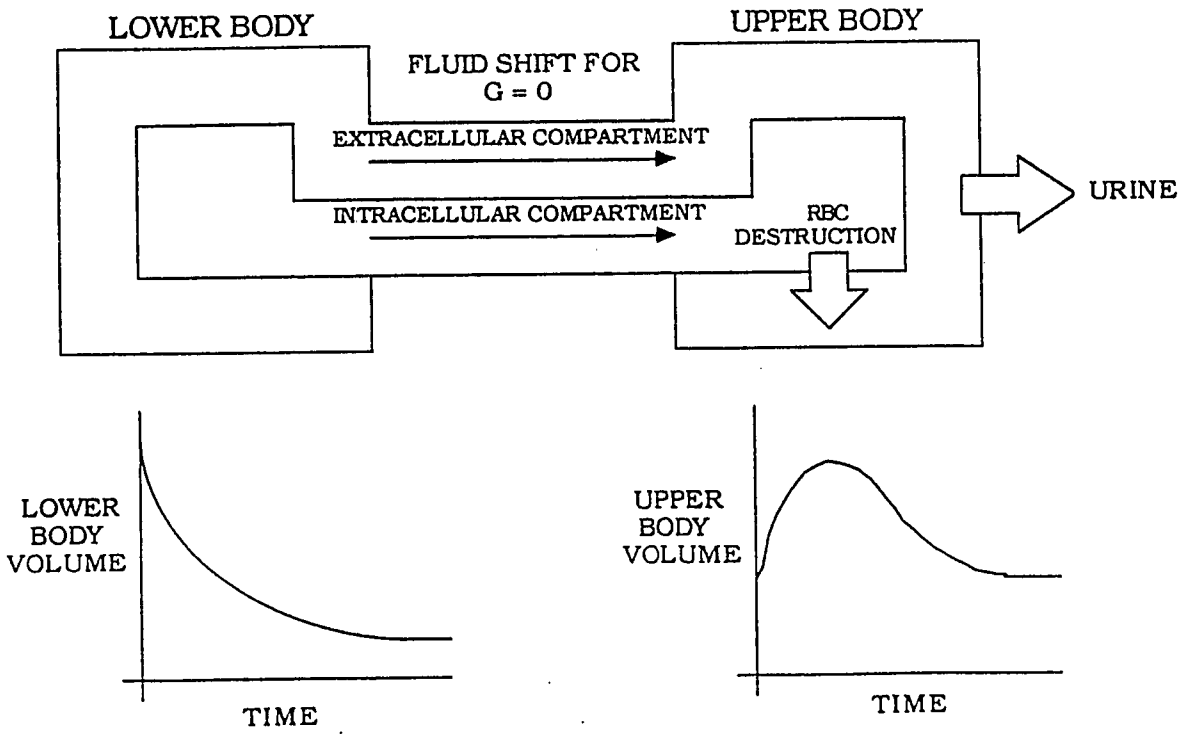

Figure 33: Fluid and electolyted transfer used in the proposed model to simulated the body's response to weightlessness.

head-down tilt is often used to simulate weightlessness since the initial weight loss and amount of fluid transferred from the legs is similar to that which was observed during the Skylab missions (Blomquist, Nixon, Johnson & Mitchell, 1980).

Data from simulation studies using 5° head-down tilt have shown that about 1 liter of fluid shifts from the legs over a two-hour period and the functional relationship between the fluid shift rate and time is an exponential decay (Blomquist, Nixon, Johnson & Mitchell, 1980). For the proposed model, the following fluid and electrolyte shift rates were used:

$$\text{Fluid volume shift (liters)} = 0.0135\exp(-0.015t) \qquad (86)$$

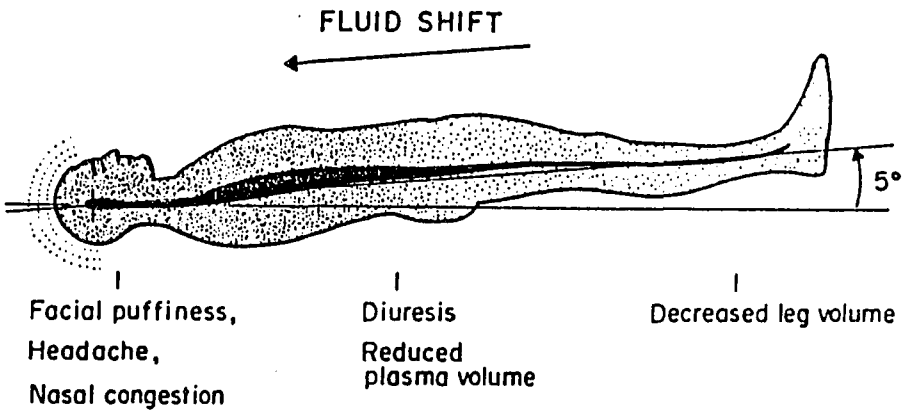

Figure 34: Summary of physiological responses to weightlessness simulation by 5° head-down tilt. (taken from Hargens, 1982)

$$\text{Sodium shift (mEq)} = 0.0608\exp(-0.015t) \tag{87}$$

$$\text{Other osmotic components shift (mEq)} = 1.15\exp(-0.015t) \tag{88}$$

where 0.9 liter of fluid shifts from the lower extremities to the upper body and 4.05 mEq of sodium and 76.49 mEq of other osmotic species are transferred from the intracellular to the extracellular compartment by red blood cell destruction. Antidiuretic hormone levels, aldosterone levels, and urine flow rates predicted by the proposed model are compared with actual data in Figures 35, 36, and 37.

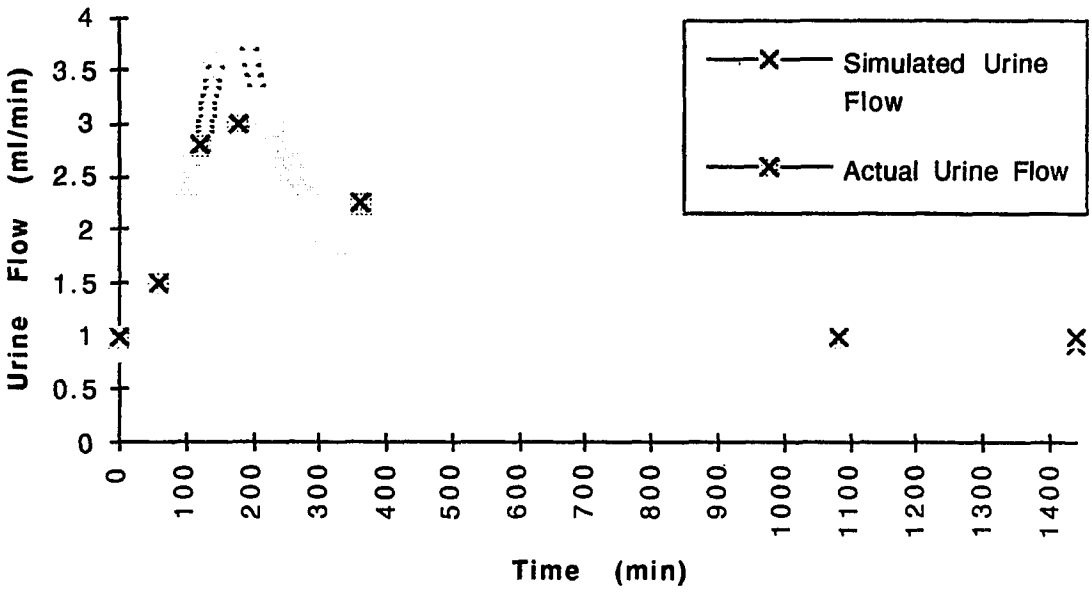

Figure 35: Results predicted the model following exposure to microgravity. Actual data was obtained from 5° head-down tilt experiments. (actual data taken from Blomquist, et al., 1980)

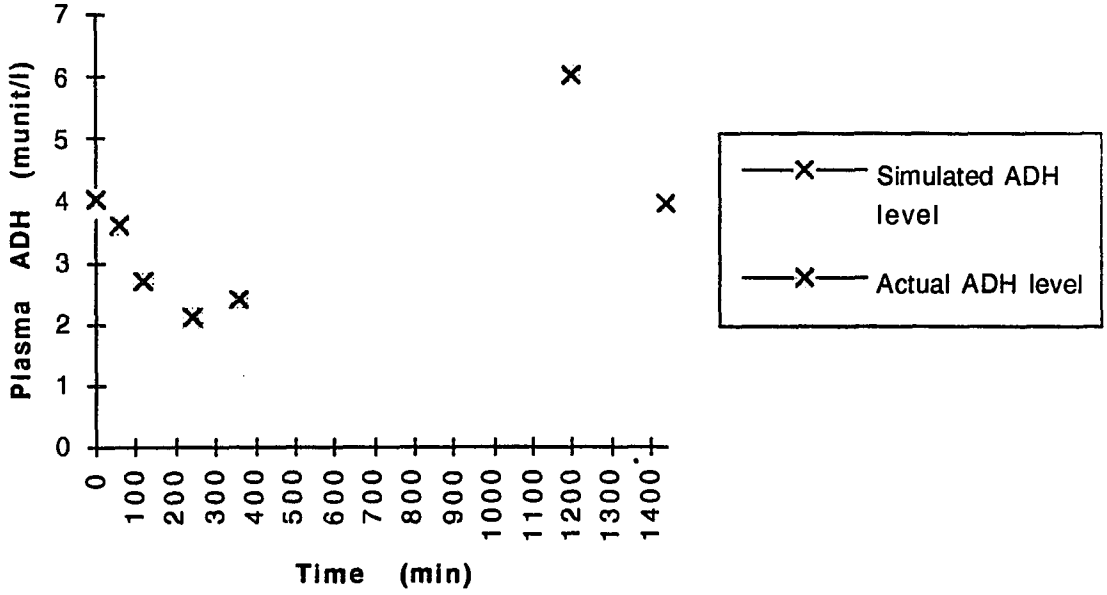

Figure 36: Antidiuretic hormone levels predicted by the model following the exposure to microgravity. Actual data was obtained from 5° head-down tilt experiments. (actual data taken from Blomquist,et al., 1980)

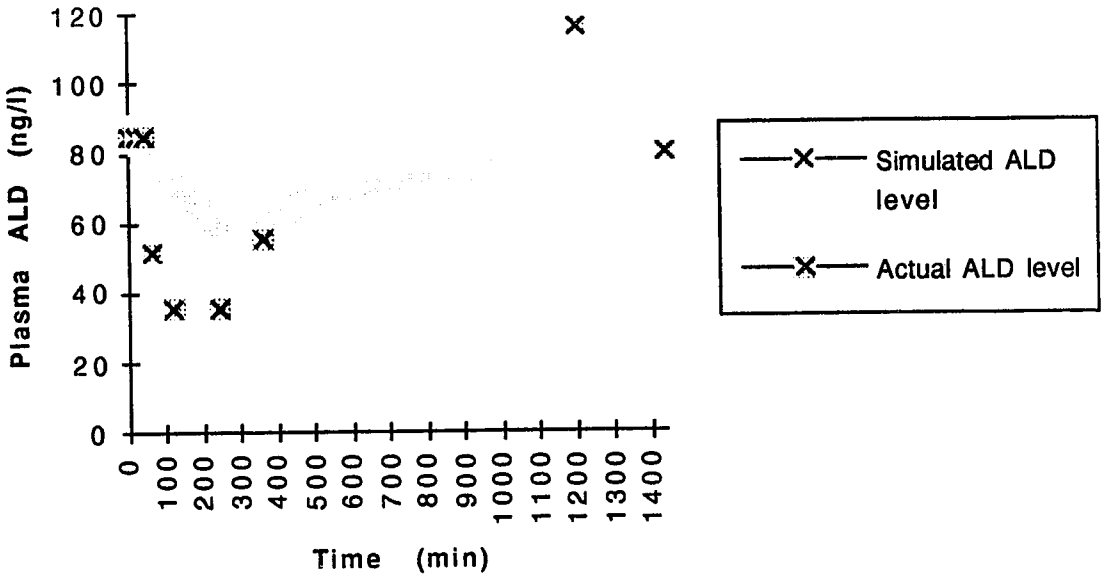

Figure 37: Aldosterone levels predicted by the model simulation following the elimination of the hydrostatic pressure gradient in the blood column. Actual data was obtained from 5° head-down tilt experiments (actual data taken from Blomquist et al., 1980)

Mechanisms which control the human water and sodium balances are incompletely understood not only under conditions of weightlessness, but also on earth (Gerzer & Drummer, 1992). As shown in Figure 35, as well as Figures 23 and 24, the proposed model reasonably predicts the urine flow rate for a variety of conditions. Figures 36 and 37 show that the proposed model also predicts the general pattern of hormone fluctuations after exposure to weightlessness. These results suggest that the control mechanisms considered by the proposed model, which include ADH, the renin-angiotensin-aldosterone system, and arterial pressure, are the primary controllers of human water regulation and sodium regulation. In other words, if a primary regulator was neglected by the proposed model, the fairly similar results shown in Figures 23, 24, and 35 would not be

expected. Other factors have been found to affect kidney function, such as natriuretic peptides and neurotransmitters. However, when considering long-term regulation, arterial pressure and plasma levels of ADH and aldosterone should reasonably describe kidney function.

Thermoregulation

Other space flight conditions which may affect the proposed model include the barometric pressure and the chemical composition of the atmosphere. The atmospheric composition varies depending upon the ambient humidity, which determines the amount of water in the atmosphere, and upon which gas is used to dilute oxygen. These factors should mainly influence the thermoregulation model without having much, if any, effect on the kidney model. Under space flight conditions, a pressurized cabin containing an artificial gas atmosphere protects the crew against the hostile effects of space and provides a source of oxygen. Parameters such as barometric pressure and chemical composition may vary widely depending upon design characteristics of the life support system. The chemical composition of the atmosphere depends in part on the barometric pressure, since the partial pressure of oxygen must be kept above a level required to keep the crew members well oxygenated. The choice of the diluting gas will affect convective heat transfer between the crew and their environment. For example, It has been found that at a pressure of 1 atmosphere, a helium-oxygen mixture is twice as effective at

cooling than air (Webb, 1975). Evaporative losses will depend upon the ambient humidity since the maximum evaporation rate (E_{max}) and the insensible water loss (j) increase as the water vapor pressure decreases. Heat and mass transfer coefficients may also vary since these parameters are dependent upon the barometric pressure. Variations in the barometric pressure and composition of the atmosphere can easily be considered in the model by using the appropriate value for the water vapor pressure in equations 68 and 73, the appropriate value for the convective heat transfer coefficient in equations 71 and 81, and the appropriate value for the mass transfer coefficient in equation 73.

Figure 38 illustrates the effect of varying the relative humidity while keeping the ambient temperature and pressure constant. In other words, only the percentage of water in the ambient air is changing. As expected, decreasing the relative humidity, which decreases the ambient water vapor pressure, increases the sweating efficiency so the body is able to maintain more normal temperatures.

Figure 39 shows how the body core temperature varies as the convective heat transfer coefficient is changed by considering different gas compositions. Therefore, in this figure, the ambient temperature, pressure, and humidity remain the same however the gas which dilutes the oxygen is changing. As expected, an oxygen-helium atmosphere, which approximately doubles the convective heat transfer coefficient relative to an oxygen-nitrogen atmosphere (Webb, 1975), provides additional cooling for the body.

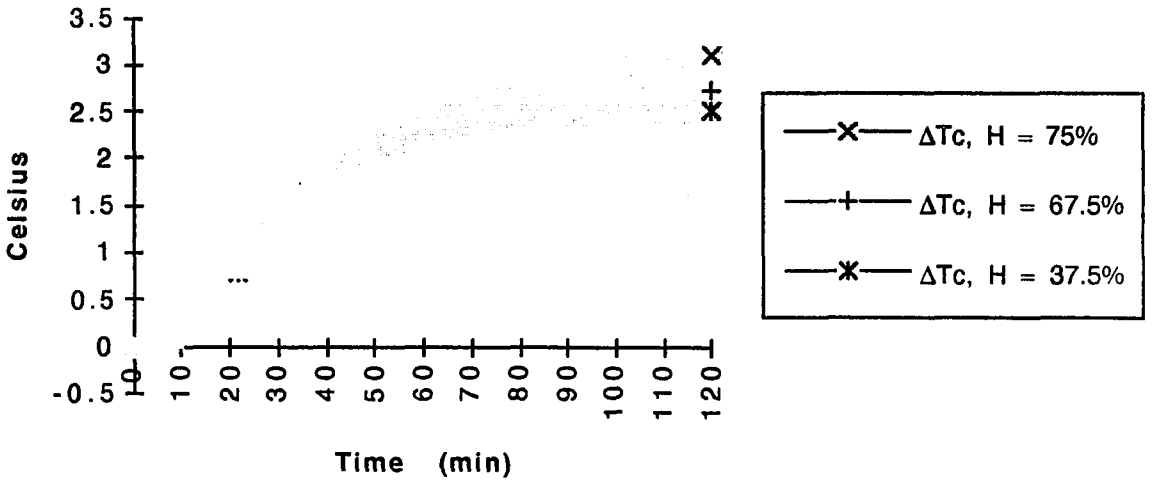

Figure 38: The effect of varying the ambient humidity on the core temperature of an exercising individual. M_E = 6.2 kcal/m^2·min, T_a = 33°C, P = 1 atm, still air, t-shirt and shorts.

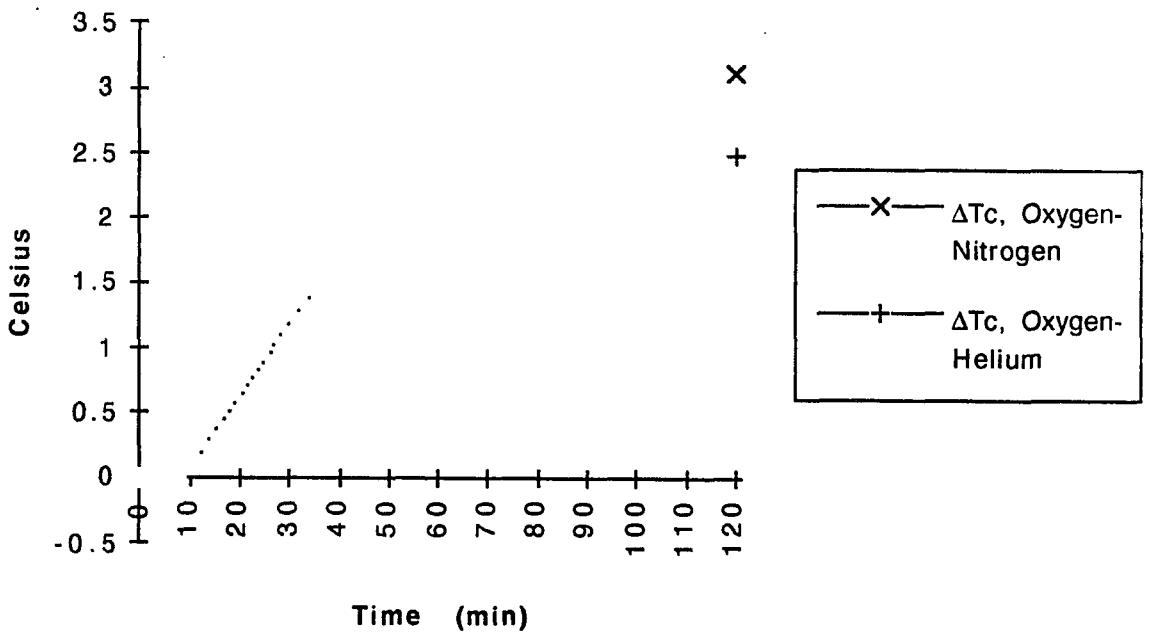

Figure 39: The effect of changing the atmospheric gas composition on the core temperature of an exercising individual. M_E = 6.2 kcal/m^2·min, T_a = 33°C, H = 75%, still atmosphere, t-shirt and shorts.

Varying the barometric pressure while keeping the ambient temperature and humidity constant will affect the rate at which water vapor and heat are transferred from the body. The relationship between barometric pressure and the convective heat and mass transfer coefficients can be estimated from the ideal gas law and the kinetic theory of low-density gases. The convective heat transfer coefficient is equal to the sum of that for natural convection and that for forced convection.

$$h_c = h_{c,f} + h_{c,n} \tag{89}$$

Similarily, for the convective mass transfer coefficient,

$$h_d = h_{d,f} + h_{d,n} \tag{90}$$

The Nusselt number, which is a dimensionless form of the convective heat transfer coefficient, can be expressed as a function of the Reynolds number and Prandtl number for forced convection and as a function of the Grashof number and Prandtl number for natural convection (Geankoplis, 1978).

$$Nu = \frac{h_{c,f}L}{k} = 0.6\left(\frac{Lv\rho}{\mu}\right)^{0.5}\left(\frac{C_p\mu}{k}\right)^{0.3} = 0.6(Re)^{0.5}(Pr)^{0.3} \tag{91}$$

$$Nu = \frac{h_{c,n}L}{k} = 0.55\left(\frac{L^3\rho^2 g\beta\Delta T}{\mu^2}\right)^{0.25}\left(\frac{C_p\mu}{k}\right)^{0.25} = 0.55(Gr)^{0.25}(Pr)^{0.25} \tag{92}$$

To convert a heat transfer correlation into the analogous mass transfer correlation, it is often only necessary to substitute the appropriate mass transfer dimensionless groups (Seagrave, 1971). Therefore, the Sherwood number, which is a dimensionless form of the convective mass transfer coefficient, can be expressed as a function of the Reynolds number and Schmidt number for forced convection and as a function of the mass transfer Grashof number and Schmidt number for natural convection.

$$Sh = \frac{h_{d,f}L}{\rho D_{AB}} = 0.6\left(\frac{Lv\rho}{\mu}\right)^{0.5}\left(\frac{\mu}{\rho D_{AB}}\right)^{0.3} = 0.6(Re)^{0.5}(Sc)^{0.3} \quad (93)$$

$$Sh = \frac{h_{d,n}L}{\rho D_{AB}} = 0.55\left(\frac{L^3\rho g\Delta\rho_a}{\mu^2}\right)^{0.25}\left(\frac{\mu}{\rho D_{AB}}\right)^{0.25} = 0.55(Gr_{AB})^{0.25}(Sc)^{0.25} \quad (94)$$

Where the constants in the above four equations are valid for flow normal to a single cylinder (Geankoplis, 1978).

Since a pressurized space cabin will typically be at low pressure (approximately1 atm), ideal gas behavior can be assumed. From the ideal gas law, the density is proportional to pressure and inversely proportional to temperature.

$$\rho \alpha \frac{P}{T} \quad (95)$$

From the kinetic theory of low-density gases, it can be shown that the diffusivities for momentum, mass, and thermal energy are proportional to

temperature to the three halves power and inversely proportional to pressure (Bird, Stewart, & Lightfoot, 1960).

$$D_{AB} \alpha \frac{k}{\rho C_p} \alpha \frac{\mu}{\rho} \alpha \frac{T^{3/2}}{P} \tag{96}$$

For an ideal gas, the heat capacity, C_p, will be a function of temperature and independent of pressure (Smith & Van Ness, 1975). Between 0°F and 100°F, the heat capacity of air remains relatively constant (Geankoplis, 1978). From this information and after several algebraic steps, the following can be shown.

$$h_{c,f} \alpha h_{c,n} \alpha \frac{P^{1/2}}{T^{1/4}} \tag{97}$$

$$h_{d,f} \alpha h_{d,n} \alpha \frac{P^{1/2}}{T^{1/4}} \tag{98}$$

Consequently,

$$h_c \alpha \frac{P^{1/2}}{T^{1/4}} \tag{99}$$

$$h_d \alpha \frac{P^{1/2}}{T^{1/4}} \tag{100}$$

Figure 40 shows the effect of changing the convective heat and mass transfer coefficients by varying the ambient pressure. For these results, the

ambient temperature, humidity, and diluting gas, which is nitrogen, remain constant.

To observe pronounced differences for the results shown in figure 40, a warm, humid, and windy environment had to be considered. In this environment, convective heat and mass transfer are the primary mechanisms for cooling the body. Furthermore, since the humidity was high, the sweat evaporation rate was determined by E_{max}, the maximum evaporative capacity of the environment. As shown by equation 73, E_{max} is proportional to the convective mass transfer coefficient. As expected, the higher pressure environment, which had a larger mass transfer coefficient,

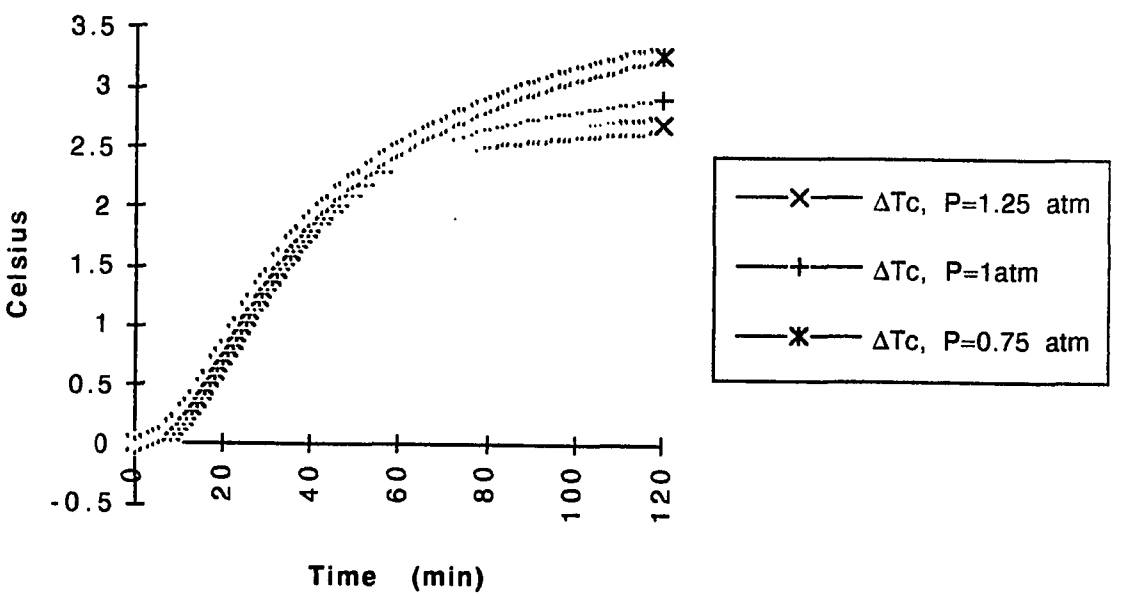

Figure 40: The effect of changing the atmospheric pressure on the core temperature of an exercising individual. M_E = 6.2 kcal/m^2·min, T_a = 35°C, H = 75%, air velocity = 5 m/s, t-shirt and shorts.

allowed for a higher sweat evaporation rate and for a more normal body temperature to be maintained.

Equations 99 and 100 predict that the convective heat and mass transfer coefficients will also be a function of temperature. However, variations in pressure should be much greater than variations in temperature since these equations refer to the absolute temperature . For an air environment, the pressure can vary from about 0.7 atmospheres to over 1.4 atmospheres, or by over 100%, and still provide an appropriate amount of oxygen for human life (Malkin, 1975). A resting adult human can maintain thermal control between about 293K and 305K (Hull, 1988) which is a temperature variation of about 4%. From equations 99 and 100, changing the temperature from 293K to 305K would change the convective heat and mass transfer coefficients by only 1%. Therefore, under most normal circumstances, the variation of the convective heat and mass transfer coefficients with temperature will be insignificant.

For microgravity, equations 92 and 94 predict that the natural convective heat and mass transfer coefficients will be insignificant, since the Grashof number approaches zero as the gravitational force, g, approaches zero. Therefore, when considering heat and mass transfer in space, natural convection can be neglected. This may have been expected without knowledge of the correlations, since the driving force for natural convection is density differences in the fluid.

Calcium Balance

The plasma concentration of calcium is approximately 10 mg/dl but can normally vary between 9.2 and 10.4 mg/dl (Guyton, 1976). These narrow limits are necessary since a larger depletion or elevation of calcium in the extracellular fluid causes extreme effects. Calcium ion concentrations affect the sodium permeability of excitable membranes (Martini, 1989). When calcium concentrations fall below normal, which is termed hypocalcemia, the nervous system becomes progressively more excitable. The nerve fibers can become so excitable that they begin to discharge spontaneously, initiating nerve impulses that pass to the skeletal muscles where they elicit tetanic contraction (Guyton, 1976). Conversly, when calcium concentrations rise above normal, which is termed hypercalcemia, the nervous system is depressed.

The digestive system, skeletal system, and renal system are all involved with maintaining appropriate levels of calcium in the extracellular fluid. The relationship between these organ systems and extracellular calcium levels is shown in Figure 41.

Studies of astronauts have revealed abnormal losses of calcium and reduced bone density as a result of weightlessness incurred during space flight (Hattner & McMillan, 1968). Similar findings have also been observed for persons confined to bedrest for long periods of time (Schneider, LeBlanc, and Rambaut, 1989). The precise mechanism of this calcium loss in not yet known, however, it is believed to be a result of reduced mechanical stresses

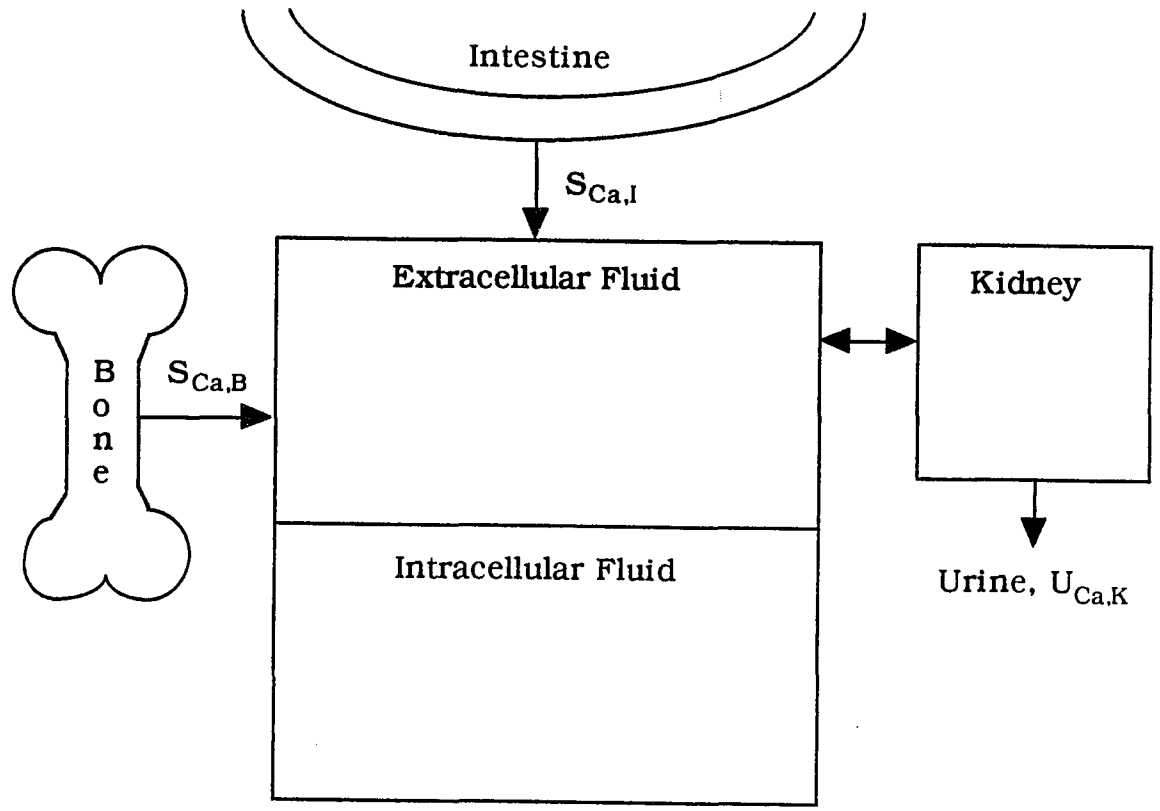

Figure 41: Relation between extracellular calcium and intestine, bone, and kidney.

on weight bearing bones (Hattner & McMillian, 1968 and Luken, Arnaud, Taylor, Baylink, 1993). The proposed mechanism which describes this calcium loss is shown in Figure 42. Each step of this mechanism has been studied individually and these steps will now be thoroughly discussed in numerical order.

Step 1 A primary function of the skeletal system is to provide support for the soft tissues of the body. The force of gravity acting on one's body mass mechanically stresses weight bearing bones as they move within the earth's gravitational field. Therefore, as step 1 of Figure 42 illustrates,

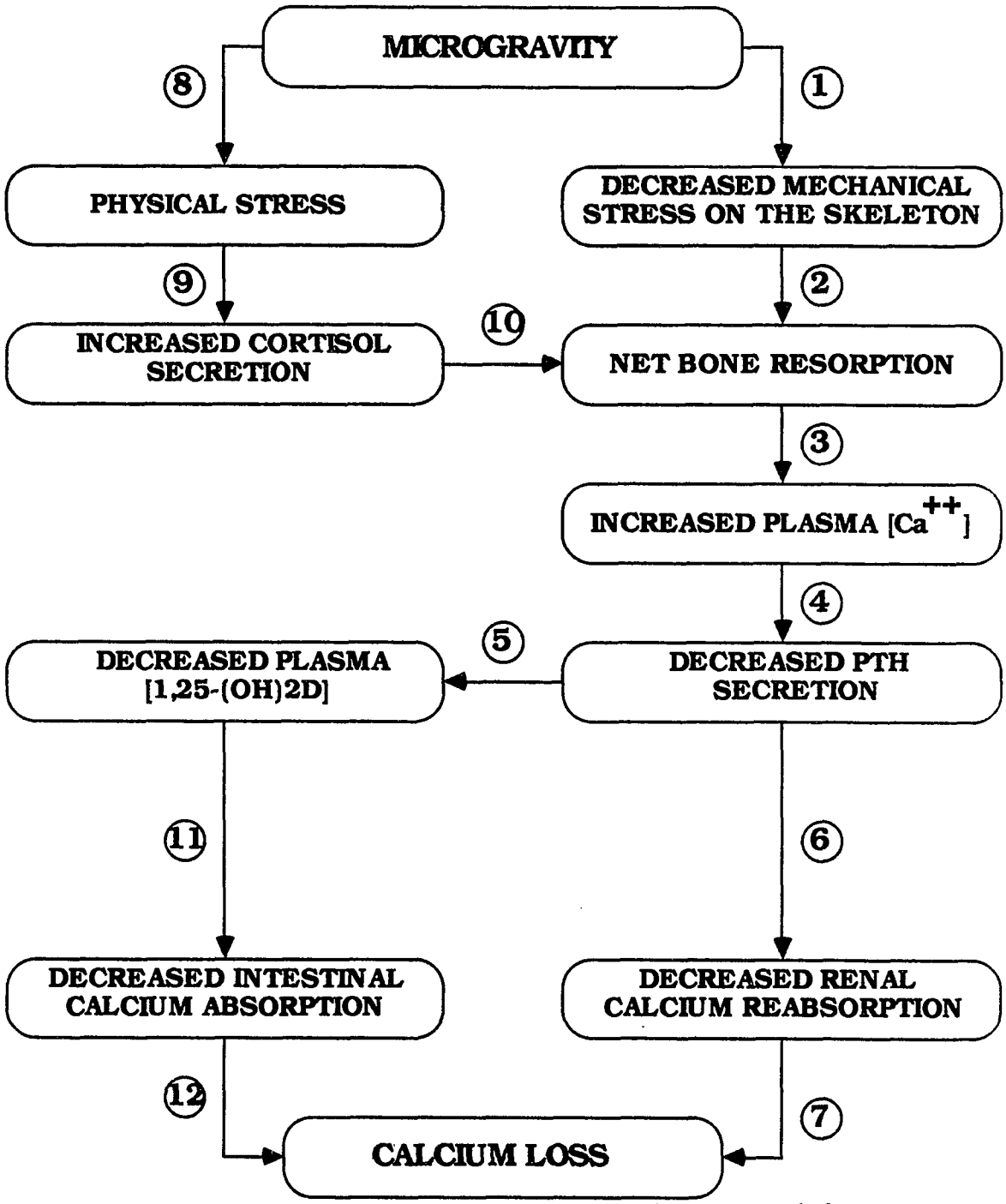

Figure 42: Proposed mechanism of calcium loss during weightlessness.

an environment with reduced gravity, which reduces body weight, or prolonged bed rest, which reduces bone stressing body movement, will decrease the amount of mechanical stress to which the skeletal system is exposed.

Step 2 Reduced mechanical stress on weight bearing bones causes the body to begin reabsorbing bone material, as step 2 suggests. Under normal conditions, the skeletal system is continually being remodeled and the rate of bone formation approximately equals the rate of bone destruction. The deposition of bone at points of compressional stress has been suggested to be caused by a piezoelectric effect as follows: Compression of bone causes a negative potential in the compressed areas and a positive potential elsewhere in the bone (Guyton, 1986). It has been shown that minute quantities of current flowing in bone increases the activity of bone producing cells at the negative end of the current flow, which could explain the increased bone deposition at compressive sites (Guyton, 1986). Electrical stimulation of bone has been found to decrease bone loss during limb immobilization (Kenner, Gavrielson, Lovell, and Marshall, 1975). Furthermore, increased bone density as a result of exercise is most likely carried out through this mechanism.

Bone calcium is of two types: exchangable calcium which accounts for about 0.5% of the total bone calcium, and stable calcium which accounts for the other 99.5% (see Figure 43). Bone material is formed by bone producing cells. Newly formed bone material makes up the exchangable pool and the calcium in this new bone material is freely exchanged with that of the extracellular fluid. Mineral that has been deposited and allowed to

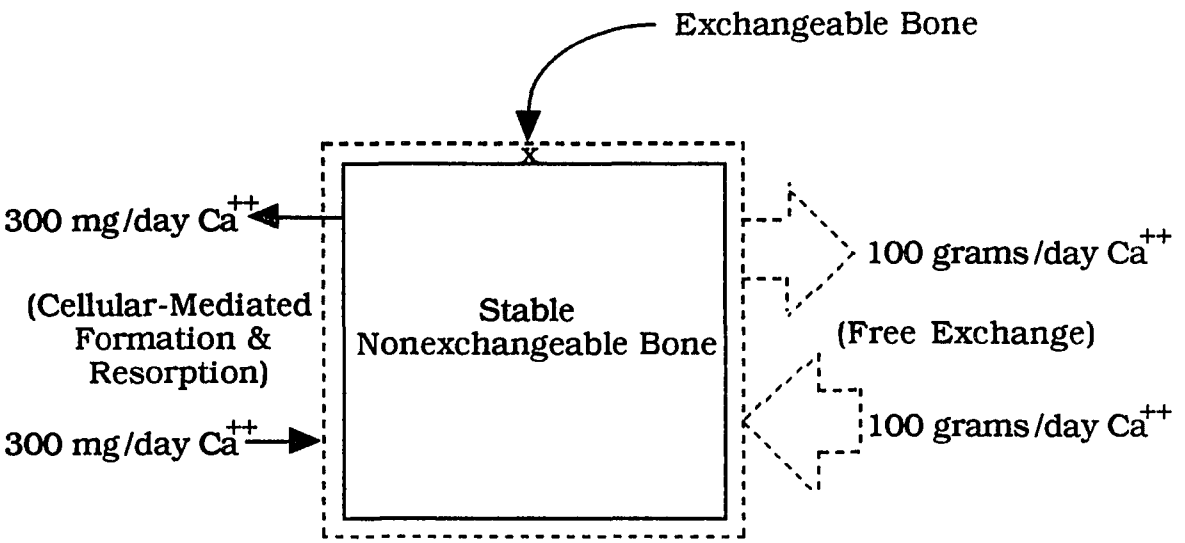

Figure 43: Calcium turnover in newly formed exchangable bone and older, more stable, nonexchangeable bone. (Adapted from Brown & Stubbs, 1983)

stabilize makes up the stable calcium pool. Calcium in the stable pool is not freely exchangeable with extracellular calcium and is released into the extracellular fluid only during cell-mediated bone resorption. Consequently, the calcium turnover rate is approximately 1000 times greater in the exchangeable pool than in the stable pool. The two mechanisms in which calcium can be transfered between bone material and extracellular fluid are the free exchange system and the bone formation-resorption system.

The main function of the free calcium exchange system is to eliminate large fluctuations of plasma calcium. However, in the absence of bone formation and resorption, which is cell mediated and hormonally regulated, the free exchange system can only sustain a plasma calcium level of 7 mg/dl (Ganong, 1991). Thus, the fine control system of bone formation and

resorption is essential for maintaining the plasma calcium at its normal level of 10 mg/dl (Brown & Stubbs, 1983). By shifting the ratio of bone formation to bone resorption, the bone formation-resorption system has a substantial effect on plasma calcium. Consequently, in terms of regulating plasma calcium, the free exchange system provides rapid, coarse buffering whereas the formation-resorption system is associated with more precise, long-term control. During space flight, the plasma calcium concentration varies by less than 10% (Leach, 1981) and should not greatly affect the rates at which calcium is transferred by the free exchange system since this system only provides coarse control. However, this plasma calcium concentration variation will most likely affect the bone formation-resorption system since this system provides fine control. Therefore, for the proposed model, changes in the free calcium exchange system will be considered insignificant and the following discussion is concerned mainly with the bone formation-resorption system.

Bone consists of crystalline salts which are deposited on an organic matrix which is mostly collagen fibers. The salts are mainly composed of calcium and phosphate, and the formula for the primary bone salts, or hydroxyapatites, is shown below:

$$Ca^{++}_{10-X}(H_3O^{+})_{2X}\bullet(PO_4)_6(OH^{-})_2$$

Cells which produce bone material are called osteoblasts. These cells produce collagen fibers on which the hydroxyapatite crystals can be

deposited. The concentrations of calcium and phosphate ions in the extracellular fluid are greater than those required to cause precipitation of hydroxyapatite. However, inhibitors present in most body fluids prevent such precipitation (Guyton, 1986). One theory of bone mineralization holds that osteoblasts secrete a substance which neutralizes the inhibitor(s) that prevents hydroxyapatite crystallization, thereby allowing for mineralization of the collagen fibers (Guyton, 1986 and Boskey, 1981). Crystallization theory predicts that the rate of crystallization will vary linearly with the solute concentration of the supersaturated solution (Geankoplis, 1978). Subsequently, the rate at which calcium is removed from the plasma and formed into bone salts, R_f, should be a function of the plasma calcium ion concentration, the inhibitor concentration, and the area of bone being mineralized.

$$R_f = f\{ [Ca^{++}], [\text{inhibitor}], (\text{area})\} \tag{101}$$

For a given inhibitor concentration and bone surface area, the crystallization rate should vary linearily with the plasma calcium ion concentration:

$$R_f = K_1[Ca^{++}] \tag{102}$$

where K_1 may be a function of temperature but will be constant in this situation, since body temperature is approximately constant.

Cells which break down bone material are called osteoclasts. These cells attach to the bone surface which is to be resorbed and dissolve bone by secreting acid and enzymes at the bone surface. The enzymes presumably digest or dissolve the organic matrix of the bone, while the acid causes solution of the bone salts (Guyton, 1986). The rate at which calcium is reabsorbed from the bone salts, R_r, should be a function of the bone calcium concentration, the acid concentration, and the bone area affected by the osteoclasts.

$$R_r = f\{ [Ca], [acid], (area)\} \tag{103}$$

The bone calcium concentration, [Ca], remains constant since only the bone surface is involved in the reaction. Therefore, for a given acid concentration and bone area, the reabsorption rate should remain constant.

$$R_r = K_2 \tag{104}$$

The relationship between bone formation and bone resorption is illustrated in Figure 44.

The rates of bone formation and resorption have been measured under normal and bed rest conditions (Lockwood, Vogel, Schneider, and Hulley, 1975). It was found that during bed rest, both the bone formation and bone reabsorption rates increased. However, a greater increase was observed for the bone reabsorption rate. From these rates and equations

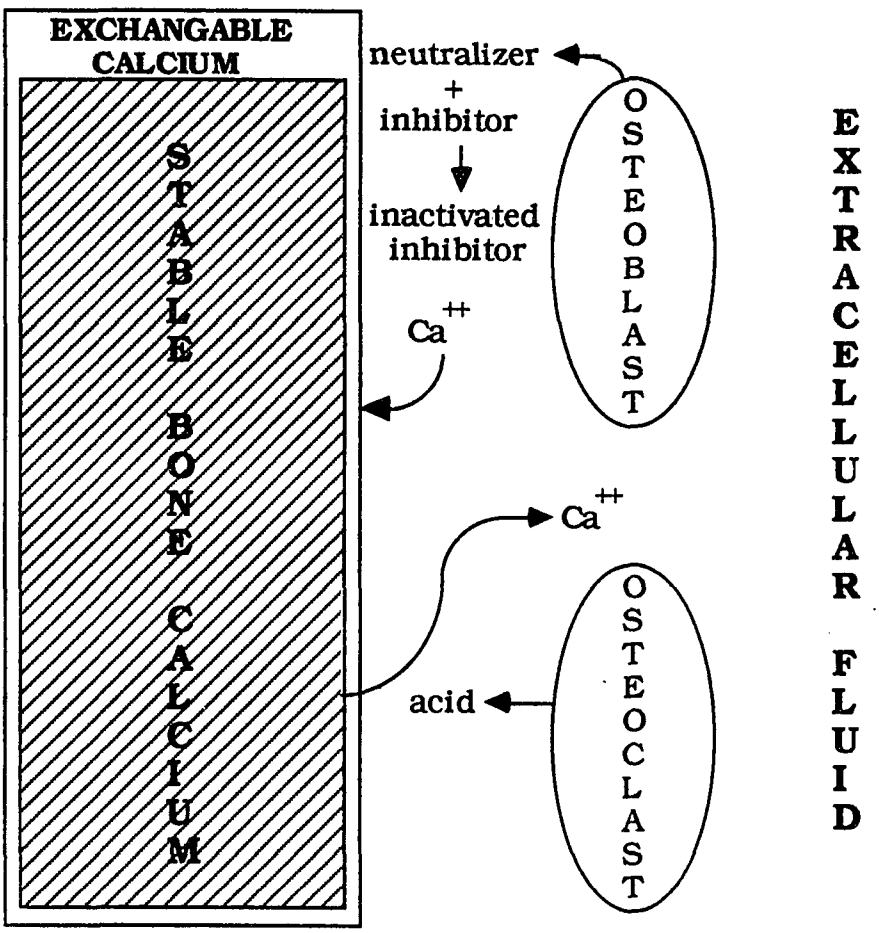

Figure 44: Relationship between bone formation and bone resorption.

102 and 104, the constants K_1 and K_2 can be estimated under normal and bed rest conditions. This estimation assumes that a particular inhibitor concentration, bone formation area, acid concentration, and bone resorption area are associated with earth's environment and bed rest conditions. For example, to determine K_1 for bed rest, specific values for the inhibitor concentration and the bone formation area are assumed for anyone exposed

to bed rest. This assumption is only an approximation, since bone areas affected by the osteoblasts and osteoclasts, inhibitor concentrations, and acid concentrations will most likely vary somewhat among individuals. Using the assumed typical values for these parameters, the following can be calculated.

K_1 = 9.27 l/day	earth conditions
K_2 = 510 mg/day	earth conditions
K_1 = 13.5 l/day	bed rest conditions
K_2 = 815 mg/day	bed rest conditions

The bone formation rate and resorption rate during weightlessness has not yet been measured. However, it has been observed that calcium release from the bones is about 4.2 times greater during space flight than during bed rest (Rambaut & Johnston, 1979). The proposed model requires the rate of calcium release from the bones (see equation 105), which is the difference between the bone resorption rate and the bone formation rate, and not the specific values for these rates. Therefore, to determine the rate of calcium release from the bones during weightlessness, the bed rest K values can be used to calculate the bone formation and resorption rates, and the difference between these rates is multiplied by 4.2

Step 3 Plasma calcium exists in two forms. Approximately 45%, or 4.5 mg/dl, is bound to plasma proteins whereas the remaining 55%, or

5.5mg/dl, is ionized. It is the free, ionized calcium which is released from the bones, absorped by the intestines, and filtered by the kidneys. Therefore, for the proposed model, bound calcium concentrations will be assumed to remain constant, and ionized calcium concentrations will vary with bone, intestinal, and renal activity.

From step 2, it was shown that a weightless state increases the rate at which calcium ions are released from the bones into the extracellular fluid compartment. Since the plasma compartment makes up part of the extracellular fluid compartment, increasing the input of calcium ions into the extracellular fluid will tend to increase the plasma calcium ion concentration. The calcium ion concentration should be uniform throughout the extracellular compartment because calcium ions are relatively small and can easily cross vessel walls (see Figure 4). From a calcium ion mass balance on the extracellular compartment, the calcium ion concentration can be estimated over time.

$$V_E \frac{d[Ca^{++}]}{dt} = S_{Ca,B} + S_{Ca,I} - U_{Ca,K} \qquad (105)$$

The net rate at which calcium ions are released by the bones, $S_{Ca,B}$, can be determined by the difference between the bone reabsorption rate and the bone formation rate (see equations 102 and 104). The net rate at which calcium is absorbed by the intestines, $S_{Ca,I}$, will be described by step 11. Calcium is excreted from the body in the feces and urine. Since $S_{Ca,I}$ is the net intestinal absorption rate, the fecal loss of calcium will be included in

this term. Urinary calcium loss, $U_{Ca,K}$, which depends upon kidney function, will be described by step 6.

Step 4 Three hormones regulate the plasma ionized calcium concentration: 1,25-dihydroxycholecalciferol (1,25-$(OH)_2D_3$), parathyroid hormone (PTH), and calcitonin. The role of calcitonin seems to be minor when compared to that of PTH and 1,25-$(OH)_2D_3$ (Ganong, 1991) and will therefore be neglected in the proposed model. PTH acts to increase the formation rate of 1,25-$(OH)_2D_3$ and this action will be discussed when considering step 5.

PTH is an 84 amino acid peptide which is synthesized and secreted by the chief cells of the parathyroid gland. Humans have four parathyroid glands located behind the thyroid gland. PTH has a direct action on bone and kidney and an indirect action, via 1,25-$(OH)_2D_3$, on the intestines. The main action of this hormone is to maintain proper plasma levels of ionized calcium. Through a feedback mechanism, the PTH secretion rate is regulated by the concentration of ionized calcium in the plasma. When ionized calcium levels are low, the secretion rate of PTH is increased. PTH increases the rate of calcium release from the bones by stimulating osteoclasts, thereby increasing bone resorption, inhibiting osteoblasts, and thereby decreasing bone formation (West, 1985). PTH also acts on the renal tubules by increasing the amount of calcium reabsorbed by the distal nephron (West, 1985). These actions tend to increase plasma levels of ionized calcium. When plasma ionized calcium levels are increased, the secretion rate of PTH decreases and the opposite actions occur. A previous

study has found a linear relationship between PTH secretion and the plasma level of calcium. This relationship is shown below.

$$S_{PTH} = -0.0749[Ca^{++}] + 5.62 \qquad (106)$$

The plasma concentration of PTH over time can be estimated from a material balance on this hormone. Equation 107 assumes that PTH is confined mainly to the plasma compartment since this assumption was also made when considering plasma levels of aldosterone, renin, and angiotensin II.

$$(V_{pl})\frac{d[PTH]}{dt} = S_{PTH} - D_{PTH}[PTH] \qquad (107)$$

PTH is deactivated in the body by the liver, kidneys, and bones (Martin, 1985). From steady state considerations, where $\frac{d[PTH]}{dt} = 0$, from the normal plasma PTH concentration, 450 pg/ml, and from equation 106, the destruction rate, or clearance, of this hormone, D_{PTH}, can be determined.

$$D_{PTH} = 3334 \text{ liter/day} \qquad (108)$$

Step 5 Vitamin D_3, or cholecalciferol, is produced in the skin of mammals through a reaction involving sunlight. In the liver, cholecalciferol is converted to 25-hydroxycholecalciferol, and this reaction does not appear to be stringently regulated. 25-Hydroxycholecalciferol has a normal plasma

level of about $3.0x10^{-2}$ mg/l. 25-Hydroxycholecalciferol is then converted to 1,25-dihydroxycholecalciferol in a regulated reaction involving an enzyme located in the cells of the proximal tubule. The normal plasma level of 1,25-dihydroxycholecalciferol is about $3.0x10^{-5}$mg/l.

The plasma 1,25-$(OH)_2D_3$ concentration can be estimated over time with the following mass balance.

$$(V_{pl})\frac{d[1,25\text{-}(OH)_2D_3]}{dt} = S_{1,25\text{-}(OH)_2D_3} - D_{1,25\text{-}(OH)_2D_3}[1,25\text{-}(OH)_2D_3] \quad (109)$$

PTH increases the formation rate of the physiologically active vitamin D metabolite, 1,25-dihydroxycholecalciferol (1,25-$(OH)_2D_3$). As plasma levels of PTH decrease, the formation rate of 1,25-$(OH)_2D_3$ will decrease with a consequent decrease in the plasma 1,25-$(OH)_2D_3$ level. The steady state relationship between the plasma level of PTH and 1,25-$(OH)_2D_3$ has previously been studied and is shown below (Gallagher, Riggs, & DeLuca, 1980).

$$[1,25\text{-}(OH)_2D_3] = 0.0667[PTH] \quad (110)$$

1,25-$(OH)_2D_3$ has a half-life of about 15 hours (West, 1985). Therefore, if the secretion rate was zero, after 15 hours the plasma concentration of this hormone would be half of the initial concentration. In other words, half of the plasma would be cleared of 1,25-$(OH)_2D_3$. Using an average plasma

volume of 3 liters, the disappearance rate, or clearance, of this hormone can be determined.

$$D_{1,25\text{-}(OH)_2D_3} = \frac{1.5 \text{ liters}}{15 \text{ hours}} = 0.1 \frac{\text{liter}}{\text{hour}} = 2.4 \frac{\text{liter}}{\text{day}} \quad (111)$$

From steady state considerations, where $\frac{d[1,25\text{-}(OH)_2D_3]}{dt} = 0$, the secretion rate can be determined with equations 109, 110, and 111.

$$S_{1,25(OH)_2D_3} = 1.6[PTH] \quad (112)$$

The primary target organ for $1,25\text{-}(OH)_2D_3$ is the intestine. This hormone, which increases the intestinal absorption of calcium, will be disscussed in detail when considering step 11.

Step 6 The renal handling of calcium determines the urinary output of this electrolyte and therefore must be considered in the calcium balance. The plasma calcium which is bound to plasma proteins is not filtered by the kidney, however, the ionized plasma calcium is filterable. The renal handling of ionized calcium appears to be coupled to the handling of sodium. In the proximal tubule, calcium reabsorption parallels the reabsorption of sodium and water, and the calcium concentration therefore stays approximately constant along this nephron segment (Lote, 1987). Calcium reabsorption occurs in the ascending limb of the loop of Henle (recall that the descending limb is relatively impermeable to ions). The reabsorption in this segment also appears to be coupled to sodium

reabsorption since furosemide, a diuretic which inhibits NaCl transport in the loop of Henle, also inhibits Ca^{++} reabsorption (Lote, 1987). Furthermore, studies have found identical fractions of Na^{+} and Ca^{++} are reabsorbed when the filtrate reaches the early portion of the distal nephron (West, 1985 and Lote, 1987). This apparent coupling between sodium and calcium does not hold for the distal tubule and collecting tubule. Thiazide diuretics inhibit Na^{+} reabsorption and stimulate Ca^{++} reabsorption in this portion of the nephron (Sullivan, 1982).

The fraction of Ca^{++} reabsorbed in the distal tubule and collecting duct is controlled primarily by PTH. PTH enhances Ca^{++} reabsorption in this nephron segment and will consequently decrease the urinary calcium loss. Previous studies have found that the calcium excretion rate increases severalfold in laboratory animals when the parathyroid glands are removed (Talmage, 1956 and Biddulph, Hirsch, Cooper, and Munson, 1970). In these studies, the plasma PTH concentration was likely close to zero, since PTH secretion was eliminated and PTH has a rapid destruction rate (see equation 108). For urinary calcium excretion to increase so dramatically, calcium reabsorption by the distal nephron was probably insignificant. Assuming that the same would be true for humans, a relationship between the fraction of calcium reabsorbed by the distal nephron, $FRe_{Ca++,DT}$, and the plasma PTH level can be determined. This relationship assumes that the fraction of calcium reabsorbed by the distal nephron is normal when the plasma PTH concentration is normal and that the fraction reabsorbed is insignificant when the plasma PTH level is zero.

$$FRe_{Ca++,DT} = 1366[PTH] \quad (113)$$

Step 7 A decrease in renal calcium reabsorption will increase the urinary loss of this electrolyte. The kidneys filter fluid and, consequently, remove calcium from the plasma compartment. The urinary calcium loss, $D_{Ca,K}$, is therefore used in the extracellular calcium mass balance (see equation 105). A total body mass balance on calcium is given by the following equation.

$$\frac{d(Calcium)}{dt} = \text{intestinal input - urinary loss - fecal loss} \quad (114)$$

From equations 105 and 114, it can be seen that an increased urinary calcium loss will tend to decrease the extracellular, or plasma, calcium concentration and the total amount of calcium in the body.

Step 8 Exposure to a weightless environment is physically, and perhaps mentally, stressful. Weightlessness eliminates the hydrostatic pressure gradient in the blood column of the body and consequently causes fluid in the lower extremities to be redistributed headward. This fluid shift increases the central blood volume and blood pressure. Engorgement of neck veins and facial tissues and feelings of head fullness have been observed inflight (Leach, 1979). As described by steps 1 and 2, weightlessness also reduces mechanical stresses on the skeletal system and causes bone reabsorption. Besides these two factors, other physiological changes may also occur after exposure to weightlessness. These

physiological changes will physically stress the body and will likely cause some mental stress as well.

Step 9 Cortisol, cortisone, and corticosterone are steroid hormones which are secreted from the cortex of the adrenal gland. These hormones are called glucocorticoids because of their effects on glucose metabolism. The best known action of the glucocorticoids is the stimulation of gluconeogenesis in the liver, i.e., increasing the conversion of amino acids to glucose, with a resulting rise in glucose output to the blood (Sawin, 1969). However, glucocorticoids have also been found to affect bone metabolism and 1,25-$(OH)_2D_3$ metabolism (Martin, 1985). Therefore, glucocorticoids influence the calcium balance and need to be considered by the proposed model. Since cortisol accounts for at least 95% of the glucocorticoid activity (Guyton, 1976), it is the only glucocorticiod which will be considered by the proposed model.

The cortisol concentration over time can be predicted with the following mass balance.

$$V_E \frac{d[C]}{dt} = S_C - D_C[C] \tag{115}$$

where the volume distribution of cortisol is approximately equal to the extracellular volume, V_E , and the clearance is about 144 liters/day (Vinson, Whitehouse, and Hinson, 1992). The secretion rate of cortisol, S_C, has been found to be a function of stress (Guyton, 1976).

Almost any type of stress, whether is be physical or mental, will increase the plasma level of cortisol. Some of the different types of stress that increase cortisol release are the following (Guyton, 1976):

1. Trauma
2. Infection
3. Intense cold or heat
4. Surgical operations
5. Restraining an animal so that it cannot move
6. Almost any debilitating disease

Cortisol levels have also been found to increase by up to 100% under space flight conditions (Leach, 1981). Since the stimulus for cortisol secretion, stress, is nonspecific, the relationship between cortisol secretion and stress will be difficult to describe. Furthermore, it is not completely understood why increased cortisol secretion during stressful events is of benefit to the animal (Guyton, 1976).

Cortisol secretion is controlled almost entirely by a hormone which is secreted by the anterior pituitary gland, adrenocorticotropic hormone or ACTH (Guyton, 1976). Almost any type of stress will increase within minutes the plasma levels of ACTH and cortisol. The approximate cortisol secretion rate for humans under normal conditions is 21.6 mg/day (Vinson, Whitehouse, & Hinson, 1992) and is 259 mg/day under maximum ACTH stimulation (Gray & Bacharach, 1961). From this information, an arbitrary

stress scale can be derived and used to describe the relationship between stress and cortisol secretion in the proposed model. For the stress scale, a stress level of 0 will correspond to a cortisol secretion rate of zero whereas a stress level of 10 will correspond to the maximum secretion rate, 259 mg/day. From these two data points, a linear relationship can be determined.

$$S_C = 25.9\ (SL) \tag{116}$$

where S_C is the cortisol secretion rate in mg/day and SL is the stress level. From equation 116 and the normal cortisol secretion rate, 21.6 mg/day, the normal stress level can be found to be 0.83.

The plasma cortisol level during space flight has previously been measured (Leach, 1981). From this data, the stress level during space flight can be calculated from equations 115 and 116. This relationship is given below:

$$SL = 0.0197(FT) + 0.83 \qquad \text{for } FT \leq 30 \text{ days} \tag{117}$$

$$SL = 1.42 \qquad \text{for } FT > 30 \text{ days} \tag{118}$$

where FT is the flight time in days.

Step 10 The relationship between cortisol, calcium metabolism, and calcified tissue is poorly understood (Baulieu & Kelly, 1990). However,

chronic overdosage or excessive secretion of glucocorticoids have been found to impair skeletal growth in juveniles and cause bone thinning in adults (Martin, 1985).

A previous study investigated the direct effect of cortisol on bone collagen synthesis using in vitro techniques (Dietrich, Canalis, Maina, & Raisz, 1978). In this study, the rate at which labeled amino acids were incorporated into bone material was measured. This study found that cortisol inhibited the formation of collagen fibers in isolated bones and that the degree of inhibition was related to the cortisol concentration in the supporting medium. From this data, a relationship for the ratio of the actual bone formation rate to the normal bone formation rate can be derived.

$$\frac{\text{actual collagen synthesis rate}}{\text{normal collagen synthesis rate}} = -0.00126[C] + 1.189 \qquad (119)$$

The authors of the study speculated that cortisol may inhibit the collagen synthesis rate by decreasing the proliferation rate of osteoblast precursor cells. A decreased osteoblast precursor proliferation rate should decrease the osteoblast precursor population which should subsequently decrease the osteoblast population and the area of bone covered by the osteoblasts. Decreasing the area of bone which the osteoblasts affect will most likely decrease the collagen synthesis rate and the bone mineralization rate. Assuming that the bone collagen synthesis rate and bone mineralization rate are both proportionally related to the bone area affected by the

osteoblasts, then the mineralization rate can be determined from the data as a function of cortisol concentration.

$$\frac{R_{f,actual}}{R_{f,normal}} = -0.00126[C] + 1.189 \qquad (120)$$

where R_f is the rate at which calcium is transferred from the extracellular fluid to the bone salts and was discussed in step 2. Equation 120 gives R_f as a function of the extracellular cortisol level and $R_{f,normal}$ is that rate where the cortisol level is approximately normal. Equation 102 gives R_f as a function of the extracellular calcium ion concentration. The data used to derive K_1, which is the constant used in equation 102, were obtained from individuals who should have near normal cortisol levels (Lockwood, Vogel, Schneider, & Hulley). The data used to determine K_1 under weightless conditions, were taken after 5 to 6 weeks of bed rest. The plasma cortisol level after 5 or 6 weeks of weightlessness should not have increased by more than 15% (Leach, 1981). Therefore, $R_{f,normal}$ can be estimated from equation 102 and $R_{f,actual}$ as a function of plasma calcium ion concentration and cortisol concentration can be estimated by combining equations 102 and 120.

$$R_{f,actual} = K_1[Ca^{++}]\{-0.00126[C] + 1.189\} \qquad (121)$$

where $K_1[Ca^{++}]$, from equation 102, represents $R_{f,\ normal}$.

A previous in vitro study investigated the direct action of cortisol on bone-resorbing cells (Teitelbaum, Malone, & Kahn, 1981). By varying the cortisol concentration in the support medium, it was found that cortisol stimulated bone resorption. From the data taken in the study, the following relationship can be derived.

$$\frac{\text{actual bone resorption rate}}{\text{normal bone resorption rate}} = 0.0002[C] + 0.9703 \qquad (122)$$

Glucocorticoid administration has been found to increase the number of osteoclasts and bone-resorbing sites (Teitelbaum, Malone, & Kahn, 1981). Therefore, cortisol may increase the bone resorption rate by increasing the osteoclast population and consequently the bone area affected by the osteoclasts. The rate at which calcium is transferred from the bone salts to the extracellular compartment, R_r, is given by equation 104. The constant used in this equation, K_2, was calculated for conditions where the cortisol level should have been near normal. Using a procedure similar to that used to determine $R_{f,actual}$ as given by equation 121, a relationship for $R_{r,actual}$ can be derived.

$$R_{r,actual} = K_2\{0.0002[C] + 0.9703\} \qquad (123)$$

The net rate at which calcium is transferred between bone and the extracellular compartment as a function of plasma calcium ion levels and

plasma cortisol levels will be given by the difference between equations 121 and 123.

Step 11 The intestine is the principal target for 1,25-$(OH)_2D_3$, although the hormone also has a small affect on the kidney (West, 1985). The effect of 1,25-$(OH)_2D_3$ on the renal handling of sodium and calcium has previously been studied (Puschett, Fernandez, Boyle, Gray, Omdahl, & DeLuca, 1972). It was found that by increasing the plasma 1,25-$(OH)_2D_3$ concentration approximately 23 times above normal, the fractional sodium and calcium excretion decreased 26 and 36 %, respectively. Under conditions where the plasma calcium concentration varies by 10% or less, as for bed rest and space flight, the plasma 1,25-$(OH)_2D_3$ concentration will not vary by more than 3 times normal (Guyton, 1986). Therefore, the effect of 1,25-$(OH)_2D_3$ on the renal handling of sodium and calcium should be minimal and will be neglected by the proposed model.

The amount of calcium which an individual ingests can vary widely depending upon their customs and preferences. The average U.S. resident typically takes in between 600 and 1600 mg of dietary calcium per day (Brown & Stubbs, 1983). Of this ingested calcium, 30% to 80% will be absorbed. The fraction of calcium absorbed by the intestine depends mainly upon the calcium regulating hormones, specifically 1,25-$(OH)_2D_3$.

Calcium is absorbed by the intestines through both passive and active transfer (West, 1985, and Ganong, 1991) and in the absence of 1,25-$(OH)_2D_3$, both of these transfer mechanisms are impaired (Raisz, 1977). With regard to calcium transport, 1,25-$(OH)_2D_3$ has two main effects on

intestinal epithelial cells (the cells that line the lumen of the intestine). The first effect is that 1,25-$(OH)_2D_3$ stimulates the formation of a calcium-dependent ATPase. This ATPase is involved in the system which actively tranfers calcium out of the intestine (Ganong, 1991). Secondly, 1,25-$(OH)_2D_3$ causes the formation of a calcium binding protein in the cytoplasm of the epithelial cells. This calcium binding protein binds with intracellular calcium ions and thereby prevents the build-up of toxic calcium levels (West, 1985). Additionally, calcium binding protein may facilitate passive absorption since it lowers the intracellular calcium ion concentration. The calcium absorption rate appears to be proportional to the amount of calcium binding protein, and this protein can remain in epithelial cells for several weeks after 1,25-$(OH)_2D_3$ has been removed from the body (Guyton, 1976). To summarize, 1,25-$(OH)_2D_3$ increases intestinal calcium absorption by causing the formation of a calcium-dependent ATPase, which is involved with active calcium transport, and by causing the formation of a calcium binding protein, which may aid in passive calcium transport.

Calcium enters the intestine with ingested food and with gastrointestinal secretions such as bile, saliva, and pancreatic juice. Since the amount of calcium which is secreted into the gastrointestinal tract is not regulated or controlled, it remains fairly constant (Brown & Stubbs, 1983). The exact amount of calcium secreted into the intestine is not known and literature values can vary by several fold (Brown & Stubbs, 1983, and Davenport, 1982).

The fraction of ingested calcium absorbed by the intestine, $FAb_{Ca^{++},int}$, as a function of the plasma 1,25-$(OH)_2D_3$ concentration has been measured in a previous study (Gallagher, Riggs, & DeLuca, 1980). A relationship between these two variables has been derived from this experimental data and is given below.

$$FAb_{Ca^{++},int} = 10{,}000[1{,}25(OH)_2D_3] + 0.200 \quad (124)$$

Equation 124 gives the fraction of ingested calcium which is absorbed by the intestine. This amount is determined by ingesting a dose of radioactive tracer, ^{47}Ca, and then measuring the amount of the tracer excreted with the feces. Since the tracer calcium can only be excreted or absorbed, the fraction of calcium absorbed is equal to 1 minus the fraction of calcium tracer excreted. Currently, there is no method available for directly measuring the fraction of secreted calcium which is absorbed (Brown & Stubbs, 1983). A previous model of calcium metabolism in man assumed that digestive juice calcium enters the lumen towards the beginning of the gastrointestinal tract so that the fraction of secreted calcium absorbed is approximately equal to the fraction of ingested calcium absorbed (Holdsworth, 1977). Using this assumption, the amount of calcium secreted into the intestine can be determined by considering the steady state situation. At steady state, the net amount of calcium absorbed by the intestine, which is the amount absorbed minus the amount secreted, is equal to the amount of calcium lost in the urine. From the kidney model,

the fraction of sodium reabsorbed by the proximal tubule and loop of Henle can be calculated. The fraction of calcium reabsorbed by these nephron segments is approximately equal to the fraction of sodium reabsorbed. The amount of calcium reabsorbed by the distal tubule and collecting ducts can be determined from equation 113. The daily amount of calcium excreted with the urine, 178 mg/day, is then given by the amount of calcium filtered by the kidneys multiplied by one minus the fraction reabsorbed. The amount of calcium filtered can be found by multiplying the glomerular filtration rate by the normal plasma calcium ion concentration. The amount of calcium secreted into the intestine can then be estimated from the following mass balance. Equation 125 assumes a typical value of 1000 mg/day for the amount of calcium ingested and that under normal conditions, 50% of the ingested and secreted calcium is absorbed.

$$0.5(1000\ \frac{mg}{day} + \text{secreted } Ca^{++}) - \text{secreted } Ca^{++} = 178\ \frac{mg}{day} \qquad (125)$$

The left hand side of equation 125 represents the net amount of calcium absorbed by the intestine whereas the right hand side represents the urinary calcium loss. From solving equation 125, the amount of calcium secreted into the intestine can be found to be 644 mg/day. This procedure gives a maximal value for the amount of secreted calcium since it assumes a maximal fractional absorption for the secreted calcium.

Step 12 A decreased intestinal absorption of calcium will subsequently increase the amount of calcium which is lost in the feces.

From equation 114, which is a mass balance on total body calcium, it can be seen that by increasing the fecal loss term, the amount of calcium in the body tends to be reduced.

Using the information given in the previous twelve steps, the transient urinary and fecal loss of calcium can be estimated. Figures 45 through 50 compared results predicted by the model to that of actual data for bed rest, space flight, and head-down tilt.

From Figures 46 and 48, it can be seen that actual intestinal calcium absorption increases during approximately the first two weeks of bed rest and space flight. However, the model predicts that intestinal calcium absorption will decrease during this time. The model's results occur because plasma calcium levels are elevated (see Figure 49) and this leads to a decreased secretion rate and plasma level of PTH. PTH regulates the

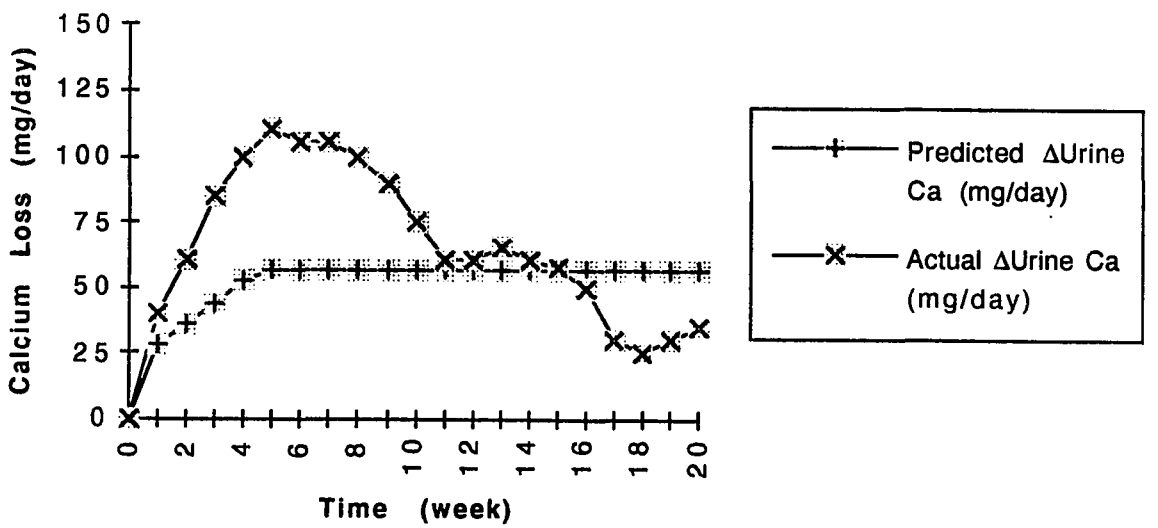

Figure 45: Urinary calcium excretion during prolonged bed rest. (actual data taken from Arnaud, Schneider, and Morey-Holton, 1986)

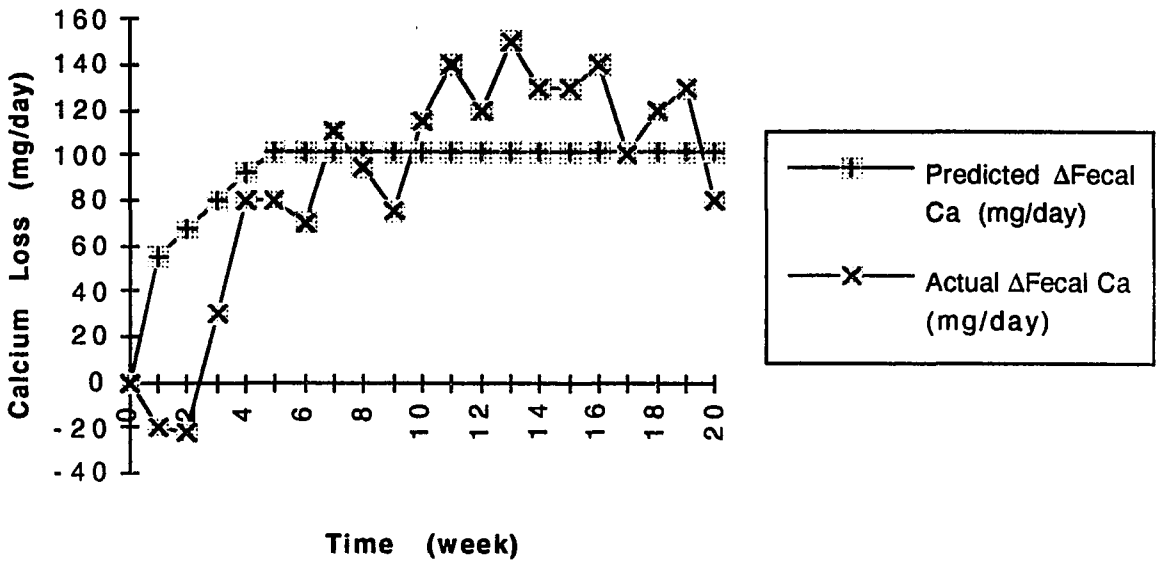

Figure 46: Fecal calcium excretion during prolonged bed rest. (actual dat taken from Arnaud, Schneider, and Morey-Holton, 1986)

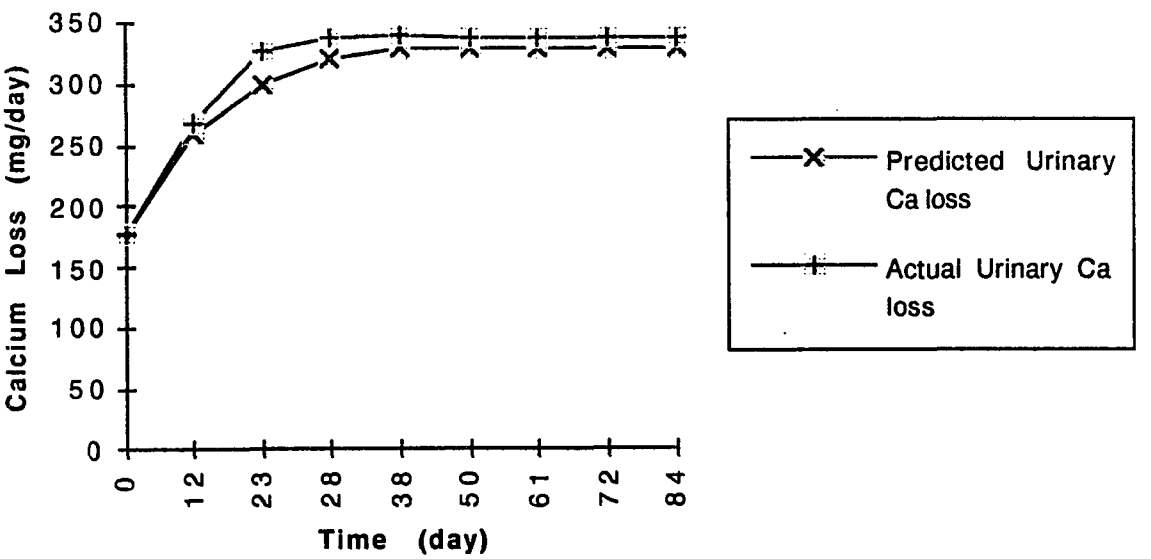

Figure 47: Urinary calcium excretion during space flight. (actual data taken from Rambaut & Johnston, 1979)

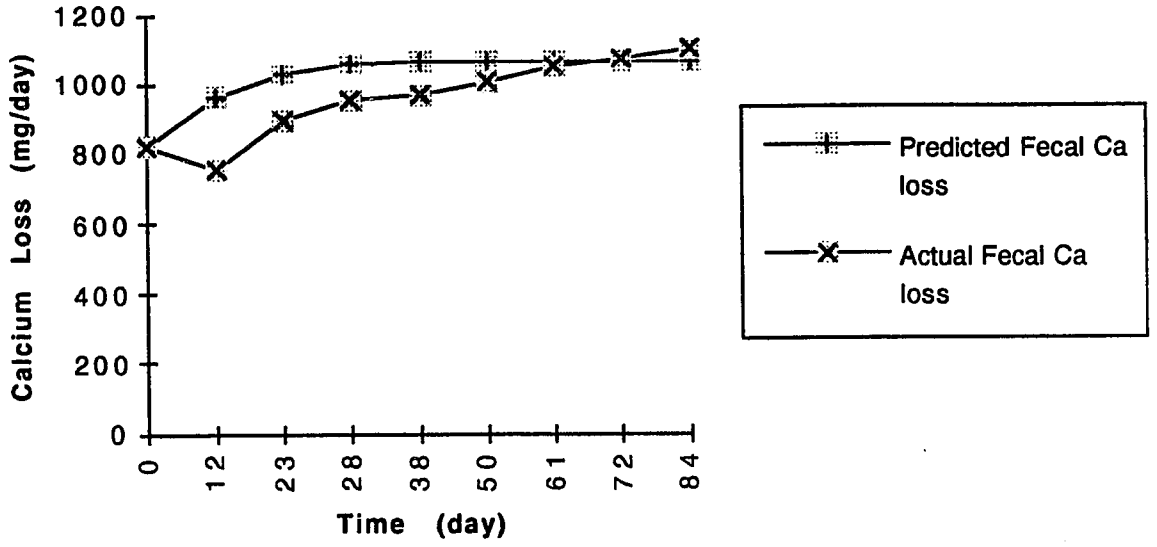

Figure 48: Fecal calcium excretion during space flight. (actual data taken from Rambaut & Johnston, 1979)

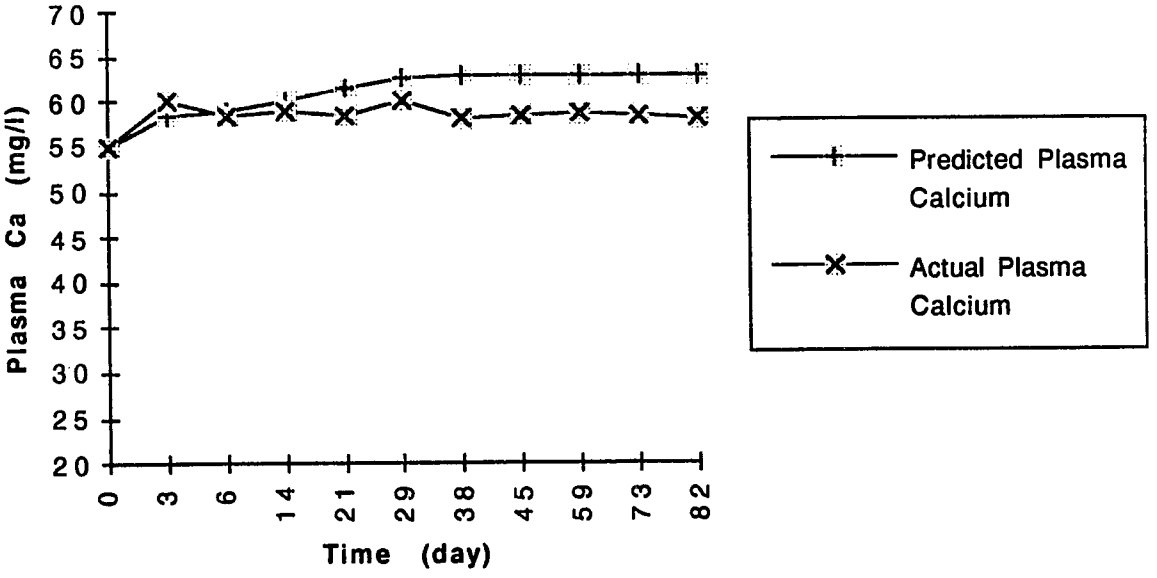

Figure 49: Plasma calcium levels during space flight. (actual data taken from Rambaut & Johnston, 1979)

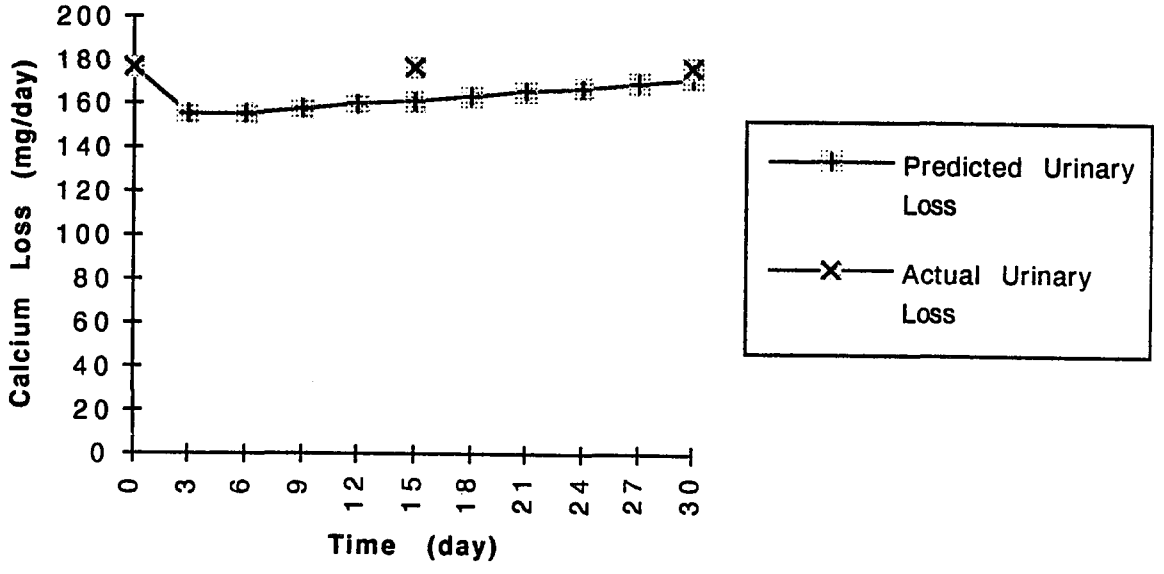

Figure 50: Urinary calcium excretion during head-down tilt where the sodium intake was restricted to 110 meq/day. (actual data taken from Arnaud, 1993)

formation rate of 1,25-$(OH)_2D_3$, therefore, the plasma level of 1,25-$(OH)_2D_3$ should also decrease. 1,25-$(OH)_2D_3$ is the primary regulator for intestinal calcium absorption. Consequently, the model predicts that intestinal calcium absorption will be decreased throughout weightlessness or bed rest. Skylab studies have found that actual plasma PTH levels can increase during the initial period of weightlessness even though plasma calcium levels are also elevated (Rambaut & Johnston, 1979). Although calcium ion concentration in the plasma is the primary regulator of PTH secretion, many other agents, such as epinephrine, dopamine, Mg^{++}, and Na^{+}, can also affect the PTH secretion rate (Martin, 1985). An increased plasma PTH concentration would most likely lead to an increased plasma 1,25-$(OH)_2D_3$

level and, subsequently, increased intestinal calcium absorption as is seen in Figures 46 and 48.

For bed rest, space flight, and head-down tilt, the model predicts that a new steady state will be attained after 30 days which is the time that cortisol secretion becomes constant (see equations 116, 117, and 118). Figure 47 tends to agree with this prediction, whereas Figure 45 does not. It has been predicted that the bones may lose 25% of their calcium after one year of space flight (Rambaut & Johnston, 1979), and, if this rate continues, the bones will be completely depleted of calcium after four years. Therefore, it is not possible for the steady state to continue after four years. Most likely, the rate of calcium of loss from the body will go to zero well before four years. The bones of paraplegic people do not completely decalcify even after many years. The actual data in Figure 45 suggest that urinary calcium loss begins to decrease after about 16 weeks. The bed rest study was conducted over a twenty week period, and the space flight study was conducted over only a twelve week period. Consequently, a decline in calcium loss may not yet have occurred, and data from longer space flights are needed to see if the calcium loss rate will eventually go to zero.

For the head-down tilt study, the sodium intake was restricted to about 110 meq/day. A normal sodium intake is about 170 meq/day. As can be seen in both the actual data and model prediction in Figure 50, restricting the sodium intake decreases the rate at which calcium is lost with the urine. This phenomenon occurs because a low sodium intake requires the body to conserve sodium, thereby causing the kidneys to

reabsorbed a greater fraction of this electrolyte. Since sodium transport and calcium transport are coupled in nephron segments prior to the distal tubule, the renal reabsorption rate for calcium is also increased. This maintains a relatively high plasma calcium level, and, from equation 102, it can be determined that the bone formation rate should also increase, thereby decreasing the net rate at which the bones lose calcium.

To summarize, a low sodium diet causes the kidneys to reabsorb a larger amount of sodium and calcium. This maintains a normal plasma sodium level and a relatively higher plasma calcium level. An increased amount of calcium in the plasma increases the rate at which bone material is formed and thereby decreases the overall loss of bone calcium.

EXERCISE

The thermoregulation model was developed to include the effects of exercise. However, several changes must be made to the kidney model for the inclusion of exercise. These changes involve variations that occur in the circulatory system and endocrine system during exercise. For the circulatory system, the arterial pressure, which determines the glomerular filtration rate at rest (see equation 10), will vary during exercise. The release rates of hormones which affect renal function, such as ADH and renin, will also change during exercise.

If the variations of glomerular filtration and hormone secretion with exercise are included, the urinary output of sodium and water during exercise can be determined by combining the proposed kidney model with the thermoregulation model. To connect the layered cylinder model with the kidney model, metabolically produced water and water lost from the body through respiration and perspiration is determined from the layered cylinder model. These flows of water are then included in the body water compartments used in the kidney model. Sensible perspiration, insensible perspiration, and water lost through respiration are losses from the extracellular fluid as shown in Figure 3. Water produced through the metabolism of food is created in the intracellular compartment since this process occurs within the cells.

At rest, the kidneys receive about 22% of the cardiac output, or 1100 ml/min, whereas the muscles typically receive 20%, or 1000 ml/min

(McArdle, Katch, & Katch, 1991). During exercise, the working muscles require more oxygen and, therefore, a higher blood flow rate. An increase in cardiac output, which occurs during exercise, accounts for a portion of the increased blood flow to the muscles. However, blood is also shunted from tissues which can tolerate a temporary reduction in blood flow and redirected to the muscles. As a result, during maximum exercise, the kidneys receive only about 1% of the cardiac output, or 250 ml/min, whereas the muscles receive about 88%, or 22,000 ml/min (McArdle, Katch, & Katch, 1991). Table 2 gives the blood flow to various tissues during rest, light exercise, moderate exercise, and maximum exercise.

The primary kidney model parameter affected by variations in the blood distribution is the glomerular filtration rate (GFR). The glomerular filtration rate tends to decrease during heavy exercise as does renal blood flow (Lamb, 1984). As mentioned above, since exercising muscles require a greater blood flow, and the kidneys, which are not a major organ of exercise,

Table 2: Estimated distribution of cardiac output during rest, light exercise, moderate exercise, and maximum exercise in a moderate environment. Values are given in ml/minute and the percent of total cardiac output that each tissue receives is shown in parenthesis (values taken from McArdle, Katch, & Katch, 1991)

Organ	Rest	Light Exercise	Moderate Exercise	Maximum Exercise
Kidneys	1100 (22%)	900 (10%)	600 (3%)	300 (1%)
Muscles	1000 (20%)	4500 (47%)	12,500 (71%)	22,000 (88%)
Brain	700 (14%)	750 (8%)	750 (4%)	750 (3%)
Skin	300 (6%)	1500 (15%)	1900 (12%)	600 (2%)
Heart	200 (4%)	350 (4%)	750 (4%)	1000 (4%)

do not require more blood, blood is shunted from the kidneys to the working muscle. As a result, renal blood flow decreases. The glomerular filtration rate, which depends mainly on the hydrostatic pressure within the glomerular capillaries, also tends to decrease during exercise, but the decrease is less marked than that of renal blood flow (Noble, 1986). The greater stability of the glomerular filtration rate is most likely caused by a balance in constriction between the afferent and efferent arterioles (Noble, 1986). Constriction of the afferent arteriole has the effect of reducing glomerular blood flow, reducing glomerular hydrostatic pressure, and consequently reducing the glomerular filtration rate. However, constriction of the efferent arteriole tends to increase the glomerular hydrostatic pressure and increase glomerular filtration. This mechanism is illustrated in figure 51. It is believed that the afferent arteriole constricts when the arterial pressure increases and causes more stretch or tension in the wall of the arteriole (Lote, 1987). The efferent arteriole constricts in response to low perfusion pressures and angiotensin II may be involved in this process (Ganong, 1991). Additionally, constriction of the renal arterioloes during exercise is most likely also controlled by activity in the renal sympathetic nerves (O'Connor, 1982).

The model predicts that the glomerular filtration rate is solely a function of arterial pressure since the arterial pressure mainly controls the glomerular hydrostatic pressure at rest. To include the effects of exercise in the kidney model, the glomerular filtration rate as a function of the exercise level must be known. Previous studies have found that renal blood flow and

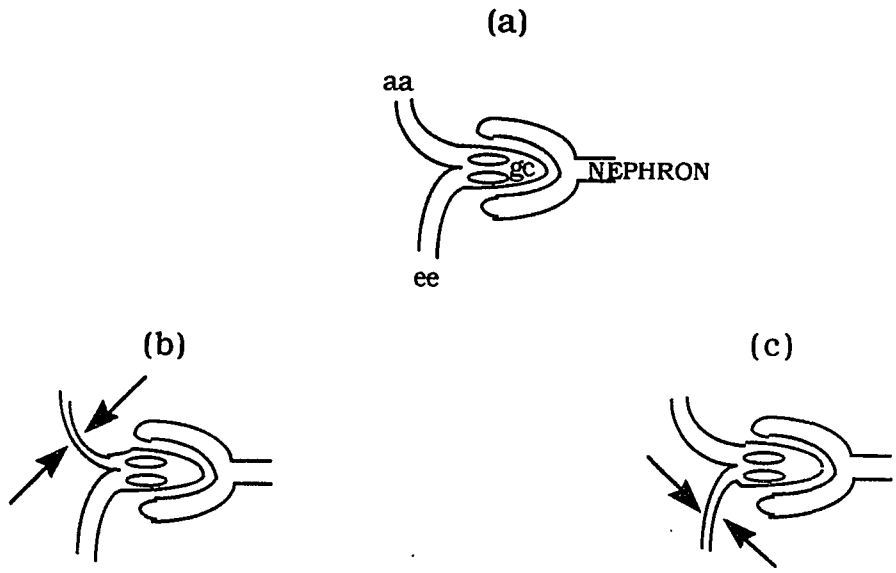

Figure 51: Diagram to show the ways in which vasoconstriction can occur in the afferent arterioles (aa) and efferent arterioles (ea) on either side of the glomerular capillary bed (gc) to help stabilize the GFR. (a) Normal situation, such as would occur at a mean arterial blood pressure of 100 mm Hg. (b) Afferent arteriolar constriction which reduces the glomerular capillary pressure below what it would otherwise be. (c) Efferent arteriolar constriction increases the glomerular capillary pressure. (adapted from Lote, 1987)

glomerular filtration are not substantially reduced when the exercise level is less than 40% of the maximal oxygen uptake ($VO_{2,max}$). This suggests that for exercise levels up to 40% $VO_{2,max}$, the associated increase in cardiac output and arterial pressure is not great enough to cause the arterioles to constrict. Under these conditions the original relationship between glomerular filtration rate and the arterial pressure (see equation 10) may be

used. The arterial pressure as a function of $\%VO_{2,max}$ has previously been measured (McArdle, Katch, & Katch, 1991) and this relationship is estimated by the following expression.

$$P_{ar} = 0.54(\%VO_{2,max}) + 96 \qquad \text{for } \%VO_{2,max} \leq 40\% \qquad (126)$$

The glomerular filtration rate can then be determined by calculating P_{ar} from equation 126 and then GFR from equation 10.

When the oxygen uptake is greater than 40% of the maximum oxygen uptake, the glomerular filtration rate decreases approximately linearly with $\%VO_{2,max}$ (Lamb, 1984). This can be interpreted as meaning that, for exercise levels over 40% of $VO_{2,max}$, the associated increase in cardiac output and arterial pressure is great enough to cause the afferent arterioles to constrict. An approximate relationship between glomerular filtration and $\%VO_{2,max}$ is shown below where $\%GFR_{rest}$ is the glomerular filtration rate expressed as a percent of the resting value.

$$\%GFR_{rest} = -1.2(\%VO_{2,max}) + 150 \qquad \text{for } \%VO_{2,max} > 40\% \qquad (127)$$

The glomerular filtration rate can then be determined by multiplying $\%GFR_{rest}$ by the normal resting glomerular filtration rate.

The glomerular filtration rates determined from equations 126 and 127 represent filtration rates which are averaged over the exercise period. Therefore, once exercise begins, these equations predict that the glomerular

filtration rate immediately changes to a new value. In actuality, the glomerular filtration rate will change over time once exercise begins. One method used to determine the actual glomerular filtration rate is to measure the creatinine clearance. Since the renal tubules reabsorb and secrete only small amounts of creatinine, the renal clearance of this compound can be used to estimate the glomerular filtration rate (Ganong, 1991). The data used to determine equation 127 were obtained from creatinine clearance measurements (Lamb, 1984). For these measurements, a urine sample was taken once immediately following 60 minutes of exercise. These clearance measurements would then yield the average glomerular filtration rate for the entire exercise period. An investigation measured the creatinine clearance several times during a 30 minute exercise period and the results of this experiment are shown in Figure 52 (Raize, Au, & Scheer, 1958). From Figure 52, it can be seen that the glomerular filtration rate changes approximately exponentially with time. Therefore, the glomerular filtration rate as a function of $\%VO_{2,max}$ and time can be estimated by the following expression.

$$GFR = [(GFR_{rest} - D)(\exp(-ct)] + D \qquad (128)$$

where GFR_{rest} is the resting glomerular filtration rate, c is a time constant, and D is the new steady state value which the glomerular filtration rate approaches. D is a function of $\%VO_{2,max}$ and is approximately 133% of the average glomerular filtration rate when $\%VO_{2,max} \leq 40\%$ and approximately

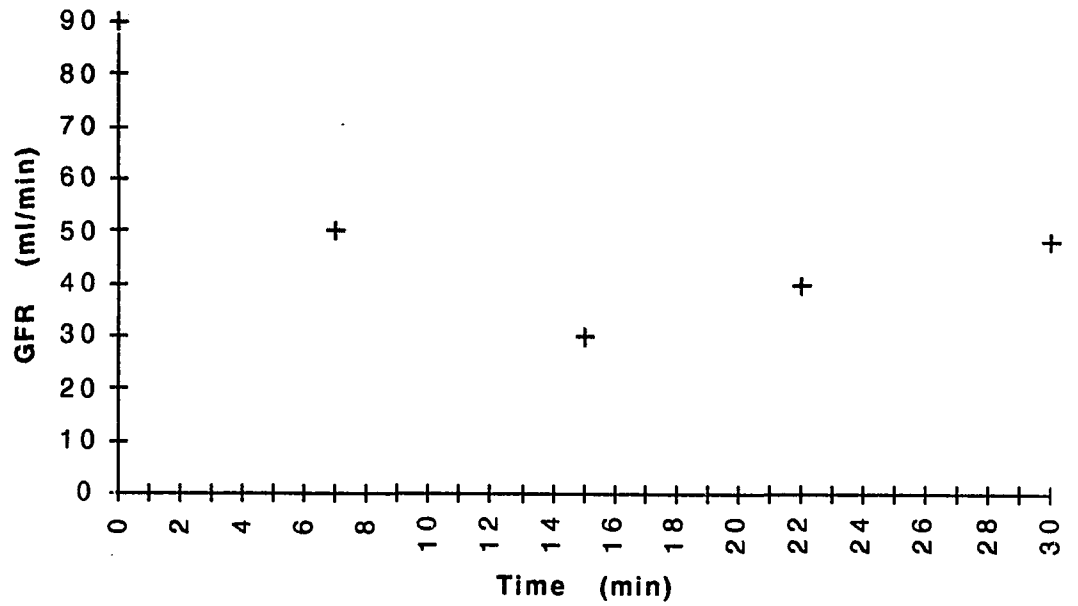

Figure 52: Glomerular filtration rate (GFR) during exercise as determined by creatinine clearance measurements. %VO2,max is approximately 53%. (Actual data taken from Raisz, Au, & Scheer, 1958)

67% of the average glomerular filtration rate when $\%VO_{2,max} > 40\%$ (Raisz, Au, & Scheer, 1958). The time constant, c, can be determined by averaging the function given by equation 128 over the exercise time and then comparing the result to the average glomerular filtration rate given by equation 127.

$$GFR_{ave} = \frac{1}{t}\int_0^t \{[(GFR_{rest} - D)(\exp(-ct)] + D\}dt \qquad (129)$$

Every variable in equation 129 is known except for c. GRF_{ave} is estimated by equation 126 or 127, D is determined from GRF_{ave}, and GFR_{rest} is the glomerular filtration rate at rest. From the data used to determine equation 127, which gave average creatinine clearances over 60 minutes of exercise, c can be determined. From this data and equation 129, c can be found to be approximately 0.04 min^{-1}.

Previous investigations have found that exercise increases the secretion rate of ADH, renin, and consequently angiotensin II and aldosterone (recall the renin-angiotensin-aldosterone system as shown in Figure 15). The precise stimuli for ADH release during exercise are not currently known, but the primary factors are believed to be blood volume and plasma osmolality (Convertino, Keil, Bernauer, & Greenleaf, 1981). As shown by equations 31 through 36, the kidney model assumes that ADH secretion is a function of blood volume and plasma osmolality. Therefore, variations in the ADH secretion rate during exercise should already be included in the kidney model. Results from a previous study suggest that the increased renin secretion rate is cause by reduced blood flow to the kidney (Convertino, Keil, Bernauer, & Greenleaf, 1981). This finding is consistent with the kidney model since in the model it is assumed that renin secretion is controlled primarily by the sodium flow rate in the distal nephron. Decreased blood flow to the kidneys will consequently decrease the glomerular filtration rate and therefore the sodium flow rate within the nephron. In summary, the stimuli which most likely control ADH and renin secretion during exercise are included in the initial kidney model.

A previous study measured the renal response to various rates of exercise for five subjects (Kachadorian & Johnson, 1970). For each trial of the experiment, the subjects drank 300 ml of water before exercising and then spent 60 minutes on a treadmill. The urine which accumulated during the 60 minutes of exercise was immediately collected. An average urine flow rate was then determined from the urine volume. Average urine flow rates predicted by the proposed model are compared with the actual data in Figure 53.

An investigation by Raisz, Au, and Scheer (1958) studied the renal concentrating mechanism during heavy exercise (Raisz, Au, & Scheer, 1958). In these experiments, subjects performed step exercises which consisted of stepping up and down a 17 inch step every three seconds. The metabolism for this step height and stepping rate should be about 8 times the basal rate (Noble, 1986) or about 53% of $VO_{2,max}$. The subjects abstained from fluids for 20 hours prior to the exercise and were intravenously infused with 100 mUnits of ADH. Using these experimental conditions with the proposed model, the urinary output of sodium and water can be estimated. Results predicted by the model are compared with actual data in Figures 54 and 55.

From Figures 53, 54, and 55, it can be seen that the proposed model reasonably predicts the urinary water and sodium loss during exercise. The urine flow rate increases with light exercise, as shown in Figure 53, but decreases with heavier exercise levels, as shown in Figures 53 and 54.

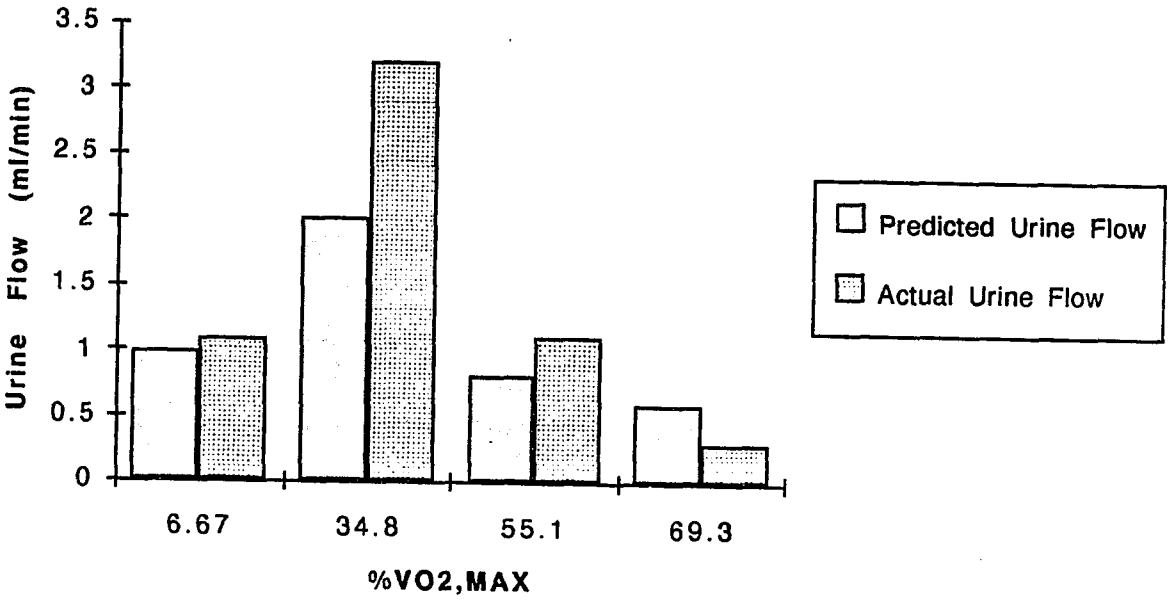

Figure 53: Predicted and actual average urine flow rates for various levels of exercise. The flow rates represent an average value for the 60 minute exercise period. T=16°C and H=50%. (actual data taken from Kachadorian & Johnson, 1970)

Figure 55 demonstrates that the urinary loss of sodium also decreases with heavier exercise levels.

The proposed model has considered how space flight and exercise individually affect the human water and electrolyte balance. Since exercise is used in space flight to reduce bone mineral loss and muscle mass loss, the next logical step would be to predict how exercising in space would affect the human water and electrolyte balance. By including the variation of glomerular filtration during exercise in the model used to predict the effects of space flight, the water and electrolyte balance can be predicted for exercising in space. Currently, experimental data on how the kidneys

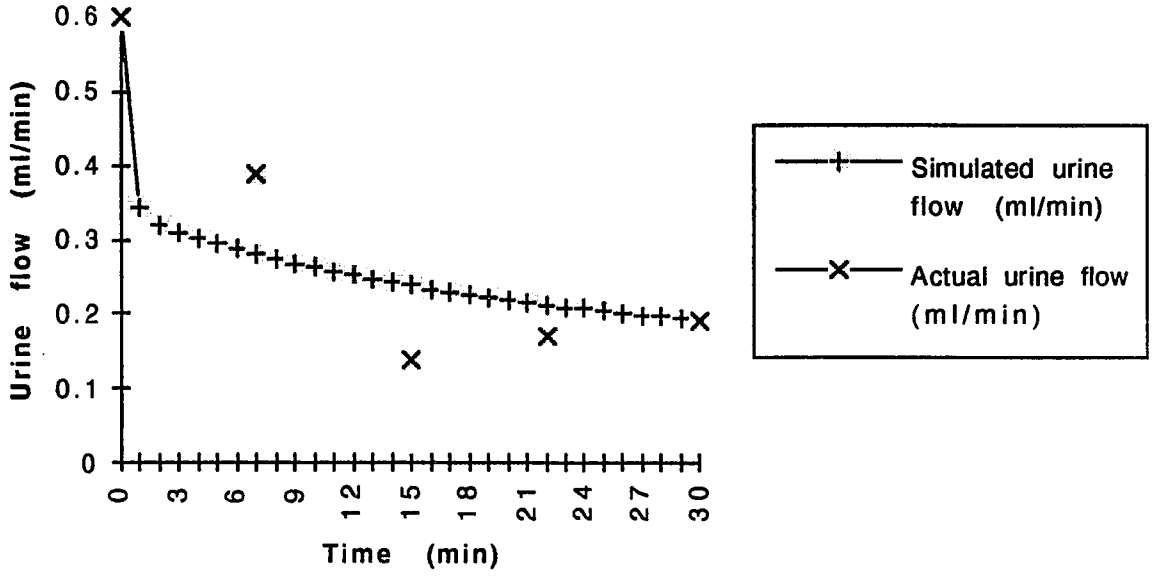

Figure 54: Simulated and actual urine flow rate during exercise at approximately 53% of $VO_{2,max}$. 100 munits of ADH were intravenously infused immediately prior to exercise. (Actual data taken from Raisz, Au, & Scheer, 1958)

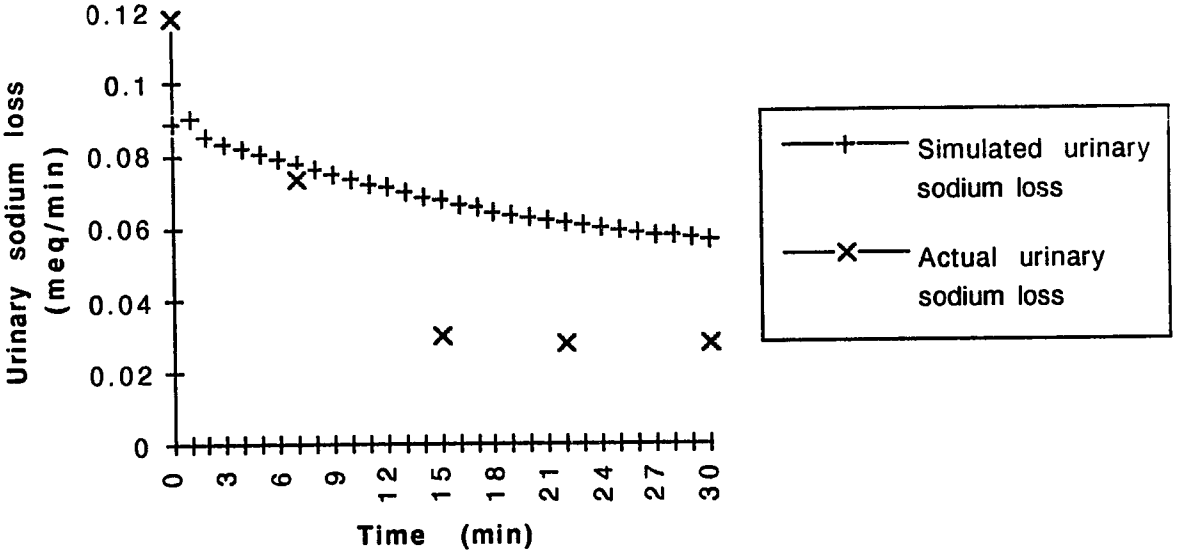

Figure 55: Simulated and actual urinary sodium loss during exercise at approximately 53% of $VO_{2,max}$. 100 munits of ADH were intravenously infused immediately prior to exercise. (Actual data taken from Raisz, Au, & Scheer, 1958)

respond to exercise in space are not available. Including the proposed effects of exercise and space flight on kidney function may or may not adequately predict renal function during exercise in space. Therefore, these calculations are not made since any predictions given by the model at this time would be mostly speculative.

CONCLUSIONS

The water, sodium, and calcium balance on earth or during space flight can be predicted and described by modeling kidney function and the associated endocrine system. The relationships used in the model may be determined either from experimental data or from mass balances. Water loss through perspiration, which is derived from the extracellular compartment, depends on body temperature. The sensible perspiration rate, or sweat rate, depends on core and skin temperature. Insensible perspiration, which is water lost from the lungs and skin by diffusion and evaporation, depends on body temperature and the ambient conditions. A thermoregulation model can be used to estimate body core, muscle, and skin temperature and the associated perspiration rates. With the kidney model and thermoregulation model, the output of water, sodium, and calcium from the body can be predicted. The bodily balance of these substances is then determined by subtracting the output flows from the input flows.

Space flight conditions may be included in the model by considering the effect on microgravity on the body. During weightlessness, fluid which is normally pooled in the lower extremities is redistributed headward. The model considers this fluid shift by dividing body water into an upper and lower compartment and then transferring fluid from the lower compartment to the upper compartment. The kidneys are contained in the upper body and therefore respond to the upper body water compartment. Since the

upper body water compartment becomes expanded during weightlessness, the kidneys increase the urinary output of fluid until the upper water compartment returns to a normal volume.

Exercise may be included in the model by considering the effects of activity on glomerular filtration. During light exercise, the increased blood pressure increases the glomerular filtration rate. During moderate and heavy exercise, glomerular filtration is reduced due to constriction of the afferent arterioles. Consequently, the urinary output tends to increase for light exercise levels and decrease for heavier exercise levels.

This model has incorporated nephron reabsorption characteristics, arterial pressure, antidiuretic hormone level, aldosterone level, and parathyroid hormone level into the mathematical equations used to describe kidney function. Consequently, mechanisms by which the human body regulates water, sodium, and calcium are included in the model. Methods of reducing the harmful effects of space flight or exercise on the human water, sodium, and calcium balance can therefore be explained by the model. For instance, a low sodium diet or bone stressing exercise can prevent bone loss during weightlessness. Additionally, new methods for preventing undesired space flight effects or exercise effects may perhaps be derived from this model.

The success of long-term space flight critically depends upon the design characteristics of the life support system, because this system is responsible for providing an environment which can comfortably sustain human life. Since the crew can bring only a limited amount of materials into space, the

life support system will also need to recycle as much materials as possible especially for long-termed space flight. The design of such systems must therefore include aspects of the crew's physiology and of the mechanical equipment which maintains the environment. This research provides some of the required physiological information and descriptions.

BIBLIOGRAPHY

Arnaud, S. B., V. S. Schneider, and E. Morey-Holton. 1986. Effects of inactivity on bone and calcium metabolism. Pages 49-76 in Vernikos, J., and H. Sandler eds. Inactivity: physiological effect. Academic Press, San Diego.

Arnaud, S. B., M. Navidi, and J. Harper. 1993. Urinary calcium loss and dietary sodium. Research and Technology 1993. Ames Research Center, Moffett Field, California.

Astrand, P. O., and K. Rodahl. 1970. Textbook of work physiology. McGraw-Hill Book Company, New York. 669 pp.

Baldes, E. J., and F. H. Smirks. 1934. The effect of water drinking, mineral starvation, and salt administration on the total osmotic pressure of the blood in man, chiefly in relation to the problems of water absorption and water diuresis. J. Physiol. 82:62-74.

Baulieu, E. E., and P. A. Kelly. 1990. Hormones. Chapman and Hall, New York. 697 pp.

Biddulph, D. M., P. F. Hirsch, C. W. Cooper, and P. L. Munson. 1970. Effect of thyroparathyroidectomy and parathyroid hormone on urinary excretion of calcium and phosphate in the golden hamster. Endocrinology 87:1346-1350.

Bird, R. B., W. E. Stewart, & E. N. Lightfoot. 1960. Transport Phenomena. John Wiley & Sons, New York. 780 pp.

Blank, I. H. 1952. Factors which influence the water content of the stratum corneum. J. Invest. Dermat. 18:433-440.

Blomquist, C., J. V. Nixon, R. L. Johnson, and J. H. Mitchell. 1980. Early cardiovascular adaptation to zero gravity simulated by head-down tilt. Acta Astronaut. 7:543-553.

Boskey, A. L. Current concepts of the physiology and biochemistry of calcification. Clin. Orthop. 157:225-257.

Brown A. M., and D. W. Stubbs. 1983. Medical physiology. John Wiley and Sons, New York. 914 pp.

Candas, V., J. P. Libert, and J. J. Vogt. 1979. Human wettedness and evaporative efficiency of sweating. J. Appl. Physiol. 46:522-528.

Carre, M., O. Ayigbede, L. Miravet, and H. Rasmussen. 1974. The effect of Prednisolone upon the metabolism and action of 25-hydroxy and 1,25-dihydroxyvitamin D_3. Proc. Nat. Acad. Sci. 71(8):2996-3000.

Chesney, R. W., R. B. Mazess, A. J. Hamstra, and H. F. DeLuca. 1978. Reduction of serum-1,25-dihydroxyvitamin-D_3 in children receiving glucocorticoids. Lancet:1123-1125.

Coffey, M. V., and R. C. Seagrave. 1972. A model of neonatal thermoregulation. Preceedings of the San Diego Biomedical Symposium 11:219-226.

Coleman, T. G., R. A. Norman, and R. D. Manning. 1975. Equilibrium between extracellular and intracellular fluid. Pages 225-242 in Guyton, A. C., A. E. Taylor, and H. J. Granger eds. Circulatory physiology II: Dynamics and control of the body fluids. W. B. Saunders Company, Philadelphia.

Convertino, V. A., L. C. Keil, E. M. Bernauer, and J. E. Greenleaf. 1981. Plasma volume, osmolality, vasopressin, and renin activity during graded exercise in man. J. Appl. Physiol.: Respirat. Environ. Exercise Physiology. 48: 657-664, 1980.

Cowley, A. W. 1975. Role of thirst and vasopressin in control of body fluid osmolality and volume. Pages 274-290 in Guyton, A. C., A. E. Taylor, and H. J. Granger eds. Circulatory physiology II: Dynamics and control of the body fluids. W. B. Saunders Company, Philadelphia.

Cussler, E. L. 1982. Diffusion. Cambridge University Press, Cambridge. 525pp.

Davenport, H. W. 1982. Physiology of the digestive tract. Year Book Medical Publishers, Chicago. 245 pp.

Davies, C. T. M. 1979. Thermoregulation during exercise in relation to sex and age. J. Appl. Physiol. 42:71-79.

Dean, R. F. A., and R. A. McCance. 1949. The renal responses of infants and adults to the administration of hypertonic solutions of sodium chloride and urea. J. Physiol. 109:89-97.

DeHaven, J. C., and N. Z. Shapiro. 1970. Simulation of the renal effects of antidiuretic hormone. J. Theor. Biol. 28:261-286.

Dietrich, J. W., E. M. Canalis, D. M. Maina, and L. Raisz. 1979. Effects of glucocorticoids on fetal rat bone collagen synthesis in vitro. Endocrinology 104:715-721.

Doty, S. E. 1992. A model for predicting insensible water loss in premature neonates. M.S. Thesis. Iowa State University, Ames, IA.

Frye, A. J., and E. Kamon. 1983. Sweating efficiency in acclimated men and women exercising in humid and dry heat. J. Appl. Physiol. 54(4):972-977.

Gagge, A. P. 1973. A two-node model of human temperature regulation in FORTRAN. Pages 142-148 in J. F. Parker, and V. R. West eds. Bioastronautics data handbook. NASA, Washington, D. C.

Gagge, A. P., J. A. J. Stolwijk, and Y. Nishi. 1971. An effective temperature scale, based on a simple model of human physiological regulatory response. ASHRAE Trans. 77:247-262.

Gallagher, J. C., B. L. Riggs, and H. F. DeLuca. 1980. Effect of estrogen on calcium absorption and serum vitamin D metabolites in postmenopausal osteoporosis. J. Clin. Endocrinol. Metab. 51:1359-1364.

Ganong, W. F. 1991. Review of medical physiology. 15th ed. Appleton and Lange, Norwalk, Connecticut. 754 pp.

Geankolis, C. J. 1978. Transport processes and unit operations. Allyn and Bacon Inc., Boston. 650 pp.

Gerzer, R., and C. Drummer. 1992. Hormonal control of body fluid metabolism. Acta Astronaut. 27:109-114.

Givoni, B., and R. F. Goldman. 1972. Predicting rectal temperature response to work, environment, and clothing. J. Appl. Physiol. 32(6):812-822.

Goldstein, L. J., and E. B. Rypins. 1992. A computer model of the kidney. Comput. Methods Programs Biomed. 37(3):191-203.

Gray, C. H., and A. L. Bacharach. 1961. Hormones in blood. Academic Press, New York. 655 pp.

Grimby, G. 1965. Renal clearances during prolonged supine exercise. J. Appl. Physiol. 20(6):1294-1298.

Guyton, A. C. 1986. Textbook of medical physiology. 6th ed. W. B. Saunders and Co., Philadelphia. 1200 pp.

Guyton, A. C. 1976. Textbook of medical physiology. 5th ed. W. B. Saunders and Co., Philadelphia. 1194 pp.

Guyton, A. C. 1984. Physiology of the human body. Saunders College Publishing, Philadelphia. 691 pp.

Guyton, A. C., A. E. Taylor, and H. J. Granger. 1975. Circulatory physiology II: Dynamics and control of the body fluids. W. B. Saunders Company, Philadelphia. 397 pp.

Guyton A. C., and D. B. Young. 1975. Relative unimportance of hormonal mechanisms for volume control: Their all importance for extracellular electrolyte concentration regulation. Pages 349-358 in A. C. Guyton, A. E. Taylor, and H. J. Granger eds. Circulatory physiology II: Dynamics and control of the body fluids. W. B. Saunders Company, Philadelphia.

Hargens, A. R. 1982. Fluid shifts in vascular and extravascular spaces during and after simulated weightlessness. Med. Sci. Sports Exerc. 15:421-427.

Hattner, R. S., and D. E. McMillan. 1968. Influence of weightlessness upon the skeleton: A review. Aerospace Med. 39: 849-855.

Holbrook, K. A. 1982. A histological comparison of infant and adult skin. Pages 3-31 in H. Miabach and E. K. Boisits eds. Neonatal skin. Marcel Dekker Inc., New York.

Holdsworth, C. D. 1975. Calcium absorption in man. Pages 223-262 in I. McColl and G. E. Sladen eds. Intestinal absorption in man. Academic Press, London.

Hole, J. W. 1987. Human anatomy and physiology. 4th ed. Wm. C. Brown Publishers, Dubuque, Iowa. 966 pp.

Hull, D. 1988. Thermal control in very immature infants. Br. Med. Bull. 44(4):971-983.

Johnson, A. T. 1991. Biomechanics and exercise physiology. John Wiley and Sons, Inc., New York. 493 pp.

Johnson, R. L., A. E. Nicogossian, S. A. Bergman, and G. W. Hoffler. Lower body negative pressure: the second manned Skylab mission. Aviat. Space Environ. Med. 47(3):347-353.

Kachadorian, W. A. 1972. The effects of activity on renal function. Pages 97-116 in J. F. Alexander ed. Physiology of fitness and exercise. The Athletic Institute, Chicago.

Kachadorian, W. A., and R. E. Johnson. 1970. Renal responses to various rates of exercise. J. Appl. Physiol. 28(6):748-752.

Keele, C. A., E. Neil, and N. Joels. 1982. Samson Wright's applied physiology. 13th ed. Oxford University Press, New York.

Kenner, G. H., E. W. Gabrielson, J. E. Lovell, and A. E. Marshall. 1975. Electrical modification of disuse osteoporosis. Calcif. Tiss. Res. 18:111-117.

Kimberg, D. V. 1969. Effects of vitamin D and steroid hormones on the active transport of calcium by the intestine. New England J. Med. 280:1396-1405.

Kimberg, D. V., R. D. Baerg, E. Gershon, and R. T. Graudusius. 1971. Effect of cortisone treatment on the active transport of calcium by the small intestine. J. Clin. Invest. 50:1309-1321.

Klein, R. G., S. B. Arnaud, J. C. Gallagher, H. F. DeLuca, and B. L. Riggs. 1977. Intestinal calcium absorption in exogenous hypercortisonism. J. Clin. Invest. 60:253-259.

Koeppen, B. M., and B. A. Stanton. 1992. Renal Physiology. Mosby-Year Book Publishers, Saint Louis. 167 pp.

Lamb, D. R. 1984. Physiology of exercise. MacMillan Publishing Company, New York. 489 pp.

Landis, E. M., and J. R. Pappenheimer. 1963. Exchange of substances through the capillary walls. Pages 961-1034 in Hamilton, W. F., and P. Dows eds. Handbook of physiology: Circulation. American Physiological Society, Washington, D. C.

Leach, C. S. 1981. An overview of the endocrine and metabolic changes in manned space flight. Acta Astronautica 8:977-986.

Leach, C. S. 1979. A review of the consequences of fluid and electrolyte shifts in weightlessness. Acta Astronautica 6:1123-1135.

Little, R. C. 1989. Physiology of the heart and circulation. Year Book Medical Publishers Incorporated, Chicago, Illinois. 379 pp.

Lockwood, D. R., J. M. Vogel, V. S. Schneider, and S. B. Hulley. Effect of the diphosphonate EHDP on bone mineral metabolism during prolonged bed rest. j. Clin. Endocrinol. Metab. 41:533-541.

Lote, C. J. 1987. Principles of renal physiology. Croom Helm, London. 208 pp.

Lueken, S. A., S. B. Arnaud, A. K. Taylor, and D. J. Baylink. Changes in markers of bone formation and resorption in a bed rest model of weightlessness. J. Bone Miner. Res. 8(12): 1433-1438.

Malkin, V. B. 1975. Barometric pressure and gas composition. Pages 3-64 in M. Calvin and O. G. Gazenko Eds. Foundations of space biology and medicine. National Aeronautics and Space Administration, Washington, D. C.

Martin, C. R. 1985. Endocrine physiology. Oxford University Press, New York. 1009 pp.

Martini, F. 1989. Fundamentals of anatomy and physiology. Prentice Hall, Englewood Cliffs, New Jersey. 945 pp.

Mathews, D. K., E. L. Fox, and D. Tanzi. 1969. Physiological responses during exercise and recovery in a football uniform. J. Appl. Physiol. 26(5):611- 615.

McArdle, W. D., F. I. Katch, and V. L. Katch. 1985. Exercise physiology. 2nd ed. Lea and Febiger, Philadelphia. 696 pp.

McArdle, W. D., F. I. Katch, and V. L. Katch. 1991. Exercise physiology. 3rd ed. Lea and Febiger, Philadelphia. 853 pp.

McCabe, W. L., J. C. Smith, and P. Harriott. 1985. Unit operation of chemical engineering. 4th ed. McGraw-Hill Book Company, New York. 960pp.

Nadel, E. R., R. W. Bullard, and J. A. J. Stolwijk. 1971. Importance of skin temperature in the regulation of sweating. J. Appl. Physiol. 31(1):80-87.

Nadel, E. R., K. B. Pandolf, M. F. Roberts, and J. A. J. Stolwijk. 1974. Mechanisms of themal acclimation to exercise and heat. J. Appl. Physiol. 37(4):515-520.

Nadel, E. R., E. Cafarelli, M. F. Roberts, and C. B. Wenger. 1979. Circulatory regulation during exercise in different ambient temperatures. J. Appl. Physiol.: Respirat. Environ. Physiol. 46(3):430-437.

Navar, L. G., and A. C. Guyton. 1975. Intrarenal mechanisms for regulating body fluid volume. Pages 243-261 in Hamilton, W. F., and P. Dows eds. Handbook of physiology: Circulation. American Physiological Society, Washington, D. C.

Nicogossian, A. E., C. S. Huntoon, and S. L. Pool. 1989. Space physiology and medicine. Lea and Febiger, Philadelphia. 401 pp.

Noble, B. J. 1986. Physiology of exercise and sport. Times Mirror/Mosby College Publishing, Saint Louis. 570 pp.

O'Connor, W. J. 1982. Normal renal function. Croom Helm, London. 433 pp.

Parmley, T. H., and A. E. Seeds. 1970. Fetal skin permeability to isotopic water (THO) in early pregnancy. Amer. J. Obstet. Gynec. 108:128-131.

Puschett, J. B., P. C. Fernandez, I. T. Boyle, R. W. Gray, J. L. Omdahl, and H. F. DeLuca. 1972. The acute renal tubular effects of 1,25-Dihydroxycholecalciferol. Proc. Soc. Exp. Biol. Med. 141:379-384.

Pitts, R. F. 1974. Physiology of the kidney and body fluids. Year Book Medical Publishers Incorporated, Chicago, Illinois. 315 pp.

Quinton, F. M. 1988. Structure and function of eccrine sweat glands in humans. Pages 57-88 in K. Laden and C. B. Felger eds. Antiperspirants and deodorants. Marcel Dekker, Incorporated, New York.

Raisz, L. G., W. Y. W. Au, and R. L.Scheer. 1958. Studies on the renal concentrating mechansim. III. Effect of heavy exercise. J. Clin. Invest. 38:8-13.

Rambaut, P. C., and R. S. Johnston. 1979. Prolonged weightlessness and calcium loss in man. Acta Astronautica 6:1113-1122.

Reeve, E. B., and A. C. Guyton. 1967. Physical bases of circulatory transport: Regulation and exchange. W. B. Saunders Company, Philadelphia. 381 pp.

Sawin, C. T. 1969. The Hormones. Little, Brown, and Company, Boston. 308 pp.

Scheuplein, R. J. 1978. Skin Permeation. Pages 1693 - 1730 in A. Jarrett ed. The physiology and pathophysiology of the skin. Vol. 5. Academic Press, London.

Scheuplein, R. J., and I. H. Blank. 1971. Permeability of the skin. Physiol. Rev. 51(4):702-747.

Schneider, V. S., A. LeBlanc, and R. C. Rambaut. Bone and mineral metabolism. Pages 214-221 in A. E. Nicogossian, C. Leach Huntoon, and S. L. Pool eds. Space physiology and medicine. Lea & Febiger, Philadelphia. 401 pp.

Shapiro, Y., K. B. Pandolf, and R. F. Goldman. 1982. Predicting sweat loss response to exercise, environment, and clothing. Eur. J. Physiol. 48:83-96.

Scherb, M. K. 1992. Modifications to an interactive model of the human body during exercise: With special emphasis on thermoregulation. M. E. Creative Component. Iowa State University, Ames, IA.

Siervogel, R. M., A. F. Roche, W. C. Chumlea, J. G. Morris, P. Webb, and J. L. Knittle. 1981. Blood pressure, body composition, and fat tissue cellularity in adults. Hypertension 4:382-386.

Seagrave, R. C. 1971. Biomedical applications of heat and mass transfer. Iowa State University Press, Ames, Iowa. 175pp.

Smith J. M., and H. C. Van Ness. 1975. Introduction to chemical engineering thermodynamics. McGraw-Hill Book Company, New York. 632 pp.

Sullivan L. P., and J. J. Grantham. 1982. Physiology of the kidney. Lea and Febiger, Philidelphia. 236 pp.

Talmage, R. V. 1956. Studies on the maintenance of serum calcium levels by parathyroid action on bone and kidney. Ann. NY Acad. Sci. 64:326-335.

Teitelbaum, S. L., J. D. Malone, and A. J. Kahn. 1981. Glucocorticoid enhancement of bone resorption by rat peritoneal macrophages in vitro. Endocrinology 108:795-799.

Uttamsingh, R. J., M. S. Leaning, J. A. Bushman, E. R. Carson, and L. Finkelstein. 1985. Mathematical model of the human renal system. Med. Biol. Eng. Comput. 23:525-535.

Vinson, G. P., B. Whitehouse, and J. Hinson. 1992. The Adrenal Cortex. Prentice Hall, New Jersey. 316 pp.

Webb, P. 1975. Thermal exchanges and temperature stress. Pages 94-126 in M. Calvin and O. G. Gazenko Eds. Foundations of space biology and medicine. National Aeronautics and Space Administration, Washington, D. C.

West, J. B. Best and Taylor's physiological basis of medical practice. 11th ed. Williams and Wilkins, Baltimore. 1340 pp.

ACKNOWLEDGMENTS

I would like to sincerely thank my major professor, Dr. Seagrave, for helping to make graduate school such a enjoyable learning experience. He always made his graduate students, and their work, a top priority. I would also like to thank my other committee members, Dr. M. H. Greer, Dr. G. Youngquist, Dr. C. Heath, and Dr. D. Young for being so generous with their time. Finally, I would like to thank the one who saw me through many stressful days as well as many cheerful days, my husband Mark. Graduate school was certainly a challenging experience, however, thanks to these people and the ISU Chemical Engineering Department, the last $4\frac{1}{2}$ years were invaluable!!!

Thanks also goes to the organizations that supported this research: The Iowa Space Grant Consortium and NASA Ames (Grant # NAG 2-885).